Ph D Thesis

Fabrication of Potentiometric Sensors for the Determination of Certain Metal Ions

Remalakshmy Poduval

Department of Applied Chemistry
Cochin University of Science and Technology
Kochi-22, Kerala, India

August 2006

Fabrication of Potentiometric Sensors for the Determination of Certain Metal Ions

THESIS

Submitted to Cochin University of Science and Technology
in partial fulfilment of the requirements
for the award of the degree of

DOCTOR OF PHILOSOPHY

in

CHEMISTRY

by

Remalakshmy Poduval

Department of Applied Chemistry
Cochin University of Science and Technology
Kochi – 22.

August 2006

DEPARTMENT OF APPLIED CHEMISTRY
COCHIN UNIVERSITY OF SCIENCE AND TECHNOLOGY
Kochi - 682 022.
Tel: 0484-2575804. E-mail: chem.@cusat.ac.in

Dr. K. Girish Kumar
Reader in Analytical Chemistry

31-08-2006

Certificate

Certified that the present work entitled "**Fabrication of potentiometric sensors for the determination of certain metal ions**", submitted by Mrs. Remalakshmy Poduval, in partial fulfilment of the requirements for the degree of Doctor of Philosophy in Chemistry to Cochin University of Science and Technology, is an authentic and bonafied record of the original research work carried out by her under my supervision at the Department of Applied Chemistry. Further, the results embodied in this thesis, in full or in part, have not been submitted previously for the award of any other degree.

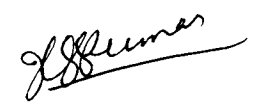

K. Girish Kumar
(Supervising Guide)

PREFACE

Potentiometric sensors or ion-selective electrodes permit a specific and quantitative determination of a substance, ranging from simple inorganic ions through amino acids to complex organic molecules. The purpose of a sensor is to provide information about our physical, chemical and biological environment. In that respect, it is a logical element in the information acquisition – processing chain. The wide range of applications, low material requirements and simplicity of the analytical procedure have not only brought potentiometric sensors into the limelight of analytical chemistry, but have promoted their use as tools for physiologists, medical researchers, biologists, geologists, environmental protection specialists etc.

This thesis presents the synthesis and characterization of seven ionophores, their use in the fabrication of potentiometric sensors and the results and discussion of fourteen sensors developed for the determination of five transition metal ions. The thesis is divided into eight chapters. A brief idea of the chapters is given below

Chapter 1 gives an introduction to the general electroanalytical techniques developed. The different types of sensors, their fabrications with examples are discussed. This chapter also gives a brief review of the important potentiometric sensors developed for the studied metal ions.

Chapter 2 is devoted to a complete description of the materials used in the present work and the experimental techniques employed for the synthesis and characterization of the ionophores, the sensor membrane preparation and the real sample preparations. The instruments used are also discussed.

Table of Contents

Chapter 1

INTRODUCTION

In many fields such as earth science, biology, environment and electronics, the knowledge about elemental distributions and chemical speciation is important[1]. The determination of metal levels especially the toxic ones both in the environment and in biological materials are increasingly demanded by the society. A number of techniques are available for the determination of metals. One of the most common and extensively used methods is the titrimetric analysis. The main advantage is that the method is precise but, a major drawback is that they are normally less sensitive and laborious[2]. A major breakthrough was the application of potentiometric, coulometric and amperometric methods in titrimetric analysis.

Another 'wet' method used is the gravimetric analysis. It is a macroscopic method usually involving relatively large samples compared with any other quantitative analytical method and a very high level of accuracy is achieved. It is concerned with the weighing of a substance that has been precipitated from solution or volatized and absorbed[3]. The need for trace level analysis led to the development of chromatographic methods, spectrophotometric methods and electroanalysis. Chromatography is mainly a separation technique. Ion chromatography is a technique used to separate and concentrate rare earths and transuranic ions. Gas chromatography which involves the separation of a mixture into its constituents by passing a moving

gas phase over a stationary sorbent is also used in the determination of cations[2]. Spectrophotometry specifically refers to the use of a spectrophotometer[4]. Quantitative applications of absorption / emission spectroscopy depend on the use of Beer's law, which relates absorbance to concentration. A number of techniques have evolved based on absorption / emission spectroscopy from simple spectrophotometric methods involving the use of a spectrophotometer, flame emission spectroscopy (FES), atomic absorption spectroscopy (AAS), atomic fluorescence spectroscopy (AFS) to the highly precise inductively coupled plasma atomic emission spectroscopy (ICP AES). Electroanalytical measurement is another technique used for trace level analysis.

One of the major research work carried out in our laboratory is the development of new techniques for the determination of metal ions in trace levels by the spectrophotometric[5-7] and the electroanalytical methods.

1.1 Electroanalysis

Electroanalysis can be defined as the application of electrochemistry to solve real-life analytical problems[8]. Each analytical technique has a specific purpose and a range of applications. Electroanalytical measurements have a number of important benefits such as[9]:

1. selectivity and specificity
2. selectivity results from the choice of electrode material
3. high sensitivity and low detection limit
4. results can be furnished in real time or close to real time
5. portable sensors with dedicated instrumentation can be fabricated for use outside the laboratory

6. miniaturized sensors for application in cases where other probes may not be usable

One important criterion for any electroanalytical measurement is that the medium between the electrodes making up the electrical circuit has to be sufficiently conducting[10]. Thus, electroanalysis is complementary to other analytical techniques. Electrochemical monitoring has many advantages; the detection limits achieved in electroanalysis make it a better alternative to the existing analytical techniques. Also, the advantage of distinguishing oxidation states is highly important. The electrochemical approach can give a rapid answer, without digestion, as to the labile fraction of a given element in a particular oxidation state, and the experiment can be performed on-site in the field. In cases where existing analytical techniques cannot be applied as they require complex and large equipment, electroanalysis provides a ready solution[8].

1.2 Electroanalytical Measurements

There are essentially three types of electroanalytical measurements and three kinds of controlling or measuring devices to implement them[11]. The three types of electroanalytical technique are as follows

1. conductimetry
2. potentiometry
3. amperometry and voltammetry

1.2.1 Conductimetry

In conductimetry, the concentration of charge is obtained through measurement of solution resistance and is therefore not species-selective. Conductimetric detectors can, however, be useful in situations where it is

necessary to ascertain, for example, whether the total ion concentration is below a certain permissible maximum level or for use as an on-line detector after separation of a mixture of ions by ion chromatography. Such situations can arise in electroremediation.

1.2.2 Potentiometry

The equilibrium potential of an indicator electrode is measured against a selected reference electrode using a high-impedance voltmeter, i.e., effectively at zero current. Thus, the current path between the two electrodes can be highly resistive. At an inert redox indicator electrode such as platinum the potential measured is a mixed potential, a function of all species present in solution and their concentrations. In ion-selective electrodes, careful choice of electrode material can give good selectivity to one particular species, in many cases, with only minimal interference from other ions.
Detection limits of the order of 100 nanomoles per litre of the total concentration of the ion present in a particular oxidation state, although down to 10 picomolar differences in concentration can be measured.

1.2.3 Voltammetry and amperometry

In voltammetry, the current is registered as a function of applied potential, more information and lower detection limits can usually be gained. Several species that react at different applied potentials can be determined almost simultaneously in the same experiment without the need for prior separation. Very low detection limits of down to the picomolar level can be reached using state-of-the-art instrumentation and preconcentration of the analyte on the electrode surface.

In amperometry, a fixed potential is applied to the electrode, which causes the species to be determined to react and a current to pass. Depending on the potential that is applied, the magnitude of the current is directly proportional to the concentration. Detection limits in the micromolar region can be obtained.

1.3 Chemical Sensors

A chemical sensor is a device which responds to a particular analyte in a selective way through a chemical reaction and can be used for the qualitative and quantitative determination of the analyte[12]. There are two parts to a chemical sensor – a region where selective chemistry takes place and the transducer. The chemical reaction produces a signal such as a colour change, emission of fluorescent light, a change in electrical potential at the surface, a flow of electrons, the production of heat, or a change in the oscillator frequency of a crystal. The transducer responds to this signal and translates the magnitude of the signal into a measure of the amount of the analyte.

Depending on the transducer type, chemical sensors are categorized into the following groups.

1. Electrochemical sensors

These include potentiometric sensors (ion-selective electrodes or ISEs) and voltammetric and amperometric sensors.

2. Optical sensors

In this class of sensors, a spectroscopic measurement is associated with the chemical reaction. They are referred to as optodes.

3. Mass sensitive sensors

These make use of the piezoelectric effect. They rely on a change in mass on the surface of an oscillating crystal which shifts the frequency of oscillation. The extent of frequency shift is a measure of the amount of material adsorbed on the surface.

4. Heat sensitive sensors

They are also known as calorimetric sensors; here, the transducer monitors the heat of a chemical reaction involving the analyte.

1.4 Potentiometric sensors

The glass electrodes[13-15] for pH measurements were the first developed potentiometric sensors that has been known since 1930s. The membrane in a pH electrode is the sodium silicate glass made by fusing a mixture of Al_2O_3, Na_2O and SiO_2. Increasing the Al_2O_3 content in the glass results in an increasing response to other monovalent cations. In 1937, Kolthoff and Sanders[16] made the first silver halide disc electrodes. In the early 1960s, Pungor[16] published his first paper on AgI-based electrodes and he along with his co-workers developed the first commercial solid state ion selective electrode. Concepts from medicine and physiology also spurred the development of potentiometric sensors. In 1964, Moore and Pressman[16] observed that neutral macrocyclic antibiotics induce ion permeation in mitrochondria, leading to the development of neutral carrier electrodes. In 1966, a major break came from the discovery by Frant and Ross that a slice of a single crystal of lanthanum fluoride attached to the end of an electrode barrel could be used to sense the fluoride ion in aqueous solution[17]. Ross and Frant teamed up and formed the Orion Research Inc. and both of them are considered as the founding fathers of ion selective electrodes. Pressed

powdered type of membranes using a sparingly soluble salt was another development as it does not require the need to grow a single crystal. An example is the silver sulphide disc[18]. The liquid membrane type of sensors[19] was first produced in 1967 and the major break through occurred in 1970 when a polymer film with sensing properties was produced by immobilizing the electroactive component into poly(vinyl chloride) [20]. A number of PVC plasticized membrane sensors have been developed using different types of electroactive species (ionophores). Ruzicka *et al*[21] were the first to introduce liquid state electrode based on carbon in 1970. The development of sensors using spectral grade graphite powder, nujol oil and metal salts of low solubility in a plastic body was described by Mesaric and Dahmen[22] in 1973. In 1980, Heineman *et al* described the first use of a polymer film chemically modified carbon paste electrode (CMCPE)[23].

Research in the field of development of potentiometric sensors is gaining more and more attention and a number of potentiometric sensors have been developed for the cations like alkali, alkaline earth, transition metals, lanthanides etc; for anions like Cl^-, NO_3^-, perchlorate etc. ; for drugs like terazosin, diclofenac etc[24-33].

1.4.1 Technique

Potentiometric sensors make use of the development of an electrical potential at the surface of a solid material when it is placed in a solution containing ions which can exchange with the surface. The magnitude of the potential is related to the number of ions in the solution and the measurement of the cell potential is made under a 'zero current' condition. Species recognition is achieved through a chemical equilibrium reaction at the sensor surface.

Consider a metal rod dipped into its metal salt solution. The metal comprises of a periodic network of positive ions and a pool of mobile electrons.

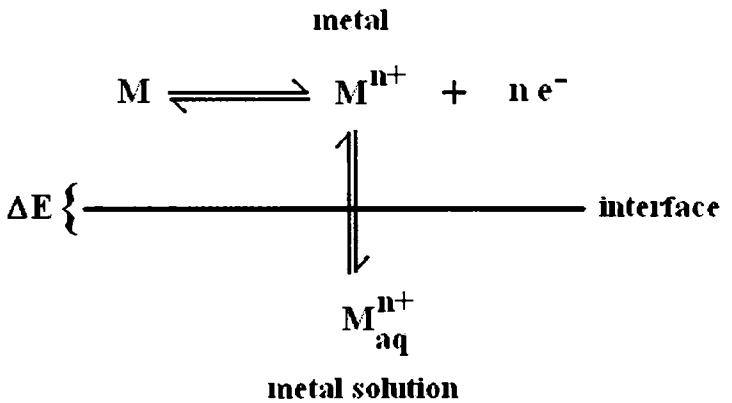

Figure 1.1 – Interfacial potential for a metal

A few M^{n+} ions at the surface distribute into the aqueous solution in the region of the surface and become hydrated (M^{n+}_{aq}) which leaves an equivalent number of free electrons on the metal side of the solution/metal interface as depicted in the Figure 1.1. Thus there is a charge separation, which gives rise to an electrical potential difference.

1.4.2 Classification

Based on the physical state of the substances forming the electrode membrane[18,34], potentiometric sensors are classified into

1. Ion-selective electrodes with solid membranes

The membrane can be either homogeneous (a single crystal, a crystalline substance or a glass which is considered to be a solid with regard to the immobility of the anionic groups) or heterogeneous, where a crystalline substance is built into a matrix made from a suitable polymer.

2. Ion-selective electrodes with liquid membranes

In this case, the sensor membrane is represented by a water-immiscible liquid in which is dissolved a substance capable of exchanging the ion in solution for which the sensor is selective.

Another classification based on the membranes used in potentiometric sensors are

1. Glass membranes

These are selective to ions such as H^+, Na^+ etc.

2. Sparingly soluble inorganic salt membranes

This type consists of a section of single crystal or the pressed powdered disc of an inorganic salt which is seen to show selectivity to certain ions.

3. Polymer-immobilized ionophore membranes

In these, an ion-selective complexing agent or ion-exchanger is immobilized in a plastic matrix such as poly(vinyl chloride).

4. Gel-immobilized and chemically bonded enzyme membranes

These membranes use the highly specific reactions catalyzed by enzymes. The enzyme is incorporated into a matrix or bonded onto a solid surface.

1.5 Aspects of Sensors

1.5.1 Recognition elements

The key component of any sensor is the ionophore or electroactive component or the modifier which imparts the selectivity that enables the sensor to respond selectively to a particular analyte, thus avoiding interferences from other substances. Schiff bases, complexes, ion association complexes, calixarenes, crown ethers etc. have been tested for their use as ionophores.

1.5.2 Performance factors

1. Selectivity

This is the most characteristic property of a sensor – the ability to discriminate between different substances and this is a function of the selective component.

2. Sensitivity range and detection limits.

This refers to the concentration range of the analyte for which the sensor behaves in a Nernstian manner. The lower level is the detection limit and the precise definition according to IUPAC convention is that it is the concentration of analyte at which the extrapolated linear portions of the calibration graph intersects the baseline – a horizontal line corresponding to zero change in response for several decades of concentration change[35].

3. Nature of solution

Conditions such as pH and the non aqueous content are taken into consideration.

4. Response time

The response time is the average time for the sensor to reach a potential within ±1 mV of its final equilibrium value. The practical response time of the sensor is calculated by measuring the time required to achieve 95% of the equilibrium potential from the moment of addition of 1.0×10^{-5} M M^{n+} solution.

5. Working lifetime

The lifetime of a sensor refers to the period of time during which the sensor can be used for the determination of the analyte and it is determined by the stability of the selective material.

1.5.3 Areas of application

The applicability of the sensors for continuous real time monitoring of certain analytes in the environment or in the online and offline processes in the industry are of great importance. In addition to pollution applications, farming, gardening, veterinary science and mining are all areas where sensors are needed for environmental monitoring.

1.6 A brief review on important potentiometric sensors for metal ions.

As part of the present investigations, potentiometric sensors have been developed for the following metals – Mn^{2+}, Ni^{2+}, Cu^{2+}, Hg^{2+} and Pb^{2+}. A brief review on the potentiometric sensors for the titled metal ions is presented below.

1.6.1 Manganese

There are only few reports on manganese sensors in literature and so far none of them have been commercialized. Buchanan and Seago[36] reported the use of two electroactive components $MnHPO_4$ in $MnCl_2$ and $MnCO_3$ in $MnCl_2$ which were impregnated into silicone rubber matrix. Though the sensors fabricated responded to Mn^{2+} test solutions; they were not 'specific' in their response to towards Mn^{2+} ions; but rather it showed a response to the total free cations in solution. The use of an electrode with manganese(II) telluride-silver sulphide disc was explored by Hirata and Higashiyama[37]. This sensor showed a non Nernstian response of 25 mV/pM and was selective relative to alkali-metal and alkaline-earth metal cations, but no other performance characteristics were described. The group of Lal[38] published their results where a membrane consisting of a cation exchange resin (Dowex 50 WX-4) in an epoxy resin matrix was proposed for Mn^{2+} ion

determinations, but the sensor gave a super Nernstian response. Midgley and Mulcahy[39] reported the use of manganese(IV) oxide with a graphite/PTFE substrate in the fabrication of a solid type manganese sensor. The results show that the sensor gave a near Nernstian response to Mn^{2+} ions but the main practical problem was the slow response time of ~20 min and also, the pH had to be precisely controlled (maintained at pH 4.0 acetate medium). Agarwala and Chattopadhyaya[40] studied the response characteristics of sensor fabricated with tetrapyridine Mn(II) thiocyanate precipitate as the ionophore which had a good working pH range of 2.3 – 8.8, but the response was only near Nernstian. Sun and Qi[41] fabricated a sensor using permanganate ion while Dong[42] determined the Mn^{2+} ions in solutions using a crystal ion-selective electrode. Singh *et al*[43] reported the use of a pentaazamacrocyclic manganese complex in the construction of a PVC-plasticized membrane sensor. Unfortunately, most of the developed manganese sensors have some problems like narrow working concentration range, high response time, poor selectivity and high detection limit.

1.6.2 Nickel

Extensive efforts have been made by researchers to develop sensors for the estimation of nickel especially as it is used in many catalytic processes and occurs in many industrial effluents. Morazzani-Pelletier and Baffier[44] studied collodion and paraffin membranes embedded with nickel salts. Pungor *et al*[45] developed impregnated silicone rubber membrane electrodes incorporating nickel(II) dimethylglyoxime complex which showed response to Ni^{2+} ions. The silicone rubber membranes impregnated with nickel dimethylglyoximate, nickel acetylacetonate (dehydrate and anhydrous), nickel carbonate and nickel orthophosphate were prepared by

Buchanan and Seago[36] and the results showed that the membranes containing the chelates nickel dimethylglyoximate and nickel acetylacetonate dihydrate failed to show response towards cations. Dobbelstein and Diehl[46] studied the response of a sensor containing nickel dimethylglyoximate in epoxy polyester and phenol formaldehyde membranes. Hirata and Higashiyama[37] demonstrated the use of sintered nickel selenide and telluride discs in the determination of Mn^{2+} ions over the concentration range 10^{-1} to 10^{-5} M. Though the sensors responded in a Nernstian manner, the selectivity was poor with strong interferences from silver, copper(II), mercury(II), iron(III), sulphide and chloride. Liquid membrane type sensors were reported with different ionophores like O,O' diisobutyl dithiophosphatonickel(II) in chlorobenzene by Materavo *et al*[47]; bis(tetraethylammonium) bis(dithiobenzophenazine) nickelate in nitrobenzene by Luca *et al*[48] and nickel diethyldithiocarbamate in chloroform by Smirnova *et al*[49]. Lal *et al*[50] reported the use of a nickel complex of 1,4,8,11-tetraazacyclotetradecane in araldite as the membrane disc for the fabrication of a liquid exchange type sensor. Hampton *et al*[51] suggested the use of 1,4,7,10-tetraoxacyclododecane as the electroactive component in the fabrication of a sensor for nickel but the characteristics like shelf life and pH range was not studied. Aswathi *et al*[52] reported a membrane sensor incorporating nickel bis(2-ethylhexyl) phosphate as ionophore. Bhatt and Thakkar[53] constructed a sensor by incorporating a nickel(II) complex of isonitrosopropiophenone in styrene butyl methacrylate co-polymer which gave a non-Nernstian response to Ni^{2+} ions. Rao *et al*[54] investigated the responses of a membrane prepared by dissolving a 1:1 ratio of a chelating ion-exchange resin and PVC in THF. Gupta and co-workers[55-58] published four reports where porphyrins, 5,7,12,14-tetramethyldibenzotetraazaannulene, dibenzocyclamnickel(II) and

dibenzo-18-crown-6 were investigated as electroactive materials for preparing PVC based membrane sensors. Jain *et al*[59,60] reported the use of different electroactive components; macrocyclic compounds in PVC and polystyrene binders and two nickel chelates of schiff bases in PVC membrane sensors for the determination of Ni^{2+} ions. Crown ethers such as 1,10-dibenzyl-1,10-diaza-18-crown-6 reported by Mousavi *et al*[61] and dibenzodiaza-15-crown-4 reported by Shamsipur and Kazemi[62] were used as neutral carriers in the construction of a PVC based membrane sensor. The group of Ganjali[63,64] suggested two ionophores; a thiopyran derivative as the electroactive material in the construction of a PVC membrane sensor and a coated graphite PVC-membrane sensor based on benzylbis(thiosemicarbazone). A PVC-based membrane of 1,5-diphenylthiocarbazone was discussed in detail by Abbaspour and Izadyar[65] while the group of Singh reported a polystyrene based 3,4,11,12-dibenzo-2,5,10,13-tetraoxo-1,6,9,14-tetraazacyclohexadecane[66] and also 3,4:12,13-dibenzo-1,6,10,15-tetraazacyclooctadecane[67] and dibenzo[e,k]-2,3,8,9-tetraphenyl-1,4,7,10-tetraazacyclododeca-1,3,5,7,9,11-hexaene[68] in a PVC membrane matrix. A wire sensor coated with the PVC plasticized membrane containing 1,3,7,9,13,15,19,21-octaazapentacyclooctacosane which was selective to Ni^{2+} ions was reported by Mazloum *et al*[69]. Mashhadizadeh *et al*[70,71] reported the response characteristics of two PVC membrane sensors based on two ionophores- a mercapto derivative and a schiff base. Singh and Bhatnagar[72] reported the use of carboxylated and methylated porphine while Belhamel *et al*[73] made use of a macrocyclic compound for the construction of a nickel sensor. The group of Yari[74] discussed the results of the sensor fabricated using a dioxime derivative. However, most of the reported sensors

suffer from one or the other drawbacks like narrow working concentration range, high detection limit, high response time and poor selectivity.

1.6.3 Copper

A variety of potential ion carriers have been used in the construction of sensors for Cu^{2+} ions and a commercial solid state membrane sensor based on CuS-Ag_2S has been introduced by Orion Research Inc.[75] but it suffers interferences from Hg^{+}, Hg^{2+}, Ag^{+} and Fe^{3+} ions. Chatterjee and Mitra[76] prepared clay membranes while Buchanan and Seago[36] tested the response of silicone rubber membranes impregnated with anhydrous and hydrated $CuHPO_4$ in $Cu(NO_3)_2$ but these sensors gave a sub-Nernstian response to Cu^{2+} ions. The group of Hirata[77,78,37] investigated the response of different types of sensors – a copper(I) sulphide cermanic sensor, silicone rubber membranes impregnated with copper(I) sulphide and copper(I) selenide and telluride sensors, to Cu^{2+} ions. Sharp and Johansson[79] prepared solid-state sensors from ion-radical salts of 7,7,8,8-tetracyanoquinodimethane. Neshkova and Sheytanov[80,81] developed two solid-state sensors with homogeneous membranes of CuAgSe and $Cu_{2-x}Se$ which showed response to Cu^{+} ions and not Cu^{2+} ions. Kamata *et al*[82,83] reported the use of acyclic neutral ionophores with dithiocarbamate groups in the fabrication of a copper sensor. The group of Jain[84,85] reported two types of sensors - a polystyrene based heterogeneous ion-exchanger membrane of cerium(IV) phosphomolybdate and PVC membrane sensors based on copper chelates. Sun *et al*[86] produced a novel copper sensor based on molecular deposition technique of copper phthalocyanine tetrasulphonate and bipolar pyridine salt on 3-mercaptopropionic acid modified Au electrode. Chen and Alexander[87] reported the use of tungsten oxide as the ionophore in the fabrication of a

copper sensor. Gismera *et al*[88,89] fabricated copper sensors based on copper complexes containing thiohydrazone and thiosemicarbazone ligands and also based on dithiosalicylic and thiosalicylic acids. The group of Shamsipur[90-92] reported the use of a 23-membered macrocyclic diamide, naphthol-derivative schiff base and mixed aza-hioether crowns containing a 1,10-phenanthroline sub-unit; in the fabrication of copper sensors. K. C. Gupta and D'Arc[93,94] published their results on copper sensors containing a copper(II) salicylaniline schiff base complex in styrene-co-acrylonitrile copolymer while Saleh[95] reported a copper sensor based on a cephaloridine antibiotic as ionophore in a PVC matrix. Chattopadhyaya and co-workers[96,97] successfully estimated the copper content in gun metal by using a heterogeneous coated wire Cu^{2+} ion selective electrode based on Cu(II)-cupron complex as ionophore and also used thiopentone-Cu(II) complex as the ionophore in a PVC membrane sensor for the determination of Cu^{2+} ions. Park *et al*[98] developed five novel 1,3-alternate calix[4]azacrown ethers having 2-picolyl, 3-picolyl and benzyl unit on the nitrogen atom as ionophores for copper-selective PVC membrane sensors and Gholivand and Nozari[99] used 2,2'-dithiodianiline as the neutral carrier in the fabrication of a copper sensor. Tymecki *et al*[100] discussed the thick-film graphite electrodes produced by screen-printing and it was shown that CuS-doped graphite sensors show stable and improved response to copper ions. Su *et al*[101] reported a copper sensor based on 2'-picolyl sym-dibenzo-16-crown-5 ether as membrane carrier with a super Nernstian response to Cu^{2+} ions. Ganjali and co-workers[102-104] reported a graphite sensor coated with PVC plasticized bis-2-thiophenal propanediamine membrane and two PVC membrane sensors incorporating a bis-thiophenalpropanediamine and diphenylisocyanate bis(acetylacetone) ethylenediimine as the electroactive species. Firooz *et*

al[105] constructed a coated wire copper sensor based on phenylglyoxal-α-monoxime ionophore while the group of Abbaspour[106,107] reported a carbon paste electrode modified with 3,4-dihydro-4,4,6-trimethyl-2(1H)-pyrimidine thione and a PVC membrane sensor incorporating dithioacetal as ionophore for the potentiometric determination of Cu^{2+} ions. Coated wire and coated disc copper sensors based on Cu(II) complex with cyclized salophen were reported by Al-Saraj *et al*[108,109] for the determination of Cu^{2+} ions in aqueous solutions. Sadeghi *et al*[110] reported the use of a series of schiff base derivatives inorder to characterize their abilities as copper ion carrier in PVC membrane sensors. Yoshimoto *et al*[111] studied the response of the sensor based on hydrotris(3-isopropylpyrazolyl)methane in a poly(vinyl chloride) matrix. V. K. Gupta and co-workers[112-114] fabricated three PVC plasticized membrane sensors based on ethambutol-copper complex, bis(acetylacetone)propylenediimine and porphyrins as ionophores. A comparison between the response characteristics of sol-gel and coated wire copper sensors based on thiosemicarbazone was studied by Ardakani *et al*[115]. Singh and Bhatnagar[116] explored the response of PVC plasticized membrane sensor based on a schiff base complex derived from 2,3-diaminopyridine and o-vanillin, to Cu^{2+} ions. The group of Michalska[117,118] reported the use of conducting polymers in the construction of an all-plastic, disposable copper sensor. Fakari *et al*[119] fabricated a series of PVC membrane sensors based on different salens as carriers for the determination of Cu^{2+} ions in solutions. Two novel copper PVC membrane sensors were constructed by Hassan *et al*[120] which were based on cyclic tetrapeptide derivatives. Singh *et al*[121] studied the characteristics of two plasticized membrane sensors based on 3-(2-pyridinyl)2-H-pyrido[1,2,-a]-1,3,5-triazine-2,4(3H)-dithione and acetoacetanilide. Szigeti[122] explored the response characteristics of the sensor

fabricated using *N,N,N',N'*-tetracyclohexyl-3-thiaglutaric diamide as ionophore for the potentiometric determination of Cu^{2+} in drinking water while Oliveira *et al*[123] reported a new copper sensor incorporating a new thiophosphoril-containing macrocycle as neutral carrier. However, most of the reported sensors have limitations in that they exhibit inferences to some common ions, work over a narrow concentration range and show non-Nernstian response, limited pH range and high response time.

1.6.4 Mercury

Literature reports on mercury sensors are sparse and one is yet to achieve an efficient commercial mercury(II) sensor. One of the earliest report of a mercury sensor was by Ruzicka and Tjell[124] which was a liquid membrane electrode based on the mercury(II) complex of dithizone. Baiulescu *et al*[125-127] reported the use of Hg^{2+} chelate of diketohydrindylidine diketohydrindamino in chloroform, palladium dithizonate and PAN chelate of Hg^{2+} dissolved in chloroform in the fabrication of three liquid membrane sensors. Szczepaniank and Oleksy[128] published their results of a liquid membrane sensor based on N(O,O-diisopropylthiophosphoryl) thiobenzamide. But, these sensors suffered interferences from Ag^{+} and Fe^{3+} ions. Lai and Shin[129] reported the use of 1,4-dithia-12-crown-4 as a neutral carrier in the fabrication of a PVC membrane sensor which gave a discrimination of both Ag^{+} and Fe^{3+} ions, but while Nernstian slopes were observed for $Hg(NO_3)_2$ solution, the use of a chloride salt led to nearly complete disappearance of an emf response. In the case of the sensor fabricated using the ionophore hexathiacyclooctadecane, which was reported by Masuda and Sekido[130], there was serious interferences from Fe^{3+}, Bi^{3+} and Pb^{2+}, the effect of Ag^{+} was not mentioned. The group of Brzózka[131,132]

reported the use of two *N,N'*-substituted 1,10-diaza-18-crown-6 ethers for the fabrication of a PVC membrane sensor which exhibited a high discrimination for most of the tested ions except Ag^+ ions. Srivastava *et al*[133] constructed a solid membrane sensor using polytungstoantimonate as the electroactive phase using which they were able to estimate the metal ions in polluted waters. The group of Siswanta[134,135] used non cyclic thioethers, sulphoxides and sulphone as ionophores. Their experiments revealed that sulphoxides and thioethers were better ionophores for the mercury sensor as they had a preference for Hg^{2+} to Ag^+ ions. The sensor fabricated using *N*-hydroxylamide derivatives gave a twice Nernstian response which could be attributed to the fact that they are charged Hg^{2+} ion carriers and that at an appropriate pH, a response mechanism could prevail or alternatively, they could be responding to monocation mercury acetate[136]. Gupta *et al*[137,138] explored the response characteristics of the PVC membrane sensors fabricated using pentathia-15-crown-5 and a diamine donor ligand while the group of Shamsipur[139,140] studied the responses of PVC membrane sensors based on hexathia-18-crown-6-tetraone and dibenzodiazathia-18-crown-6-dione. Yang and co-workers[141] reported the use of two ionophores, 7,16-dithenyl-1,4,10,13-tetraoxa-7,16-diazacyclooctadecane and 7,16-di-(2-methylquinolyl)-1,4,10,13-tetraoxa-7,16-diazacyclooctadecane, for the fabrication of PVC membrane mercury sensors. Jain *et al*[142] fabricated a PVC membrane sensor incorporating 1-(2-nitro-4-methyl phenyl)-6-methyl-6-methoxy-1,4,5,6-tetrahydro-pyrimidine-2-(3H)-thione as the electroactive ingredient which gave a sub Nernstian response to Hg^{2+} ions. Marco *et al*[143] reported the use of a chalcogenide glass ISE for the determination of ultra trace level of Hg^{2+} ions in saline media. Perez-Marin[144] and co-workers fabricated a PVC membrane sensor incorporating 1,3-diphenyl thiourea. The

construction, performance and application of coated wire sensors based on three carriers, 2-mercaptobenzimidazole, 2-mercaptobenzothiazole and hexathiacyclooctadecane, were reported by Mazloum *et al*[145] while the group of Hassan[146] explored the response behaviour of a PVC membrane sensor based on ethyl-2-benzoyl-2-phenylcarbamoyl acetate. A new tetrazolium-triiodomercurate modified carbon paste sensor was tested by Abbas and Mostafa[147] and it gave a near Nernstian response and was applied for the direct determination of Hg^{2+} ions in spiked waste water, metal amalgams and dental alloys. Mahajan *et al*[148,149] explored the use of a thiosemicarbazone and *p-tert*-butyl calix[4]crown with imine units as ionophores in the fabrication of two PVC membrane sensors for the determination of Hg^{2+} ions. Two PVC membrane sensors based on a mercapto compound and bis[5-((4-nitrophenyl)azo salicylaldehyde)] were reported by the group of Mashhaizadeh[150,151] which gave near Nernstian slopes for Hg^{2+} ions. Lu *et al*[152] reported the use of a calixarene derivative containing a thiazole azo group as the electroactive component in the fabrication of a mercury sensor. A peculiar twice Nernstian response was observed at pH 6.5 and a typical response at pH 4.0. Singh *et al*[153] reported a polystyrene-based membrane incorporating 2,3,4,9,10,11-dipyridine-3,10-diaza-1,5,8,12-tetrathiacyclotetradeca-2,9-diene as ionophore. Gismera *et al*[154] constructed a carbon paste sensor chemically modified with tetraethylthiuram disulphide with super Nernstian responses to Hg^{2+} as well as Cu^{2+} ions. Ye and co-workers[155] fabricated a sensor incorporating *N,N*-dimethylformamide-salicylacylhydrazone as neutral carrier. Khan and Inamuddin[156] reported the use of polyaniline Sn(IV) phosphate composite for the fabrication of a mercury sensor. However, most of the reported sensors suffer from one or

the other drawbacks like narrow working concentration range, high detection limit, high response time and poor selectivity.

1.6.5 Lead

Hirata and Higashiyama[157,37] reported a new lead sulphide-silver sulphide-copper(I) sulphide electrode, selenide and telluride electrodes for Pb^{2+} ions but they were susceptible to interference from Hg^{+}, Hg^{2+}, Ag^{+}, and Cu^{2+} ions. A liquid membrane sensor was reported by Linder *et al*[158] where *N,N*-dioctadecyl-*N',N'*-dipropyl-3,6-dioxaoctanediamide was used as the ionophore to detect PbX^{+} (X- OH^{-}, Cl^{-}, NO_3^{-}, $CH_3CO_2^{-}$). Vlasov and co-workers[159] reported the use of chalcogenide glass sensors based on PbS-Ag_2S-As_2S_3 for the online detection of Pb^{2+} in river water but there was deviation in response characteristics on continuous usage. The group of Gupta and Jain[160-165] reported a series of sensors for the determination of Pb^{2+} ions based on different ionophores- bismuth tungstate, 15-crown-5, 4-*t*-butyl calix[4]arene, 3,4,4a,5-tetrahydro-3-methyl pyrimido-[1,6-a] benzimidazole-1(2H) thione, tetrapyrazole and calix[4]arene receptors and *N,N'*-dibenzyl-1,4,10,13-tetraoxa-7,16-diazacyclooctadecane. Sheina *et al*[166] fabricated a PVC membrane sensor based on a Pb^{2+} chelate of N-benzoyl-N-phenyl hydroxamine, but the sensor showed interferences in the presence of Hg^{2+}, Cu^{2+} and Fe^{3+}. The group of Malinowska and Brzozka[167-171] fabricated lead sensors where a group of cyclic amides and oxamides, di and tetrathioamide functional calix[4]arene derivatives, calix[6]arene thiophosphorylated were tested as potential carriers. A change in the ion-selectivity was seen in the thioamide calix[4]arene derivative where the sensor showed a response to perchlorate ion in the absence of lipophilic salts but, on the addition of potassium tetrakis[3,5-bis(trifluoromethyl)-phenyl]

borate, the sensor gave a near Nernstian response to Pb^{2+} ions. Kamata and Onoyama[172] suggested the use of methylene bis(diisobutyl dithiocarbamate) as the ionophore for the fabrication of a lead sensor but this sensor showed serious interferences in the presence of Cu^{2+}, Fe^{3+}, and Zn^{2+} ions. They rationalized that the response characteristics of the sensor was attributed to the size of the 'C' cavity of the ionophore. Sheen and Shih[173] fabricated a lead sensor based on mono benzo-15-crown-5-phosphomolybdic acid and they observed a very good pH range of 3.0 – 9.0. Anuar and Hamdam[174] reported a near Nernstian response for the sensor fabricated using polyhydroxamic acid with silicone rubber as the supporting material while Attiyat *et al*[175] reported a silver wire coated sensor using benzo-18-crown-6 as ionophore. Bakker *et al*[176] compared the response of a Pb^{2+} ion selective electrode with a Pb^{2+} optode fabricated with the same solvent polymeric membrane phase. The group of Shamsipur[177-185] fabricated a large number of sensors for lead based on different ionophores – dibenzopyridino 18-crown-6, 9,10-anthraquinone derivatives, 5,5'-dithiobis-(2-nitrobenzoic acid), 4'-vinylbenzo-15-crown-5 homopolymer, bis(anthraquinone) sulphide derivatives, ethaneamine 2,2'-[1,2-ethylenebis(oxy)]*N,N'*-bis(2-thienylmethylene), 18-membered thia crown derivative, piroxicam, anthraquinone derivative. Yang *et al*[141,186] studied the response characteristics of sensors fabricated using the ionophores dithiophene diazacrown ether derivatives, 7,16-dithenoyl-1,4,10,13-tetraoxa-7,16-diazacyclooctadecane and 7,16-di-(2-thiopheneacetyl)-1,4,10,13-tetraoxa-7,16-diazacyclooctadecane. Cadogan and co-workers[187] reported near Nernstian slopes for lead sensors fabricated with calixarene phosphine oxide derivatives as ionophore. Abbaspour and Tavakol[188] presented a PVC membrane sensor based on benzyl disulphide as ionophore but only the

selectivity coefficients were calculated for some metal ions; no other parameters were studied. Xu and Katsu[189] reported near Nernstian values for the sensor fabricated with tetrabenzyl pyrophosphate as ionophore but the sensor using diphenyl phosphinic anhydride gave a non Nernstian response. Mousavi *et al*[190,191] developed PVC membrane sensors based on 1,10-dibenzyl-1,10-diaza-18-crown-6 and capric acid while the group of Zareh[192] studied the effect of the presence of 18-crown-6 on the response of 1-pyrrolidine dicarbodithioate based lead sensor and it was observed that the response of the sensor with the immobilized 18-crown-6 was Nernstian. The lead sensor based on a calixarene carboxyphenyl azo derivative as reported by Lu *et al*[193] showed good Nernstian responses but the selectivity studies done were poor as the method adopted was the separate solution method. Hassan *et al*[194] fabricated three new PVC plasticized membrane sensors based on three newly synthesized pyridine carboximide derivatives as neutral ionophores which displayed near Nernstian responses. The group of Ardakany and Ensafi[195-197] fabricated a highly selective lead (II) coated wire sensor based on a schiff base, a sol-gel and PVC membrane sensor based on bis(thiophenal)-4,4'-methylenedianiline and a PVC membrane sensor based on 1-phenyl-2-(2-quinolyl)-1,2-dioxo-2-(4-bromo) phenyl hydrazone. Bhat *et al*[198] fabricated a coated wire sensor based on 4-*tert*-butylcalix[6]arene which was effectively used for the direct determination of Pb^{2+} ions in real samples. The lead sensor reported by Agarwal *et al*[199] was based on a heterogeneous membrane of chelating inorganic ion exchange resin (α-nitroso-β-naphthol sorbed zirconium (IV) tungstophosphate) embedded in a PVC matrix and was used for the direct determination of Pb^{2+} ions in soil samples. Jeon *et al*[200] fabricated a PVC membrane sensor based on a schiff base complex of *N,N'*-bis(salicylidiene)2,6-pyridinediamine but Cu^{2+} ions was observed to be

an interferent. Carbon paste sensors modified with dithiodibenzoic and mercaptobenzoic acids were studied by Gismera *et al*[201] of which the dithiodibenzoic acid based CMCPE sensor exhibited a more sensitive and selective response to Pb^{2+} ions. However, most of the reported sensors have limitations in that they exhibit inferences to some common ions, work over a narrow concentration range and show non-Nernstian response, limited pH range and high response time.

1.7 Scope of the present investigation

The present investigation purports to fabricate sensors for the determination of the transition metal ions such as Mn^{2+}, Ni^{2+}, Cu^{2+}, $Hg^{2+}$and Pb^{2+} at trace levels. Three different types of sensor fabrication has been adopted viz. PVC membrane sensor, CPE-PVC membrane sensor and CMCPE type of sensor and fourteen sensors have fabricated.

For all these sensors, the principal analytical parameters have been studied, including the linear response range, calibration slope, detection limit, effect of pH and non aqueous media, shelf life and selectivity. The usefulness of developed sensors has also been studied. The developed sensors have been applied for the analysis of metal ions in real samples by direct potentiometry and as an indicator electrode in potentiometric titrations. It is hoped that all the fourteen sensors developed can be used for the determination of the respective metal ion with high accuracy and precision.

Chapter 2

MATERIALS AND METHODS

This chapter describes in detail the synthesis and the characterization of each ionophore. The general method of preparation of the different types of sensors is also discussed. It also deals with the preparations of solutions of metal salts, buffer solutions, effluent samples and other real samples taken for analysis along with the details of the instruments employed for the investigations.

2.1 Reagents

High molecular weight PVC, dibutyl sebacate (DBS), perchloric acid and all the metal salts were obtained from Merck, Germany and were used as received. The other plasticizers; dioctyl phthalate (DOP), dioctyl sebacate (DOS), dioctyl adipate (DOA), dimethyl sebacate (DMS), dibutyl phthalate (DBP); the aldehydes; 1-naphthaldehyde, thiophene-2-carboxaldehyde, 2-hydroxy-5-nitrobenzaldehyde and sodium tetraphenylborate (NaTPB) and 1,3-diaminopropane were obtained from Lancaster, UK and were used without any further purification. High purity graphite powder was purchased from Sigma Aldrich Corporation, USA. Salicylaldehyde, ethylene diamine, o-phenylene diamine, thiosemicarbazide, tributyl phosphate (TBP), paraffin oil(heavy) (PO), tetrahydrofuran (THF) and other solvents were all of AnalaR grade and were procured from local vendors.

2.2 Synthesis and characterization of the ionophores

All the ionophores are Schiff bases and were prepared by the condensation of an aldehyde with an amine to give the azomethine group (C=N). The general scheme of the reaction is depicted below.

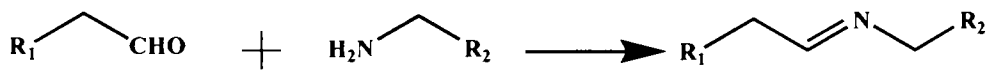

Aldehyde **Amine** **Schiff base**

They have been characterized by the elemental analysis and infrared spectroscopic methods and were found to be correct on comparison with the reported values.

2.2.1 N^1,N^2-bis(salicylidene) ethane-1,2-diamine (SED)

The schiff base, N^1,N^2-bis(salicylidene) ethane-1,2-diamine (SED), was synthesized by refluxing salicylaldehyde (0.02 mol, 2.44 g) and ethylenediamine (0.01 mol, 0.60 g) in 20 mL methanol for 1 h with stirring[202,203]. The yellow flakes that separated out was filtered, washed and recrystallized from dichloromethane. It was then dried in vacuo. The structure of the product was confirmed by analytical and spectrophotometric methods and is depicted in Chapter 3 as Figure 3.1.

CHN analysis –

Found (%) – C - 71.11, H - 6.09, N - 10.10

Cal (%) – C - 71.62, H - 6.01, N - 10.44

IR spectral details (KBr, cm^{-1}) -

3254(m), 1625(**C=N**, s), 1457(w), 1424(m), 1418(w), 1391(m), 1374(w), 1275(s), 1158(w), 1009(w), 950(m), 882(w), 840(w), 859(m), 738(s), 540(w), 464(w).

2.2.2 N^1,N^2-bis((thiophen-2-yl)methylene)ethane-1,2-diamine (TED)

The schiff base, N^1,N^2-bis((thiophen-2-yl)methylene)ethane-1,2-diamine (TED), was synthesized by refluxing thiophene-2-carboxaldehyde (0.02 mol, 2.24 g) and ethylenediamine (0.01 mol, 0.60 g) in 20 mL methanol as reported[204]. The precipitate was washed repeatedly with methanol, recrystalized from the same solvent and dried in vacuo. The structure of the yellowish brown product was confirmed by analytical and spectrophotometric methods[205]. The structure is depicted in Chapter 4 as Figure 4.1.

CHN analysis –

Found (%) – C - 58.91, H - 5.26, N - 11.10, S - 24.38

Cal (%) – C - 58.03, H - 4.87, N - 11.28, S - 25.82

IR spectral details (KBr, cm^{-1}) -

3101(m), 2847(w), 1830(w), 1628(**C=N**, s), 1427(w), 1324(m), 1282(m), 1213(m), 1189(m), 1128(w), 1019(w), 953(m), 915(m), 858(w), 840(w), 753(m), 712(s), 663(w), 518(w).

2.2.3 N^1,N^2-bis((naphthalen-1-yl)methylene) ethane-1,2-diamine (NED)

The ionophore, N^1,N^2-bis((naphthalen-1-yl)methylene) ethane-1,2-diamine (NED), was synthesized by refluxing 1-naphthaldehyde (0.02 mol, 3.12 g) and ethylenediamine (0.01 mol, 0.60 g) in 20 mL methanol for 2 h on a water bath. The white product obtained was filtered, washed and recrystallized from the same solvent[206]. Its structure was confirmed by the analytical and infrared spectral studies and is depicted in Chapter 4 as Figure 4.8.

CHN analysis –

Found (%) – C - 85.03, H - 5.49, N - 8.50

Cal (%) – C - 85.68, H - 5.99, N - 8.33

IR spectral details (KBr, cm^{-1}) -

3056(m), 2932(m), 1641(**C=N**, s), 1540(m), 1452(w), 1322(w), 1208(w), 1116(m), 976(w), 868(w), 753(w), 619(w), 521(w).

2.2.4 4-(2-hydroxybenzylideneamino)-N-(5-methyl-3-isoxazolyl) benzenesulphonamide (HIB)

The ionophore 4-(2-hydroxybenzylideneamino)-N-(5-methyl-3-isoxazolyl) benzenesulphonamide is a schiff base of 4-amino-N-(5-methyl-3-isoxazolyl) benzenesulphonamide (sulphamethoxazole) and salicylaldehyde. It was synthesized as reported elsewhere[207]: Sulphamethoxazole (0.01 mol, 2.54 g) and salicylaldehyde (0.01 mol, 1.22 g) in 100 mL methanol was refluxed for 6 h on a water bath. The orange-red product obtained was filtered, washed with methanol and chloroform and recrystallized from

methanol. The structure of HIB which is depicted as Figure 5.1 in Chapter 5 was confirmed by analytical and spectral methods.

CHN analysis –

Found (%) – C - 57.02, H - 4.25, N - 11.78, S - 8.90

Cal (%) – C - 57.13, H - 4.23, N - 11.76, S - 8.97

IR spectral details (KBr, cm^{-1}) -

3378(w), 3068(w), 2990(w), 1616(**C=N**, s), 1570(s), 1473(s), 1404(m), 1366(m), 1278(m), 1164(s), 1091(m), 1035(w), 909(m), 845(w), 748(m), 620(m), 569(s), 547(m).

2.2.5 N^1,N^2-bis(2-hydroxy-5-nitro benzylidene) propane-1,3-diamine (HPD)

The ionophore N^1,N^2-bis(2-hydroxy-5-nitro benzylidene) propane-1,3-diamine (HPD) was prepared by adding slowly a solution of 2-hydroxy-5-nitrobenzaldehyde (0.002 mol, 0.334 g in 30 mL methanol) to a solution of 1,3-diaminopropane (0.001 mol, 0.074 g in 30 mL methanol). The mixture was stirred and refluxed for 2 h on a rotamantle. The shiny yellow precipitate formed was filtered, washed, recrystallized from the same solvent and stored in vacuum. The structure of the HPD was confirmed by elemental analysis and infrared spectropscopy[208]. It is shown as Figure 5.8 in Chapter 5.

CHN analysis –

Found (%) – C - 54.90, H - 4.23, N - 14.92

Cal (%) – C - 54.84, H - 4.33, N - 15.05

IR spectral details (KBr, cm^{-1}) -

3642(w), 3325(s), 2388(m), 1610(**C=N**, s), 1537(m), 1445(m), 1325(s), 1237(m), 1207(w), 1087(w), 937(m), 896(s), 826(m), 756(w), 725(w), 622(w), 478(m).

2.2.6 1-(2-hydroxy-5-nitrobenzylidene) thiosemicarbazide (HTS)

The ionophore 1-(2-hydroxy-5-nitrobenzylidene) thiosemicarbazide (HTS) was synthesized by adding 2-hydroxy-5-nitrobenzaldehyde (0.02 mol, 3.34 g in 25 mL ethanol) to thiosemicarbazide (0.02 mol, 1.82 g in 25 mL hot distilled water). The mixture was refluxed for 6 h and the yellow precipitate filtered off, dried in vacuo and recrystallized from ethanol. The structure of HTS was confirmed by the analytical and spectroscopic methods[209]. The structure is depicted in Chapter 6 as Figure 6.1.

CHN analysis –

Found (%) – C - 39.89, H - 3.52, N - 23.94, S - 12.93

Cal (%) – C - 40.00, H - 3.36, N - 23.32, S - 13.35

IR spectral details (KBr, cm^{-1}) -

3422(s), 3321(m), 2992(s), 1607(**C=N**, s), 1541(w), 1513(w), 1432(m), 1337(w), 1101(m), 943(m), 849(m), 555(w).

2.2.7 N^1,N^2-bis(2-hydroxy-5-nitro benzylidene) benzene-1,2-diamine (HBD)

The synthesis of the ionophore N^1,N^2-bis(2-hydroxy-5-nitro benzylidene) benzene-1,2-diamine (HBD) was achieved by refluxing 2-

hydroxy-5-nitrobenzaldehyde (0.01 mol, 1.67 g) and o-phenylene diamine (0.005 mol, 0.54 g) in a 75 mL methanolic medium. The yellow precipitate formed was filtered, washed repeatedly, recrystallized from the same solvent and dried in vacuo[210]. The ionophore HBD was characterized by elemental analysis and FTIR spectroscopy and the structure is depicted in Chapter 7 as Figure 7.1.

CHN analysis –

Found (%) – C - 59.43, H - 3.02, N - 13.91.

Cal (%) – C - 59.12, H - 3.47, N - 13.79.

IR spectral details (KBr, cm^{-1}) –

3663(m), 3641(m), 3621(m), 3301(m), 2357(w), 1620(**C=N**, s), 1587(m), 1483(w), 1342(s), 1299(w), 1216(w), 1128(w), 1096(m), 984(w), 942(w), 901(w), 829(m), 795(w), 747(m), 638(w), 535(w), 499(w).

2.3 Preparation of the metal salt solution

The stock solution (1.0×10^{-1} M) of the metal salt was prepared by dissolving the appropriate amount of metal salt in a titrimetric flask and the solution was quantitatively diluted using distilled water. All the other solutions of different concentrations were made by serial dilution of the 1.0×10^{-1} M stock solutions.

2.3.1 Manganese chloride stock solution

4.9477 g of manganese chloride tetrahydrate was weighed accurately, transferred to a 250 mL titrimetric flask and was diluted to the mark with

distilled water. The stock solution was standardised by EDTA titration method[2].

2.3.2 Nickel(II) nitrate stock solution

7.2698 g of nickel nitrate hexahydrate was weighed accurately, transferred to a 250 mL titrimetric flask and was diluted to the mark with distilled water. The stock solution was standardised by EDTA titration method[2].

2.3.3 Copper(II) nitrate stock solution

6.04 g of cupric nitrate trihydrate was weighed accurately and transferred to a 250 mL titrimetric flask. The salt was dissolved in distilled water and made up to the mark. The stock solution was standardised by iodometric method[2].

2.3.4 Mercury(II) nitrate stock solution

8.5655 g of mercuric nitrate monohydrate was weighed accurately and transferred to a 250 mL titrimetric flask. Add 5 mL HNO_3 (2 M) and dissolve the salt with distilled water followed by dilution to the mark. The solution was standardised by titrating with a standard thiocyanate solution using iron(III) indicator solution[2].

2.3.5 Lead(II) nitrate stock solution

As the compound is a primary standard, further standardization was not carried out. 8.2803 g of lead nitrate was weighed accurately, transferred

into a 250 mL titrimetric flask and dissolved in distilled water. 5 mL of HNO3 (2 M) was added and the diluted to the mark.

2.4 Preparation of buffer solutions

Buffers were used to maintain the pH of the test solutions and also during the EDTA titrations. They were freshly prepared according to the Robinson Table[211].

2.4.1 pH 3.0

To 100 mL 0.1 M potassium hydrogen phthalate solution, 44.6 mL of 0.1 M HCl solution was added to give the buffer having pH 3.0.

2.4.2 pH 5.0

To 100 mL 0.1 M potassium hydrogen phthalate solution, 45.2 mL of 0.1 M NaOH solution was added to give the buffer having pH 5.0.

2.4.3 pH 6.0

To 100 mL 0.1 M potassium dihydrogen phosphate, 11.2 mL of 0.1 M NaOH solution was added to give the buffer having pH 6.0.

2.5 Preparation of the real samples

The analytical applicability of the developed sensors was tested for the determination of the metal ions in real samples.

2.5.1 Chocolate samples

Ten grams of chocolate sample was heated in a silica crucible at 400°C on an electric bunsen burner till ash is obtained. The residue was dissolved in 2 mL conc HNO_3 and again heated at 350°C for 2 h; the process was repeated till no traces of carbon are left. The final residue was treated with 0.5 mL conc HCl and 1-2 mL 70% perchloric acid and then evaporated to fumes. The solid residue was dissolved in water, filtered and then transferred quantitatively to a 100 mL titrimetric flask. The pH was adjusted to 5.0 by adding 10 mL buffer solution and then the solution was quantitatively diluted.

2.5.2 Edible oil sample

Ten grams of the hydrogenated edible oil (Dalda) was heated at 500°C for 1 h. The residue was completely dissolved in 5 mL of 0.1 M HNO_3. The solution was then transferred into a 100 mL titrimetric flask; the pH was adjusted to 5.0 by adding 10 mL buffer solution and then the solution was quantitatively diluted.

2.5.3 Effluent sample solutions (pond water, electroplating wastes, Eveready battery waste)

A small volume (5-10 ml) of the effluent sample (pond water and electroplating waste) was taken in a 100 mL titrimetric flask; the pH was adjusted to 5.0 by adding 10 mL buffer solution and then the solution was quantitatively diluted.

The Eveready battery waste sample was initially treated with a few drops of conc. nitric acid, dissolved in distilled water, filtered and then the solution

was transferred into a 100 mL titrimetric flask. The pH was adjusted to 5.0 by adding 10 mL buffer solution and then the solution was quantitatively diluted.

2.5.4 Manganese sample solutions (for standard addition)

Two different concentrations, 30 ppm (0.10807 g of $MnCl_2.4H_2O$ in 1 L) and 60 ppm (0.21614 g of $MnCl_2.4H_2O$ in 1 L) of Mn^{2+} solutions were prepared by dissolving the accurately weighed amount of salt in distilled water in 1 L titrimetric flask. The pH was adjusted to 6.0 by adding 20 mL buffer solution and then the solution was quantitatively diluted.

2.5.5 Mercury sample solutions (for standard addition)

Two different concentrations, 50 ppm (0.0854 g of $Hg(NO_3)_2.H_2O$ in 1 L) and 100 ppm (0.17081 g of $Hg(NO_3)_2.H_2O$ in 1 L) of Mn^{2+} solutions were prepared by dissolving the accurately weighed amount of salt in distilled water in 1 L titrimetric flask. The pH was adjusted to 3.0 by adding 20 mL buffer solution and then the solution was quantitatively diluted.

2.6 Sensor membrane preparation

The most important component in a sensor is the electroactive ingredient or ionophore, which is responsible for the ion recognition. There are three different types of sensors that have been studied.

2.6.1 PVC plasticized membrane sensor

This is a liquid membrane sensor and involves immobilization of the ionophore into poly(vinyl chloride) to produce a thin polymer film.

Ionophore, PVC and plasticizer were taken in percentage-weight ratios of approximately 1-7:30-33:60-69 (ionophore:PVC:plasticizer). In the case of metal ion sensors, ionic additives or anionic excluders (sodium tetraphenylborate) are added to prevent the interference from the sample anions. Its % w/w varies from 2%-5%. All the components were taken in the specified ratio and dissolved in THF. The solution was poured into glass rings struck onto a glass plate. Small disc shaped membranes were cut out and glued to one end of a hollow Pyrex glass tube using Araldite. The Pyrex glass tube was filled with the metal salt solution (internal solution) and the membrane was conditioned by dipping it in a 1.0×10^{-1} M metal salt solution.

2.6.2 CPE-PVC plasticized membrane sensor

This is a solid membrane type of sensor and requires no internal filling solution. The carbon paste was prepared by making a paste of high purity graphite and heavy paraffin oil and it was rubbed onto the open end of a capillary glass tube of 2 mm diameter. A stainless steel rod was inserted for electrical contact. The working surface of the electrode was polished with fine alumina slurries on a polishing cloth, sonicated in distilled water and dried in air. The PVC membrane solution preparation is the same as detailed before in the PVC membrane sensor. A mixture of PVC, plasticizer and membrane additive (% w/w) was dissolved in about 5-7 mL of THF. To this mixture the ionophore was added and mixed well. The polished sensor was coated by dipping into the membrane solution in THF and the solvent was evaporated. This process was repeated till a thin film was formed on the

surface and it was allowed to set overnight. The sensor was conditioned by dipping it in a 1.0×10^{-1} M metal salt solution.

2.6.3 Chemically modified carbon paste sensor (Graphite method)

This is also known as chemically modified carbon paste electrode (CMCPE). Graphite and the ionophore (referred to as modifier) (in varying % w/w ratios) were mixed thoroughly using a motor and pestle to give a homogeneous mixture. To this, acetone was added and this mixture was left overnight for the acetone to evaporate completely. It was made a paste by using tributyl phosphate or heavy paraffin oil. This paste was then packed into the open end of a glass capillary tube of 2 mm diameter and a stainless steel rod was inserted into the capillary tube for electrical contact. Appropriate packing and a smooth surface was achieved by pressing the surface of the sensor against a filter paper. The sensor was conditioned soaking in a 1.0×10^{-1} M solution of metal salt solution.

2.7 Potential measurement and calibration

All measurements were performed at ambient temperature (25±1°C) on a digital ion meter. An Ag | AgCl (silver-silver chloride) or Hg | Hg_2Cl_2, KCl (sat.) (calomel) reference electrode was used in conjunction with the developed sensor. The cell assembly for potentiometric measurements can be represented as follows:

For PVC plasticized membrane sensor -

Internal reference electrode | metal salt solution 0.1 M (internal solution) | membrane | test solution | external reference electrode

For CPE-PVC plasticized membrane sensor and Chemically modified carbon paste sensor (solid membrane type)

Reference electrode | test solution | CPE-PVC or CMCPE

The performance of the developed sensor was investigated by measuring the potential in the metal ion solutions prepared in the concentration range $1.0 \times 10^{-1} - 1.0 \times 10^{-8}$ M. The solutions were stirred and the stable potential reading was taken.

2.8 Instruments used

The CHN analysis were done on a CHN analyzer, Elementar Vario EL III and the FTIR spectra were recorded on Thermo Nicolet Avatar 370 spectrometer using KBr pellets in the range 4000 – 400 cm^{-1} at Sophisticated Test and Instrumentation Centre (STIC), Kochi.

All potentiometric experiments were carried out on a Systronics digital ion meter or Toshniwal digital ion meter and some parameters like response time was studied on BAS Epsilon electrochemical workstation.

The standard method used for the determination of metal content in real samples was the ICP-AES technique and the instrument used was Thermo Electron IRIS INTREPID II XSP DUO spectrometer.

Chapter 3

SENSORS FOR MANGANESE

This chapter details the response characteristics of two types of sensors based on a Schiff base ionophore for the determination of manganese ions. The sensors fabricated were CPE-PVC and CMCPE type of sensors. The sensors worked well over a wide concentration range of $1.0 \times 10^{-1} - 1.0 \times 10^{-6}$ *M with a fast response time. The application of the sensors as an indicator electrode in the potentiometric titration of* Mn^{2+} *against EDTA and in the determination of manganese ions in water samples by the standard addition method have also been discussed.*

Manganese is a grey white metal resembling iron. Manganese is mainly used in the making of alloys, low-cost stainless steel, dry cells and as pigments in the paint industry. Potassium permanganate is used in medicine as a disinfectant and is also a potent oxidizing agent.

Though it is an essential trace nutrient in all forms of life, in excess it is toxic. A form of Parkinson's disease-type neurodegeneration called "Manganism" has been linked to high exposure to manganese dusts and fumes. Manganese can affect the flavour and colour of food and water, and can also react with tannins present in beverages to form a black sludge sffecting both the taste and appearance. The EPA recommends 0.05 mg/l as the maximum allowable manganese concentration in drinking water[212]. The

common methods adopted for manganese analysis are titrimetry, gravimetry, atomic emission spectroscopy (AES) etc. But these methods are not convenient for analysis as they generally require sample pre-treatment and also infrastructure backup[2].

Only a few reports on manganese sensors are found in literature[36-43], and most of the reported sensors have one or the other drawbacks like long response time, narrow working concentration range, poor selectivity etc. This chapter presents the fabrication of two types of sensors incorporating a Schiff base as ionophore for the determination of Mn^{2+} ions.

3.1 Ionophore

The synthesis and characterization of the ionophore, N^1,N^2-bis(salicylidene) ethane-1,2-diamine (SED) has been discussed under Section 2.2.1 in Chapter 2.

3.2 Sensors based on SED

This ionophore SED has been used to fabricate two types of sensors; the CPE-PVC and the CMCPE type. The structure of SED is shown as Figure 3.1.

Figure 3.2 and Figure 3.3 depict the potential response of the two types of sensors towards different cations. It was found that both the sensors showed a Nernstian response to manganese ion which may be attributed to the selective complexation behaviour of the ionophore to Mn^{2+} over other metal ions, as well as the rapid ion exchange kinetics of the resulting complex at the membrane-sample interface.

3.2.1 Sensor membrane fabrication

The general method of fabrication of CPE-PVC type and CMCPE type of sensors has been discussed under Section 2.6 in Chapter 2.

The CPE-PVC type sensor involved the preparation of the CPE sensor and then the PVC membrane solution. Graphite was made a paste using paraffin oil, filled into the capillary glass tube and then polished. The best performance was obtained by using dioctyl phthalate (DOP) as the plasticizing agent and sodium tetraphenylborate (NaTPB) as anionic additive. The composition ratio for the membrane that gave the best response in terms of slope, concentration range and response time for CPE-PVC type of sensor was found to be 33:60:2:5 (PVC:DOP:NaTPB:SED) (% w/w). The polished sensor filled with the graphite paste was dipped in to the optimized PVC membrane solution repeatedly till a thin film was formed on the working surface of the sensor.

In the case of CMCPE type of sensor, the ionophore and graphite were made a paste using paraffin oil. The paste so obtained was filled into the capillary glass tube as explained in Chapter 2. The best composition ratio for CMCPE type of sensor was found to be 90:10 (graphite:SED).

The sensors were conditioned by dipping it in a 1.0×10^{-1} M manganese(II) chloride solution. The equilibration time was 2 days in the case of CPE-PVC sensor and 10 h for CMCPE type of sensor.

3.2.2 Potential measurement and calibration

Potentials were measured at 25±0.1 °C on a Systronics digital ion meter and on BAS Epsilon electrochemical workstation. An Ag | AgCl reference electrode was used in conjunction with the developed Mn^{2+} sensor.

The cell assembly for potentiometric measurements for the two types of sensors can be represented as follows:

Ag | AgCl (3.0 M KCl) | test solution | CPE-PVC based on SED or CMCPE based on SED

The performance of the developed sensor was investigated by measuring the potential in Mn^{2+} solutions (pH maintained at 6.0 by adding buffer) prepared in the concentration range $1.0 \times 10^{-1} - 1.0 \times 10^{-6}$ M. The solutions were stirred and the stable potential reading was taken.

3.2.3 Optimization of membrane composition

The optimization of the membrane composition of PVC membrane solution for CPE-PVC type sensor is important as the amount of ionophore, nature of the membrane solvent (plasticizer), plasticizer/PVC ratio and nature of the additives used, in one way or other, influences sensitivity and selectivity of the sensors. A set of ten sensors based CPE-PVC has been fabricated with different composition ratios of membrane ingredients as presented in Table 3.1. Initially the effect of a sensor, Sa_1, with no membrane coated on it was studied and this sensor showed no response to Mn^{2+} ions. The sensor fabricated without any plasticizer, Sa_2 gave a sub Nernstian slope and on the addition of the plasticizing agent, DOP, the response of the sensor improved. The sebacates and adipate gave sub Nernstian response. The amount of the ionophore was also found to affect the sensitivity of the sensors. 5% was found to be the optimum amount of ionophore and further addition of ionophore content resulted in a diminished response from the sensors which may be due to the saturation of the membrane. The presence

of lipophilic negatively charged additives (anionic excluders) improves the potentiometric behaviour of the PVC membrane by reducing the ohmic resistance and improving the response, selectivity as well as sensitivity[213-226]. The anionic excluder added was NaTPB and the optimum amount was found to be 2%. The CPE-PVC type sensor, Sa_4, with the composition ratio 33:60:2:5 (PVC:DOP:NaTPB:SED) (% w/w) was found to give the best response characteristics. Hence this sensor (Sa_4) was used for further studies.

A set of six CMCPE type sensors were fabricated with varying compositions of ionophore to graphite ratio and the results are consolidated in Table 3.2. It was observed that the sensor Sb_1 containing zero percentage of the modifier showed negligible response. However, increasing the amount of modifier up to 10% (Sb_3) had led to a sharp increase in the sensor response. On increasing the ionophore content from 10% to 50% led to an irregular pattern of the slope which could probably be due to the decrease in conductance of the sensor material. Thus the sensor Sb_3 with the composition ratio of 90:10 (graphite:ionophore) was used for further studies.

3.2.4 Working concentration range and slope

The calibration graph which is the plot of the EMF versus pMn^{2+} for the sensors Sa_4 and Sb_3 are shown as Figure 3.4 and Figure 3.5 where Sa_4 and Sb_3 denote CPE-PVC type and CMCPE type of sensors respectively. The working concentration range for both the sensors Sa_4 and Sb_3 was found to be $1.0 \times 10^{-1} - 5.0 \times 10^{-6}$ M. The slope calculated from the calibration graph was found to be 30.1 (±0.5) mV $decade^{-1}$ and 29.8 (±0.4) mV $decade^{-1}$ for the sensors Sa_4 and Sb_3 respectively. The detection limit was calculated from the graph by the intersection of the two extrapolated linear segments of

the calibration plot and was found to be 2.7×10^{-6} M and 3.8×10^{-6} M for the sensors Sa_4 and Sb_3 respectively.

3.2.5 Response time

The plot of the changes in EMF from the moment of addition of 1.0×10^{-5} M Mn^{2+} solution with respect to time for the sensors Sa_4 and Sb_3 are shown in Figure 3.6 and Figure 3.7 respectively. The practical response time for the sensors Sa_4 and Sb_3 was obtained from the plot and was found to be 20 s and 30 s respectively. The practical reversibility of the sensors Sa_4 and Sb_3 were evaluated by taking measurements for Mn^{2+} solutions with a 10-fold difference in concentration in the sequence high-to-low concentration and vice versa. The EMF versus time traces for the sensors Sa_4 and Sb_3 are shown as Figure 3.8 and Figure 3.9 respectively. The potentials remained constant for about 3 min in the case of Sa_4 sensor and 2 min for the Sb_3 sensor. The sensing behaviour of the membrane remained unchanged when potentials were recorded either from low to high concentrations or vice versa.

3.2.6 Effect of pH and non aqueous media

The pH dependence on the EMF response of the sensors Sa_4 and Sb_3 was tested for two fixed concentrations, 1.0×10^{-3} M and 1.0×10^{-4} M, over a pH range of 2.0-9.2. The pH was adjusted by introducing small drops of nitric acid (1.0 M) or sodium hydroxide (1.0 M). The results for the sensors Sa_4 and Sb_3 are shown in Figure 3.10, and Figure 3.11. It was found that the potential remained constant over a pH range of 3.0-7.0 and 3.6-6.2 for the sensors Sa_4 and Sb_3 respectively. The observed drift in potentials at higher pH may be due to the formation of some hydroxyl complexes of Mn^{2+} ion in

solution and at lower pH, the drift in potential may be because of the interference from H^+ ions.

The functioning of the sensors Sa_4 and Sb_3 was also investigated in partially non-aqueous media using methanol-water and ethanol-water mixtures. The results obtained are consolidated in Table 3.3 and it was seen that no significant change occurs in the slope for the sensors up to 25% of non-aqueous content in the case of CPE-PVC type sensor Sa_4 and 20% for the case of CMCPE-PVC type sensor Sb_3. Above the tolerance level of the sensors Sa_4 and Sb_3, the slopes gets affected which may be attributed to leaching of the ligand into the sample solution.

3.2.7 Potentiometric selectivity

The potentiometric selectivity coefficients of the sensors Sa_4 and Sb_3 towards different cations were determined by the fixed interference method[227,35]. The selectivity coefficients were determined at 1.0×10^{-2} M concentration of foreign ions and was calculated using the following equation.

$$K_{A,B}^{pot} = a_A / (a_B)^{z_A / z_B}$$

The selectivity coefficient values are consolidated in Table 3.4. The sensors Sa_4 and Sb_3 show good selectivity for Mn^{2+} ions in the presence of Na^+, K^+, NH_4^+, Mg^{2+}, Ca^{2+}, Ba^{2+} and Co^{2+}. The ions Ag^+, Pb^{2+}, Zn^{2+}, Cd^{2+} and Fe^{3+} do not interfere significantly in the functioning of the sensors. However, Cu^{2+}, Ni^{2+} and to a lesser extent Hg^{2+} may cause interference at high concentrations.

3.2.8 Lifetime or Shelf life

The potential measurements were recorded everyday over a period of time to determine the shelf life of the sensors. The operative life time for the sensors Sa_4 and Sb_3 was found to be 3 months and 4 weeks respectively. The sensors were all kept immersed in 1.0×10^{-1} M manganese(II) solution when not in use. The surface of CMCPE type sensor could be renewed by squeezing out a small amount of the paste, scrapping off the excess, polishing the new surface against a filter paper and equilibrating the sensor in the metal salt solution for 10 h.

3.2.9 Analytical applications

The utility of the sensors Sa_4 and Sb_3 was further investigated in the determination of manganese(II) in different water samples containing added Mn^{2+} ions. The preparation of the two different concentrations for each sample has been discussed under Section 2.5.4 in Chapter 2. The results presented in Table 3.5 show that the results of the determinations of manganese(II) from different water samples is quantitative.

The sensors Sa_4 and Sb_3 have been successfully applied as an indicator electrode in conjuction with Ag|AgCl in the potentiometric titration of manganese(II) chloride solution at pH 6.0. The titration curves for the sensors Sa_4 and Sb_3 are depicted in Figure 3.12 and Figure 3.13 respectively. The titration plots obtained were not the standard sigmoid shape but the plots show a sharp break point that corresponds to 1:1 stoichiometry of Mn-EDTA complex. This break point is taken as the end point of the titration.

3.3 A comparative study among the sensors Sa_4 and Sb_3 and to some of the reported sensors

The two sensors Sa_4 and Sb_3 are found to have very good response characteristics. Table 3.6 consolidates the response characteristics of the sensors Sa_4 and Sb_3. Between the two sensors, Sa_4 and Sb_3, Sa_4 is slightly better in terms detection limit, response time, working pH range, tolerance to non aqueous content and shelf life. But though the shelf life of the sensor Sb_3 is only 4 weeks, the surface could be renewed by cutting off a little of the paste, polishing it on a smooth surface and reconditioning it on 1.0×10^{-1} M of manganese(II) chloride solution. Table 3.7 presents the comparative study of the characteristics of the developed sensors with some of the reported sensors for Mn^{2+}. It can be seen that the developed sensors (Sa_4 and Sb_3) are superior in terms of working concentration range[37,39,43], slope[37,39,40], life time[37,39,40] and pH range[37,39].

Figures

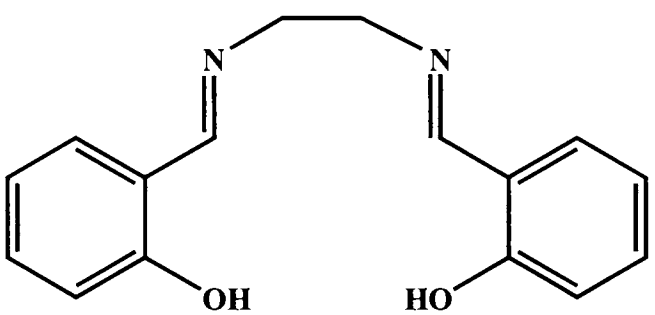

Figure 3.1 – Structure of the ionophore SED

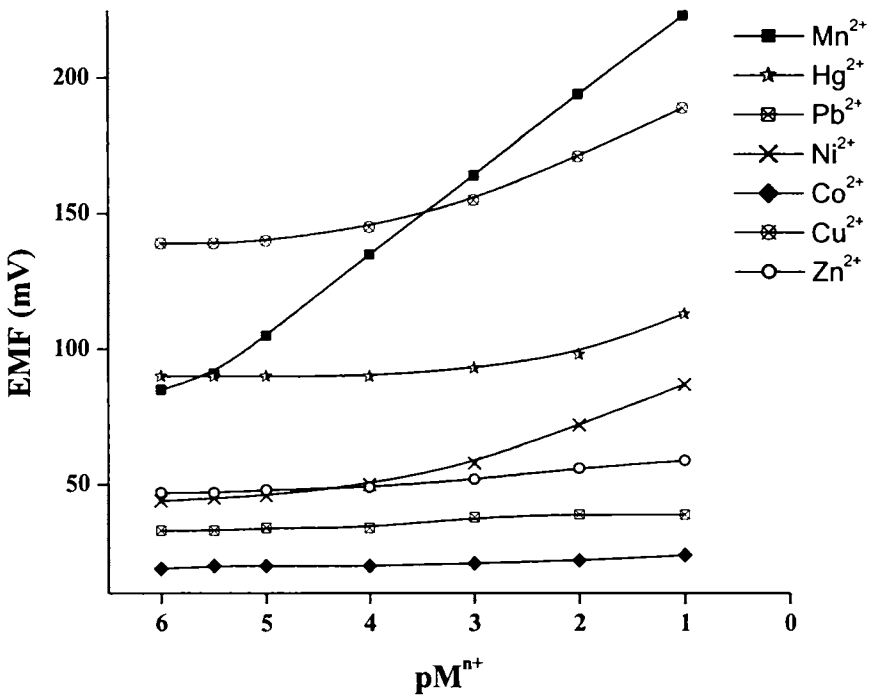

Figure 3.2 - Potential response of the various CPE type sensors based on SED.

Conditions: membrane composition ratio 33% PVC:60% DOP:2% NaTPB:5% SED; conditioned in 1.0×10^{-1} M of the corresponding cation solution for 2 days

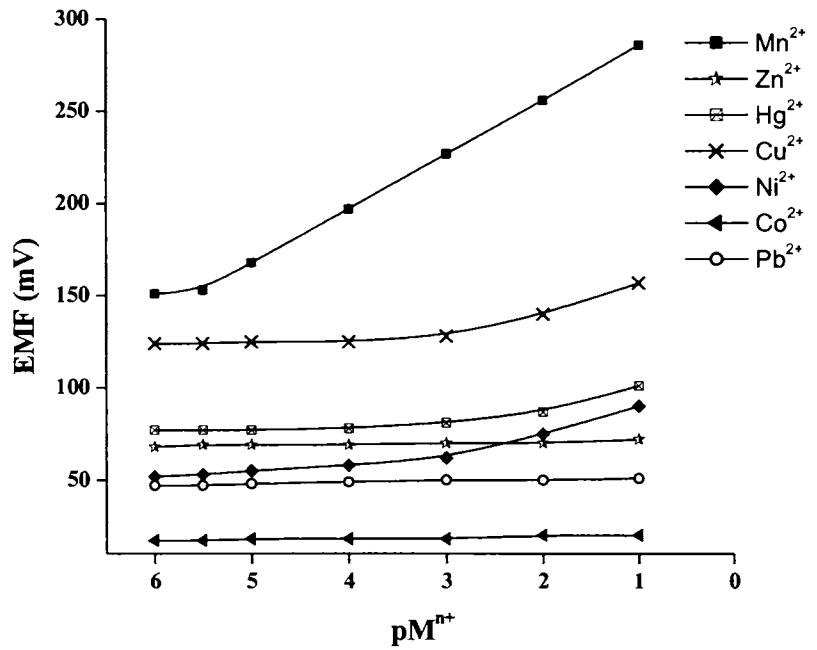

Figure 3.3 - Potential response of the various CMCPE type sensors based on SED.

Conditions: composition ratio 10% SED:90% graphite; conditioned in 1.0×10^{-1} M of the corresponding cation solution for 10 h

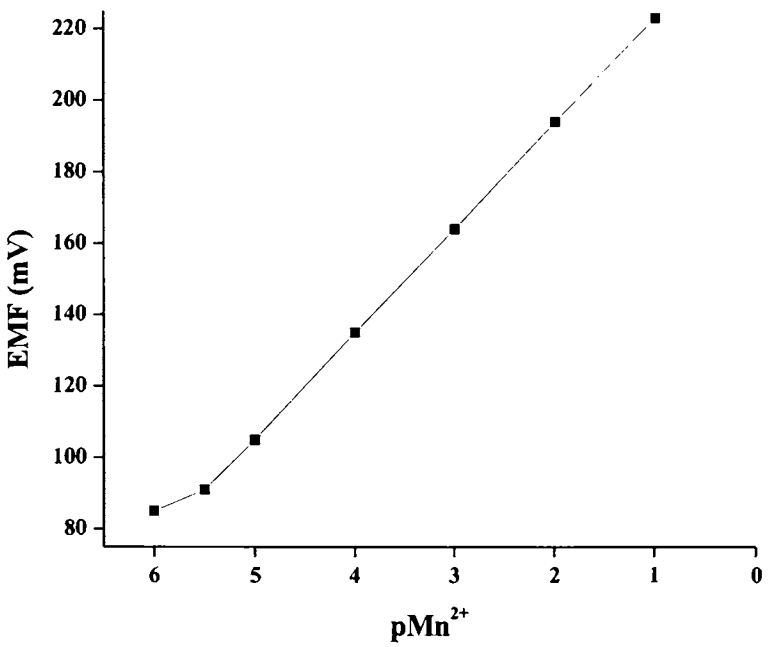

Figure 3.4 – Calibration graph of the CPE type sensor Sa_4 based on SED

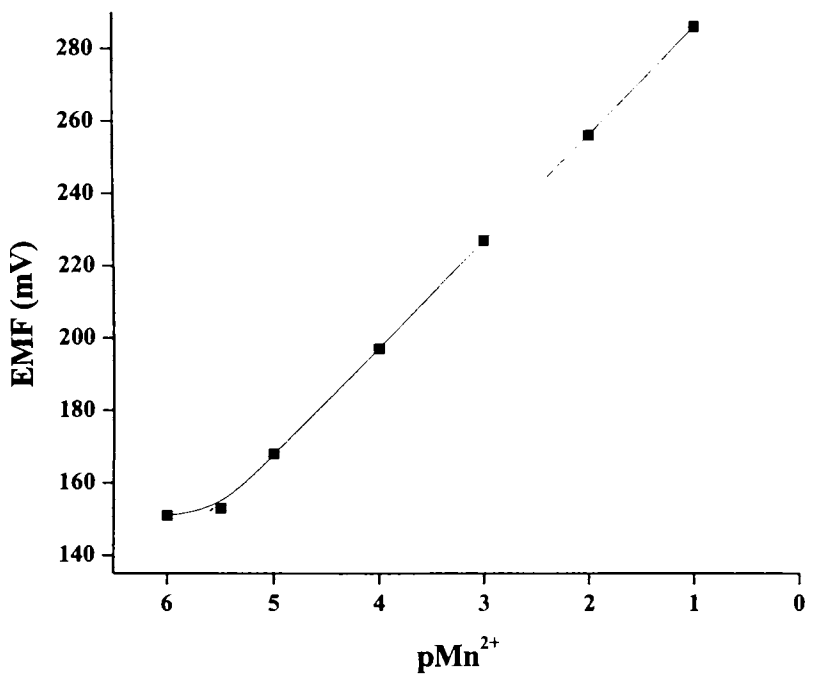

Figure 3.5 – Calibration graph of the CMCPE type sensor Sb_3 based on SED

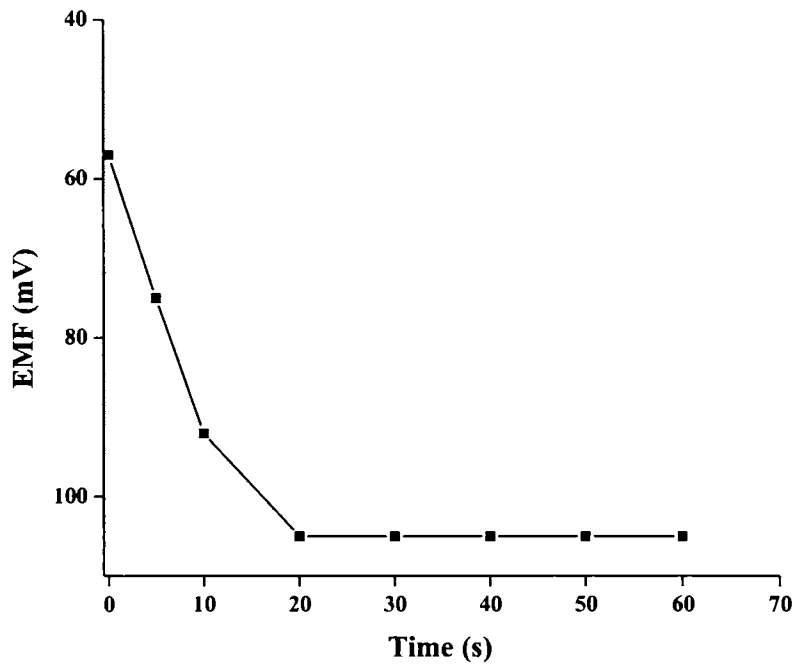

Figure 3.6 – Practical response time of the CPE type sensor Sa_4 based on SED from the moment of addition of Mn^{2+} (1.0×10^{-5} M) solution

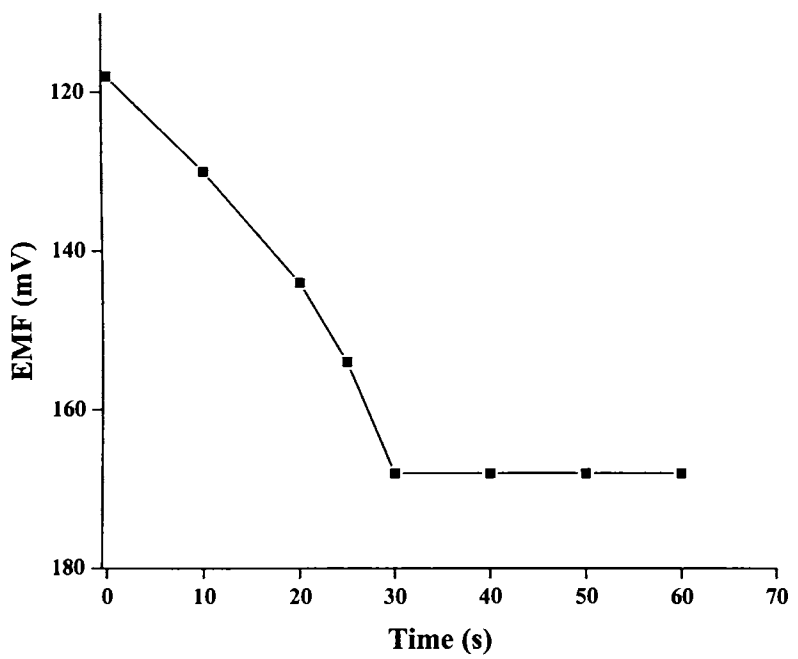

Figure 3.7 – Practical response time of the CMCPE type sensor Sb_3 based on SED from the moment of addition of Mn^{2+} (1.0×10^{-5} M) solution

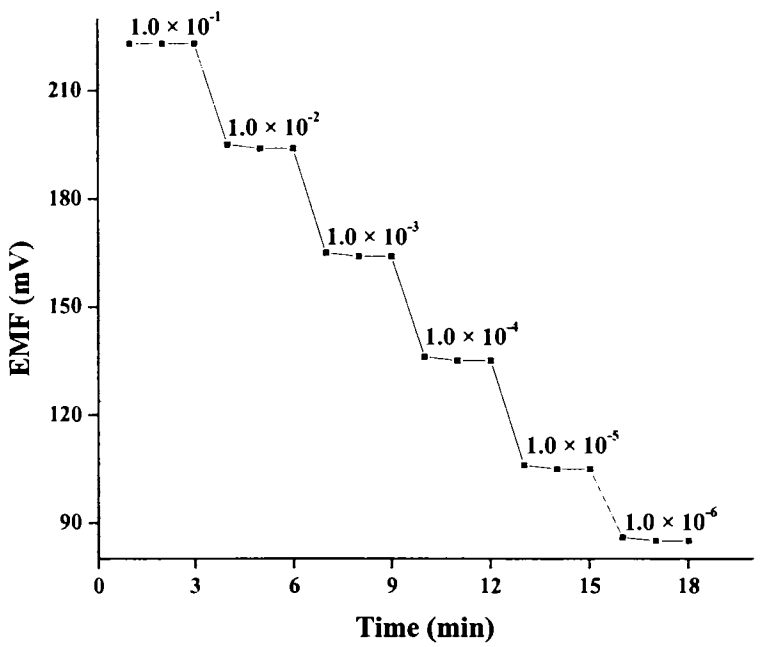

Figure 3.8 - Dynamic response time of the CPE type sensor Sa_4 based on SED for reversibility with step changes in concentration of Mn^{2+} (1.0×10^{-6} to 1.0×10^{-1} M)

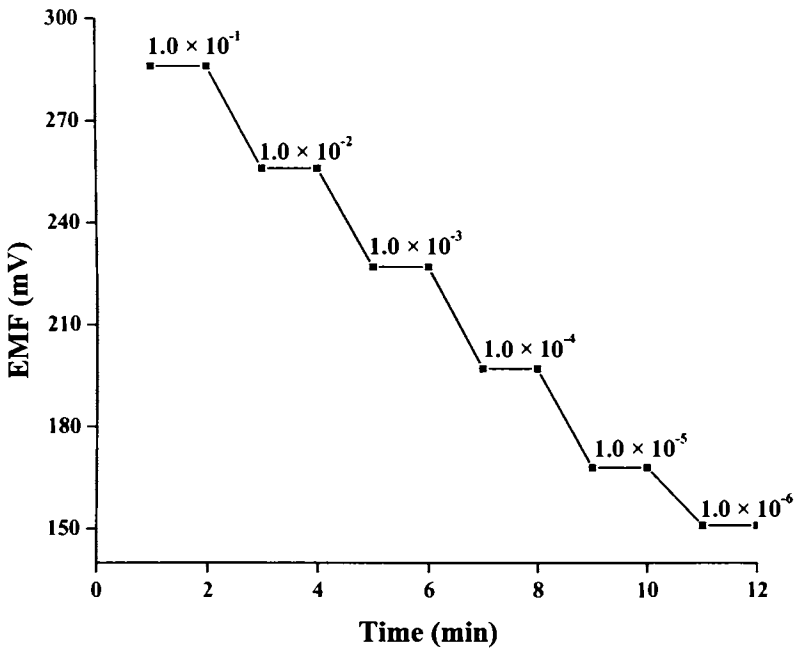

Figure 3.9 - Dynamic response time of the CMCPE type sensor Sb_3 based on SED for reversibility with step changes in concentration of Mn^{2+} (1.0×10^{-6} to 1.0×10^{-1} M)

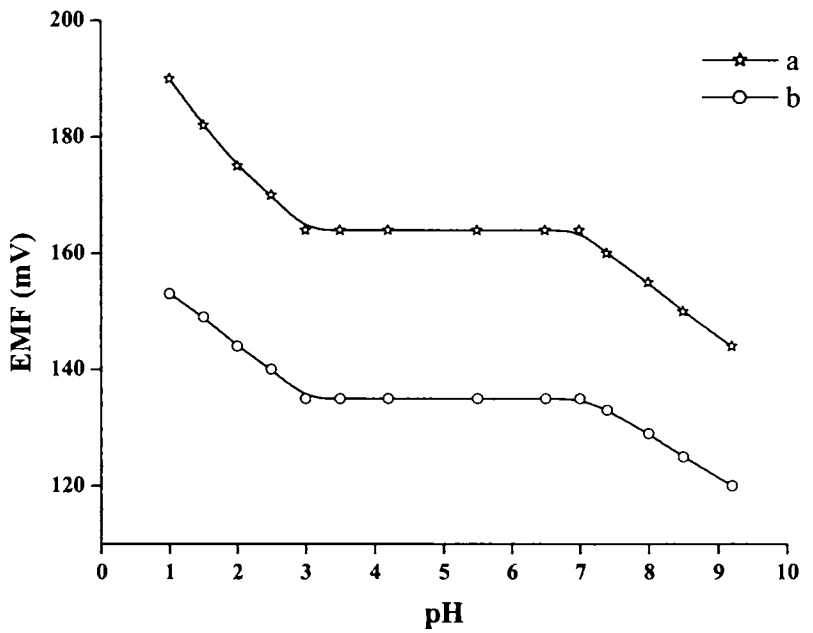

Figure 3.10 – Effect of pH on the cell potential of the CPE type sensor Sa_4 based on SED at 1.0×10^{-3} M (a) and 1.0×10^{-4} M (b)

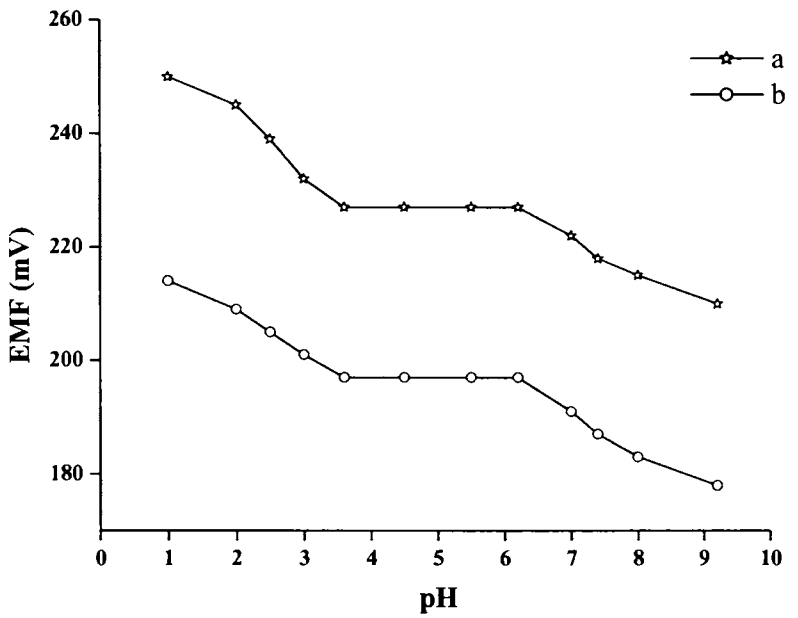

Figure 3.11 – Effect of pH on the cell potential of the CMCPE type sensor Sb_3 based on SED at 1.0×10^{-3} M (a) and 1.0×10^{-4} M (b)

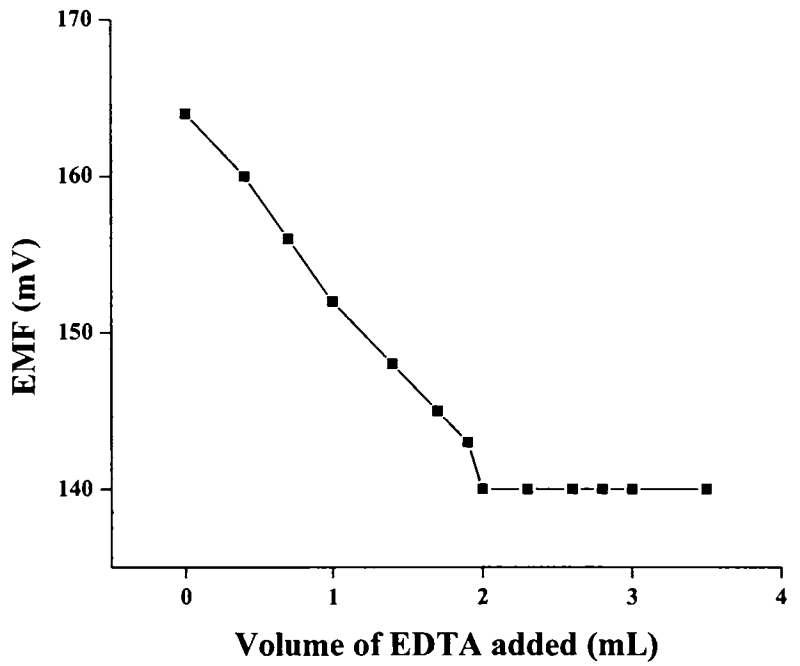

Figure 3.12 – Potentiometric titration curve of 20.0 mL of 1.0×10^{-3} M Mn^{2+} solution with 1.0×10^{-2} M EDTA using the CPE type sensor Sa_4 based on SED as an indicator electrode at pH 6.0.

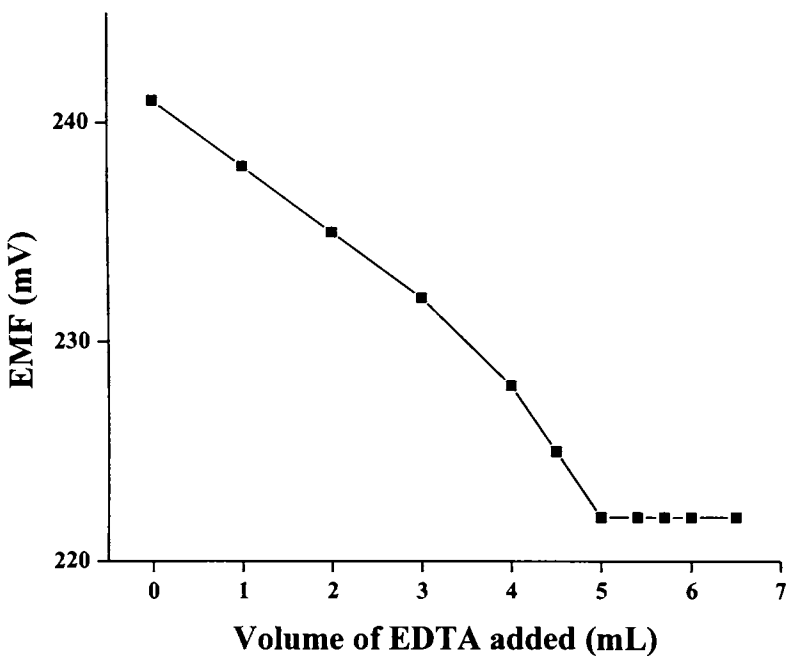

Figure 3.13 – Potentiometric titration curve of 10.0 mL of 5.0×10^{-3} M Mn^{2+} solution with 1.0×10^{-2} M EDTA using the CMCPE type sensor Sb_3 based on SED as an indicator electrode at pH 6.0.

Table 3.1 - Optimization of the PVC membrane ingredients for the CPE-PVC type of sensors based on SED[a]

Sensor	% w/w composition of each membrane				Working concentration range (M)	Slope (mV decade^{-1})	Response time (s)
	PVC	TED	Plasticizer	NaTPB			
Sa_1	0	0	0	0	$1.0 \times 10^{-1} - 1.0 \times 10^{-5}$	~0.0	90
Sa_2	93	5	0	2	$1.0 \times 10^{-1} - 1.0 \times 10^{-5}$	20.7 (±0.2)	65
Sa_3	33	2	DOP, 63	2	$1.0 \times 10^{-1} - 9.2 \times 10^{-6}$	26.9 (±0.7)	45
Sa_4	33	5	DOP, 60	2	$1.0 \times 10^{-1} - 2.7 \times 10^{-6}$	30.1 (±0.5)	20
Sa_5	33	7	DOP, 58	2	$1.0 \times 10^{-1} - 7.2 \times 10^{-6}$	25.9 (±0.4)	30
Sa_6	33	5	DBP, 60	2	$1.0 \times 10^{-1} - 7.9 \times 10^{-6}$	25.6 (±0.5)	40
Sa_7	33	5	DOA, 60	2	$1.0 \times 10^{-1} - 3.3 \times 10^{-5}$	20.1 (±0.3)	75
Sa_8	33	5	DMS, 60	2	$1.0 \times 10^{-1} - 5.2 \times 10^{-4}$	18.2 (±0.4)	50
Sa_9	33	5	DBS, 60	2	$1.0 \times 10^{-1} - 2.9 \times 10^{-4}$	16.4 (±0.7)	60
Sa_{10}	33	5	DOS, 60	2	$5.0 \times 10^{-2} - 4.3 \times 10^{-4}$	21.1 (±0.6)	45

[a] Values in parentheses are RSDs based on three replicates.

Table 3.2 - Optimization of the ionophore composition for the CMCPE type of sensor based on SED[a]

Sensor	Ionophore	Graphite	Working concentration range (M)	Slope (mV decade^{-1})	Response time (s)
Sb_1	0	100	1.0×10^{-2} - 1.0×10^{-4}	3.1 (±0.2)	100
Sb_2	5	95	1.0×10^{-1} - 9.4×10^{-6}	25.1 (±0.7)	75
Sb_3	10	90	1.0×10^{-1} - 3.8×10^{-6}	29.8 (±0.4)	30
Sb_4	20	80	1.0×10^{-1} - 5.6×10^{-5}	32.7 (±0.3)	32
Sb_5	30	70	1.0×10^{-1} - 9.0×10^{-5}	38.5 (±0.5)	48
Sb_6	50	50	1.0×10^{-2} - 3.7×10^{-4}	27.9 (±0.4)	45

[a] Values in parentheses are RSDs based on three replicates.

Table 3.3 – Effect of partially non-aqueous medium on the slope of the sensors Sa_4 and Sb_3

Non-aqueous content (% v/v)	Slope (mV decade^{-1})	
	Sa_4	Sb_3
0	30.1	29.8
Ethanol		
10	30.0	29.8
15	29.8	29.3
20	29.6	28.7
25	29.3	26.9
30	26.7	24.4
Methanol		
10	30.1	29.8
15	29.8	29.4
20	29.6	28.9
25	29.4	26.7
30	26.2	25.9

Table 3.4 – Selectivity coefficients for the sensors Sa_4 and Sb_3 using fixed interference method at 1.0×10^{-2} M concentration of interfering ion.

Interfering ion (X)	Sa_4	Sb_3
Na^+	7.3×10^{-3}	8.2×10^{-3}
K^+	5.2×10^{-3}	4.5×10^{-3}
NH_4^+	5.7×10^{-3}	6.9×10^{-3}
Ag^+	8.9×10^{-2}	7.6×10^{-2}
Mg^{2+}	5.5×10^{-3}	4.8×10^{-3}
Ca^{2+}	6.8×10^{-3}	7.2×10^{-3}
Ba^{2+}	4.6×10^{-3}	4.9×10^{-3}
Cu^{2+}	0.7×10^{0}	0.3×10^{0}
Co^{2+}	9.5×10^{-3}	7.3×10^{-3}
Ni^{2+}	8.2×10^{-1}	9.0×10^{-1}
Zn^{2+}	2.2×10^{-2}	1.9×10^{-2}
Cd^{2+}	3.2×10^{-2}	5.1×10^{-2}
Hg^{2+}	4.7×10^{-1}	3.9×10^{-1}
Pb^{2+}	2.7×10^{-2}	2.1×10^{-2}
Fe^{3+}	7.3×10^{-2}	6.5×10^{-2}

Table 3.5 – Recovery of manganese ions from two different water samples

Sensor	Tap Water Mn^{2+} (ppm)			Well Water Mn^{2+} (ppm)		
	Added	Found*	Recovery (%)	Added	Found*	Recovery (%)
Sa_4	30.00	28.83 ± 0.02	96.1	60.00	58.16 ± 0.01	96.9
Sb_3	30.00	29.47 ± 0.05	98.2	60.00	59.38 ± 0.03	99.0

*RSDs based on three replicates.

Table 3.6 – Response characteristics of the sensors Sa_4 and Sb_3

Parameter	Response characteristics	
	Sa_4	Sb_3
Working concentration range (M)	$1.0 \times 10^{-1} - 5.0 \times 10^{-6}$	$1.0 \times 10^{-1} - 5.0 \times 10^{-6}$
Slope (mV decade^{-1})	30.1 ± 0.5	29.8 ± 0.4
Detection limit (M)	2.7×10^{-6}	3.8×10^{-6}
Response time	20 s	30 s
pH range	3.0-7.0	3.6-6.2
Non aqueous tolerance limit	25%	20%
Shelf life	3 months	4 weeks

Table 3.7 -Comparison of characteristics of the sensors with some reported sensors

No.	Working concentration range (M)	Slope (mV decade^{-1})	pH range	Lifetime	Ref. No.
1	$1.0 \times 10^{-1} - 1.0 \times 10^{-5}$	Non Nernstian	NM	NM	37
2	$1.0 \times 10^{-3} - 5.0 \times 10^{-5}$	Near Nernstian	4.0	2 weeks	39
3	$1.0 \times 10^{-1} - 1.0 \times 10^{-6}$	Near Nernstian	2.3-8.8	NM	40
4	$1.0 \times 10^{-1} - 1.25 \times 10^{-5}$	Nernstian	3.0-8.0	4 months	43
5	$1.0 \times 10^{-1} - 5.0 \times 10^{-6}$	Nernstian	3.0-7.0	3 months	**Sa$_4$**
6	$1.0 \times 10^{-1} - 5.0 \times 10^{-6}$	Nernstian	3.6-6.2	4 weeks	**Sb$_3$**

*NM – not mentioned

Chapter 4

SENSORS FOR NICKEL

This chapter deals with the fabrication of two PVC plasticized membrane sensors based on two different ionophores for determination of nickel ions. The response characteristics of the developed sensors have been studied. The analytical application of the developed sensors as an indicator electrode in the potentiometric titration of nickel ions against EDTA and also for the direct determination of nickel content in real samples have been detailed in this chapter.

Nickel is a silvery white metal belonging to the iron group. It is widely used in electroplating industries and many catalytic processes. It is found in low concentrations in hydrogenated vegetable oils, milk, chocolates, cornmeal, cottonseed, oatmeal, nuts, soyabeans, raw meat etc.

Nickel monitoring has become quite essential mainly due to its toxic nature. It is a potent carcinogen and it causes acute pneumonitics, dermatitis, asthma, nasal and lung cancer[228,229]. The conventional methods such as the gravimetric method using dimethylglyoxime[230] or the spectrophotometric method[231] are not only time consuming but also have some practical inconveniences.

As part of the present investigations, two Schiff bases have been synthesized and used as the electroactive component in the fabrication of

---

PVC plasticized membrane sensors. They have been found to be highly responsive to nickel ions and have many characteristics that are far superior to the reported sensors. A comparison with a few of the reported sensors is also included in the form of a Table.

4.1 Ionophores

The synthesis and characterization of the ionophores, N^1,N^2-bis((thiophen-2-yl)methylene)ethane-1,2-diamine (TED) and N^1,N^2-bis((naphthalen-1-yl)methylene) ethane-1,2-diamine (NED), have been discussed under Sections 2.2.2 and 2.2.3 in Chapter 2.

4.2 Sensor based on TED

The ionophore TED has been used to fabricate a PVC membrane type of sensor. The structure of TED is shown as Figure 4.1.

Initially the potential response of the sensor based on TED was tested for different cations (Figure 4.2) and it was found that the sensor was highly responsive to nickel ions with respect to other ions, which may be attributed to the rapid ion-exchange process ie. the complexation and decomplexation of Ni^{2+} ions with TED at the membrane-sample interface.

4.2.1 Sensor membrane fabrication

The sensor membrane was prepared as discussed under Section 2.6.1 in Chapter 2. The best response was observed with dibutyl phthalate (DBP) as plasticizing agent and sodium tetraphenylborate (NaTPB) as anionic additive. The composition ratio that gave the best response in terms of slope, concentration range and response time was found to be 31:61:3:5 (PVC:DBP:NaTPB:TED) (% w/w). The electrode body was filled with 1.0 ×

10^{-1} M nickel(II) nitrate solution and conditioned by dipping it in a 1.0×10^{-1} M nickel(II) nitrate solution for 2 days.

4.2.2 Potential measurement and calibration

Potentials were measured at 25±0.1 °C on a Systronics digital ion meter and on BAS Epsilon electrochemical workstation. An Ag | AgCl reference electrode was used in conjunction with the developed Ni^{2+} sensor. The cell assembly for potentiometric measurements can be represented as follows:

Ag | AgCl (3.0 M KCl) | Ni^{2+} (0.1 M) | membrane based on TED | test solution | Ag | AgCl (3.0 M KCl).

The performance of the developed Ni^{2+} sensor was investigated by measuring the potential in Ni^{2+} solutions (pH maintained at 6.0 by adding buffer) prepared in the concentration range $1.0 \times 10^{-1} - 1.0 \times 10^{-7}$ M. The solutions were stirred and the stable potential reading was taken.

4.2.3 Optimization of membrane composition

A set of nine membrane compositions were investigated by varying the ratio of plasticizer to ionophore to PVC and the results are given in Table 4.1. A membrane without plasticizer was first prepared and its effect was initially studied (sensor T_1). The addition of plasticizers improves the workability of the membranes and also contributes significantly towards the improvement in working concentration range, stability and shelf life of the sensor[232,233]. The plasticizer which is compatible should exhibit high

lipophilicity to avoid leaching and also possess adequate viscosity and dielectric constant[234,235]. It was observed that the sensor T_3 with dibutyl phthalate (DBP) as plasticizer was found to give the best response in terms of the slope and the concentration range. Here, the slopes in the case of the sebacates are highly sub-Nernstian. The potentiometric response of the sensor towards Ni^{2+} ions is found to be dependent on the concentration of the ionophore used. Three different compositions (% w/w) of the ionophore were tested to obtain the optimum composition of ionophore that gives the best response characteristics. The sensitivity of the sensor was found to increase with ionophore content until a value of 5% was reached. Further addition of ionophore results in diminished response of the sensor and this may be due to some inhomogeneities and possible saturation of the membrane[236].

There is a great improvement in the potentiometric response on the addition of the anionic excluders. Such anionic excluders are beneficial for both neutral and charged carrier-based sensors[213-218]. Also, these lipophilic excluders help in reducing the membrane resistance[219] and improving the selectivity[220-222] and reducing the interference from sample anions[223-226]. It was found that the addition of sodium tetraphenylborate (NaTPB) improved the response characteristics of the sensor. The optimum level was 3%; further increase in the additive content gave no change in the response characteristics of the sensor.

Hence the sensor T_3 was used for further studies.

4.2.4 Working concentration range and slope

The plot of the EMF versus the pNi^{2+} gave the calibration graph of the sensor and the slope was calculated from the graph. The sensor T_3 gave a good working concentration range of $1.0 \times 10^{-1} - 5.0 \times 10^{-6}$ with a Nernstian

slope of 29.5 (±1.0) mV decade^{-1}. The calibration graph for the Ni^{2+} sensor based on TED is shown in Figure 4.3. The detection limit was calculated from the graph by the intersection of the two extrapolated linear segments of the calibration plot and was found to be 1.8×10^{-6} M.

4.2.5 Response time

The response time is the average time for the sensor to reach a potential within ±1 mV of its final equilibrium value. The practical response time of the sensor was calculated by measuring the time required to achieve 95% of the equilibrium potential from the moment of addition of 1.0×10^{-5} M Ni^{2+} solution. From the plot of EMF against time (Figure 4.4), the practical response time was found to be 18 s. The practical reversibility required for the Ni^{2+} sensor to reach a potential within ±1 mV of the final equilibrium value was measured by successive immersion in a series of the metal salt solution with one decade difference in concentration. This dynamic response was plotted as EMF versus time and is shown as Figure 4.5. The potentials were constant for more than 4 min. The sensing behaviour of the membrane remained unchanged when potentials were recorded either from low to high concentrations or vice versa.

4.2.6 Effect of pH and non aqueous media

The pH dependence of the sensor was examined for two fixed concentrations (1.0×10^{-3} M and 1.0×10^{-4} M) over the pH range 2.0-9.0. The pH was adjusted by adding drops of 1.0 M HNO_3 or NaOH. The results presented as Figure 4.6 reveal that the potentials are independent of pH in the range of 3.2-7.9 and it was taken as the working pH range of the Ni^{2+} sensor.

Below and above these pH values, a sharp change in potential was observed which may be due to the co-fluxing with H^+ ions at lower pH and hydrolysis of Ni^{2+} ions at higher pH values.

The utility of the sensor was also investigated in partially non-aqueous media using methanol-water and ethanol-water mixtures. The sensor worked satisfactorily in mixtures having 30% (v/v) non-aqueous content without showing any considerable change in working concentration range or slope and the results are presented in Table 4.2. Above 30%, the drift in potential may be due to the leaching of the ionophore.

4.2.7 Potentiometric selectivity

To investigate the selectivity of the developed Ni^{2+} sensor based on TED, the fixed interference method (FIM)[227,35] was adopted. The potential of the cell comprising the sensor and the reference electrode was measured for solutions of constant activity of the interfering ion (1.0×10^{-2} M), a_B, and varying activity of the primary ion, a_A. The potentials obtained versus the logarithm of the activity of the primary ion was plotted and the intersection of the extrapolated linear portions of this graph indicates the value of a_A. The $K_{A,B}^{pot}$ is calculated using the following equation.

$$K_{A,B}^{pot} = a_A / (a_B)^{z_A / z_B}$$

The selectivity coefficients were determined at 1.0×10^{-2} M concentration of foreign ions. The selectivity coefficient values are shown in Table 4.3 and the values indicate that the developed Ni^{2+} sensor based on TED is selective to the Ni^{2+} ion over a number of cations - Na^+, K^+, Mg^{2+}, Ca^{2+}, Ba^{2+}, Sr^{2+}, Cr^{3+}, Mn^{2+}, Co^{2+}, Sn^{2+}, Zn^{2+}, Cu^{2+}, Ag^+, Pb^{2+},Cd^{2+}, $Hg^{2+}$and Fe^{2+}.

4.2.8 Lifetime or Shelf life

The stability and lifetime of the Ni^{2+} sensor were tested over a period of 4 months. During this period, the sensor showed no significant deviation on the optimized response characteristics of the sensor.

4.2.9 Analytical applications

The developed Ni^{2+} sensor T_3 was successfully applied to the determination of nickel(II) in some branded Indian chocolates and wastewater sample from electroplating industries. The solutions of these samples were prepared as discussed under Section 2.5 in Chapter 2. The results presented in Table 4.4 show that the method is comparable to the standard ICP-AES[2].

The developed Ni^{2+} sensor was successfully applied as an indicator electrode in conjuction with Ag|AgCl in the potentiometric titration of Ni^{2+} solution (5.0×10^{-3} M) with an EDTA solution (1.0×10^{-2} M) at pH 6.0. The titration curve is shown as Figure 4.7 and it indicates that the amount of Ni^{2+} ions can be determined using the sensor T_3. The plot is not of sigmoid shape but the sharp break point corresponds to the stoichiometry of the Ni-EDTA complex.

4.3 Sensor based on NED

The ionophore NED has been used for the fabrication of a PVC membrane sensor. The structure of NED is shown as Figure 4.8.

Figure 4.9 shows the potential response of various NED based PVC membrane sensors towards different cations. It was seen that among the different cations tested, the sensor responded most sensitively and selectively

to Ni^{2+} ions and this may be attributed to the fast exchange kinetics at the membrane-sample interface.

4.3.1 Sensor membrane fabrication

The sensor membrane was prepared as discussed under Section 2.6.1 in Chapter 2. The best response was obtained on using dioctyl phthalate (DOP) as plasticizing agent and sodium tetraphenylborate (NaTPB) as anionic excluder. The composition ratio that gave the best response in terms of slope, concentration range and response time was found to be 31:65:2:2 (PVC:DOP:NaTPB:NED) (% w/w). The electrode body was filled with 1.0×10^{-1} M nickel(II) nitrate solution and conditioned by dipping it in a 1.0×10^{-1} M nickel(II) nitrate solution for 24 h.

4.3.2 Potential measurement and calibration

Potentials were measured at ambient temperature (25±0.1 °C) on a Systronics digital ion meter and on BAS Epsilon electrochemical workstation. An Ag | AgCl reference electrode was used in conjunction with the developed Ni^{2+} sensor. The cell assembly for potentiometric measurements can be represented as follows:

Ag | AgCl (3.0 M KCl) | Ni^{2+} (0.1 M) | membrane based on NED | test solution | Ag | AgCl (3.0 M KCl).

The performance of the developed Ni^{2+} sensor was investigated by measuring the potential in Ni^{2+} solutions (pH maintained at 6.0 by adding

buffer) prepared in the concentration range $1.0 \times 10^{-1} - 1.0 \times 10^{-7}$ M. The solutions were stirred and the stable potential reading was taken.

4.3.3 Optimization of membrane composition

Table 4.5 consolidates the results of the nine sets of membrane compositions that were studied. A membrane without plasticizer was first prepared and its effect was initially studied (sensor N_1). The use of plasticizers improves the response characteristics of the membranes by providing a smooth surface and also improving the response characteristics of the sensor[232-235]. It was observed that the sensor N_2 with dioctyl phthalate (DOP) as plasticizer was found to give the best response in terms of the slope, response time and the concentration range. The slopes in the case of the sebacates and adipates are sub-Nernstian. The amount of ionophore used was found to influence the potentiometric response of the sensor towards Ni^{2+} ions. Three different membranes were prepared by varying the composition of the ionophore and it was found that the maximum sensitivity was observed for 2% of the ionophore.

The effect of the anionic excluders was also investigated as it is well documented that the incorporation of lipophilic additives can significantly influence the performance characteristics of a membrane sensor[213-226]. It was found that the best response is for the sensor incorporating 2% of sodium tetraphenylborate (NaTPB).

4.3.4 Working concentration range and slope

The plot of the EMF versus the pNi^{2+} gave the calibration graph of the sensor and from it, the slope was calculated. The sensor N_2 gave a good

working concentration range of $1.0 \times 10^{-1} - 5.0 \times 10^{-6}$ with a Nernstian slope of 29.9 (±1.0) mV decade^{-1}. The calibration graph for the Ni^{2+} sensor based on NED is shown in Figure 4.10. The detection limit was calculated from the graph by the intersection of the two extrapolated linear segments of the calibration plot and was found to be 1.3×10^{-6} M.

4.3.5 Response time

The practical response time of the sensor was calculated by measuring the time required to achieve 95% of the equilibrium potential from the moment of addition of 1.0×10^{-5} M Ni^{2+} solution. Figure 4.11 gives the plot of EMF against time and it was found that the practical response time was 15 s. The practical reversibility required for the Ni^{2+} sensor to reach a potential within ±1 mV of the final equilibrium value was measured by successive immersion in a series of the nickel ion solutions, each having a 10-fold difference in concentration. This dynamic response is plotted as EMF versus time and is shown as Figure 4.12. The potentials remained constant for about 5 min. The sensing behaviour of the membrane remained unchanged when potentials were recorded either from low to high concentrations or vice versa.

4.3.6 Effect of pH and non aqueous media

The pH dependence of the sensor N_2 was examined for two fixed concentrations (1.0×10^{-3} M and 1.0×10^{-4} M) over the pH range 2.0-9.0. The pH was adjusted by adding drops of either 1.0 M HNO_3 or NaOH. The results presented as Figure 4.13 reveal that the potentials are independent of pH in the range of 3.6-7.4 and it was taken as the working pH range of the Ni^{2+} sensor. The observed drift in the potential values may be related to the

response of the membrane sensor to H^+ ions at pH below 3.6 and to the formation of some Ni^{2+} hydroxyl complexes at pH above 7.4.

The working of the sensor in partially non-aqueous media was also investigated using methanol-water and ethanol-water mixtures. The sensor worked satisfactorily in mixtures having 25% (v/v) non-aqueous content and the results are consolidated in Table 4.6. Above this tolerance level, the slopes gets affected which may be attributed to leaching of the ligand into the sample solution.

4.3.7 Potentiometric selectivity

The potentiometric selectivity coefficients ($K_{A,B}^{pot}$) which describes the preference of the membrane sensor for an interfering ion relative to Ni^{2+} ions, were determined by the fixed interference method (FIM)[227,35]. The $K_{A,B}^{pot}$ was calculated using the following equation.

$$K_{A,B}^{pot} = a_A / (a_B)^{z_A / z_B}$$

a_A is the value obtained from the intersection of the extrapolated linear portions of the plot of EMF versus the logarithm of the activity of the primary ion

a_B is the activity of the interfering ion, which is fixed

z_A & z_B are charge numbers of the primary ion, A and of the interfering ion, B

The selectivity coefficients were determined at 1.0×10^{-2} M concentration of foreign ions. The selectivity coefficient values are shown in Table 4.7 and

the values indicate that the developed Ni^{2+} sensor based on NED is selective to the Ni^{2+} ion over the following cations – Na^{+}, K^{+}, Mg^{2+}, Ca^{2+}, Ba^{2+}, Sr^{2+}, Cr^{3+}, Mn^{2+}, Co^{2+}, Sn^{2+}, Zn^{2+}, Cu^{2+}, Cd^{2+}, Hg^{2+}, Ag^{+}, Pb^{2+} and Fe^{2+}.

4.3.8 Lifetime or Shelf life

The stability and lifetime of the Ni^{2+} sensor were tested over a period of 4 months. During this period, the sensor showed no significant deviation on the optimized response characteristics.

4.3.9 Analytical applications

The developed Ni^{2+} sensor (N_2) was successfully applied to the determination of nickel in real samples like chocolate (Cadbury's Fruit & Nut), Vegetable oil (Dalda) and wastewater sample from electroplating industries. The solutions of real samples were prepared as discussed under Section 2.5 in Chapter 2. The results presented in Table 4.8 show that the method is comparable to the standard ICP-AES[2].

The developed Ni^{2+} sensor was also successfully applied as an indicator electrode in conjuction with Ag|AgCl in the potentiometric titration of Ni^{2+} solution (4.0×10^{-3} M) with an EDTA solution (1.0×10^{-2} M) at pH 6.0. The titration curve for Ni^{2+} solution with EDTA is shown as Figure 4.14 and it indicates that the amount of Ni^{2+} ions can be determined using the sensor N_2. A very good inflection point which shows the perfect stoichiometry of the Ni-EDTA complex was observed in the titration plot.

4.4 Comparison among sensors T_3 and N_2 and to some of the reported sensors

Both the developed sensors are found to have very good response characteristics. Table 4.9 consolidates the response characteristics of both the developed sensors. The pH range and response time values are better for the sensor T_3; but the detection limit is lower in the case of sensor N_3. Also, the conditioning time required for sensor N_2 is only 24 h whereas sensor T_3 requires 2 days. Table 4.10 lists the comparative study of the characteristics of developed sensors with some of the reported sensors for Ni^{2+}. It can be seen that the developed sensors are superior in terms of working concentration range[45,50-52,54,58,59,61,65], slope[45,50-53,64,72], life time[45,50,53,54,61,64,65,73] and pH range[45,50-52,58,59].

Figures

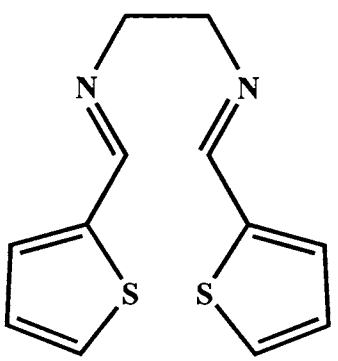

Figure 4.1 – Structure of the ionophore – TED

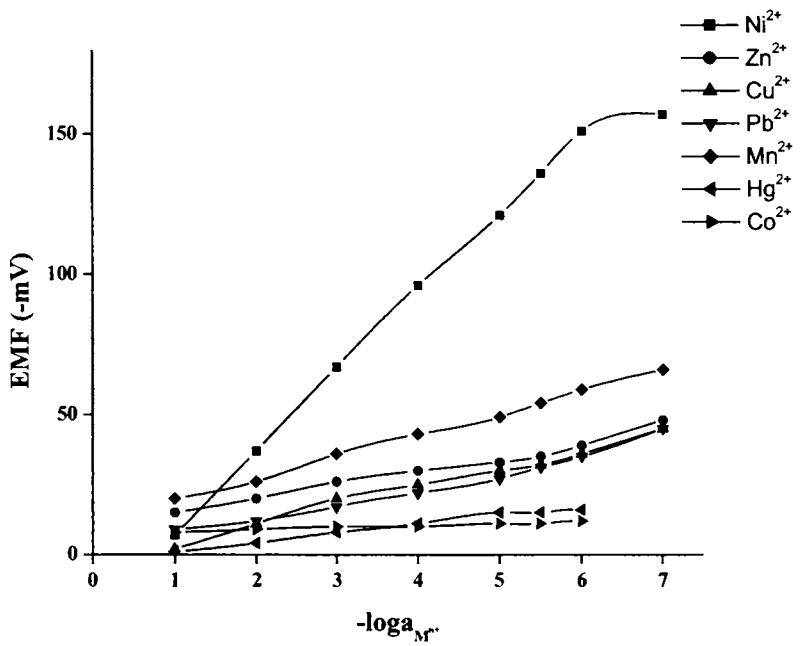

Figure 4.2 – Potential response of various sensors based on TED. Conditions: membrane composition ratio 31% PVC:61% DBP:3% NaTPB:5% TED; internal solution 1.0×10^{-1} M of each cation used and conditioned in 1.0×10^{-1} M of the corresponding cation solution for 2 days.

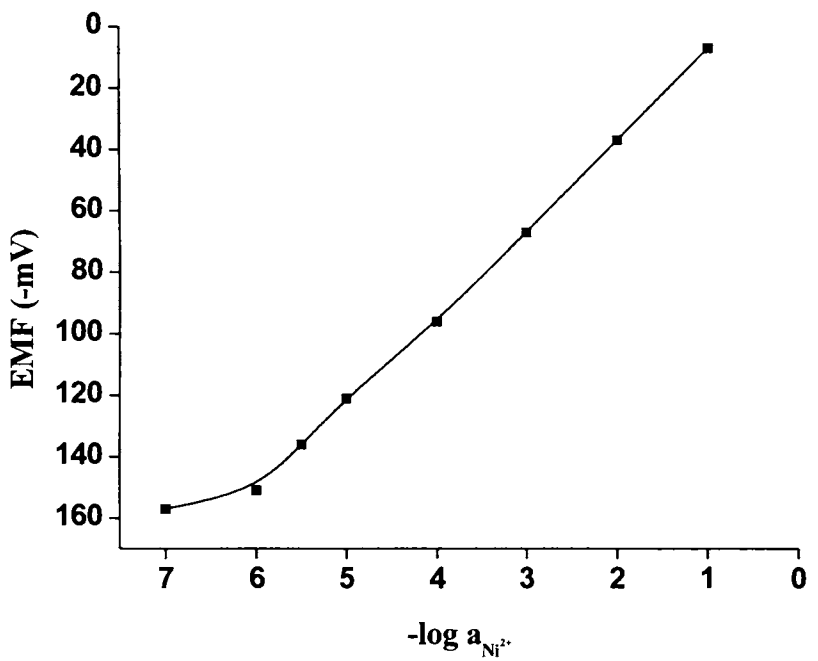

Figure 4.3 – Calibration plot of the sensor T_3 based on TED

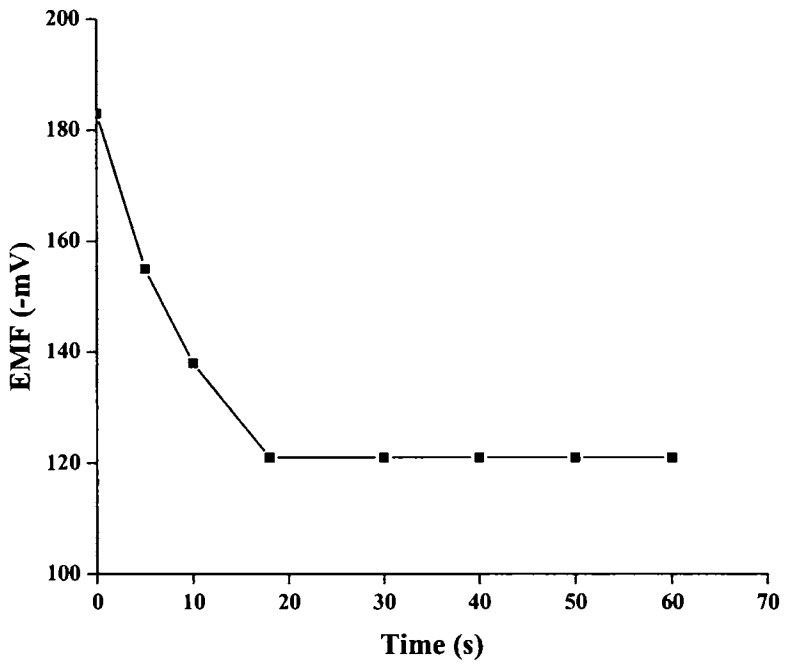

Figure 4.4 – Practical response time of the sensor T_3 from the moment of addition of Ni^{2+} (1.0×10^{-5} M) solution

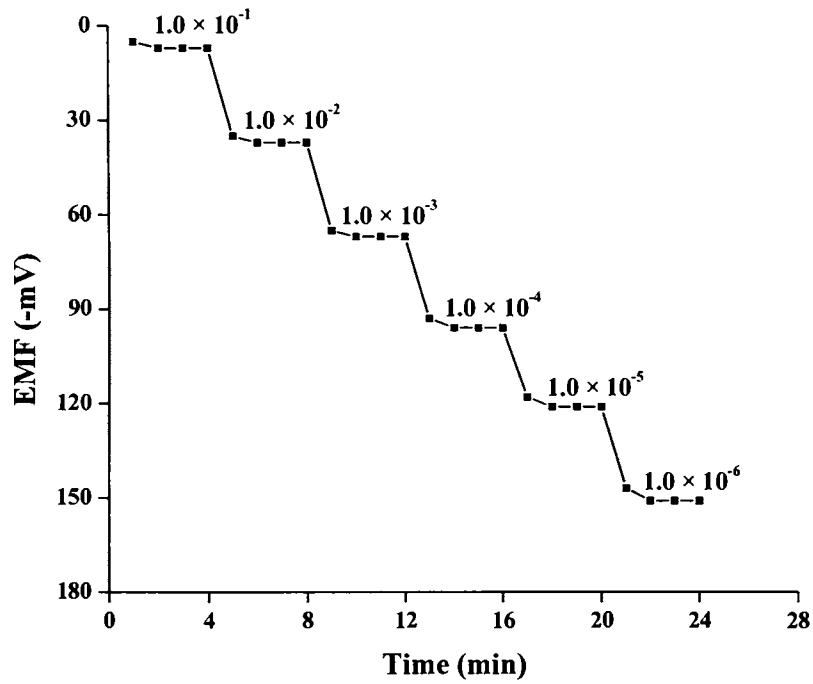

Figure 4.5 – Dynamic response time of the sensor T_3 for reversibility with step changes in concentration of Ni^{2+} (1.0×10^{-6} to 1.0×10^{-1} M)

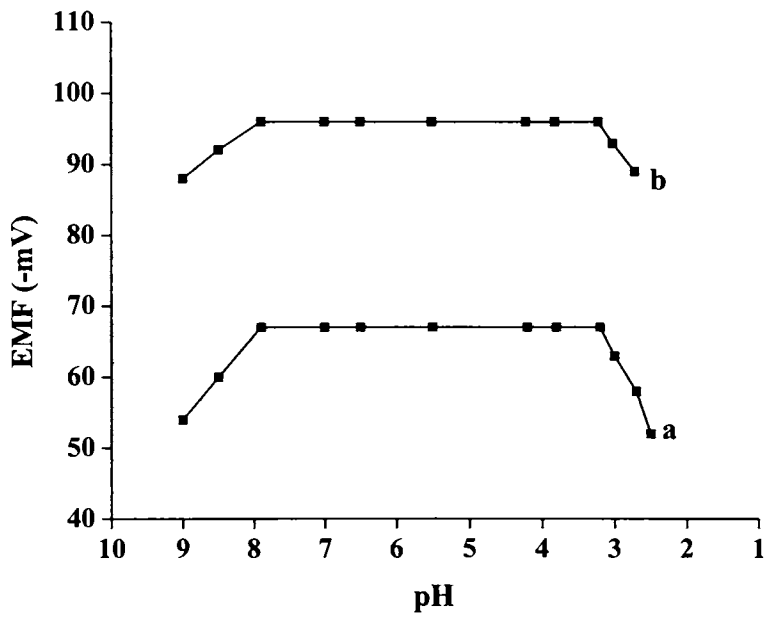

Figure 4.6 – Effect of pH on the cell potential of the sensor T_3 based on TED at 1.0×10^{-3} M (a) and 1.0×10^{-4} M (b)

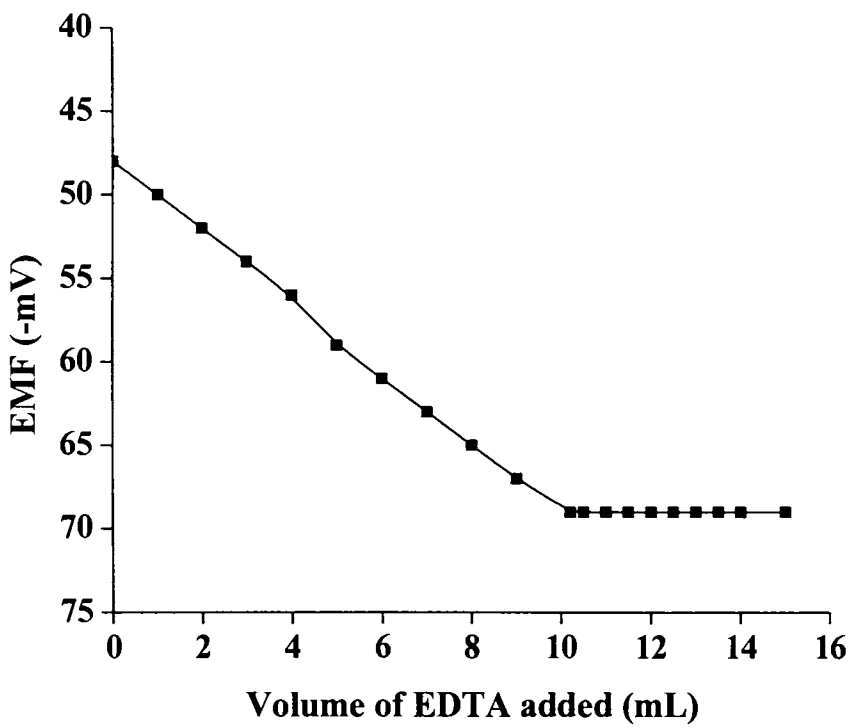

Figure 4.7 – Potentiometric titration curve of 20.0 mL of 5.0×10^{-3} M Ni^{2+} solution with 1.0×10^{-2} M EDTA using the sensor T_3 as an indicator electrode at pH 6.0.

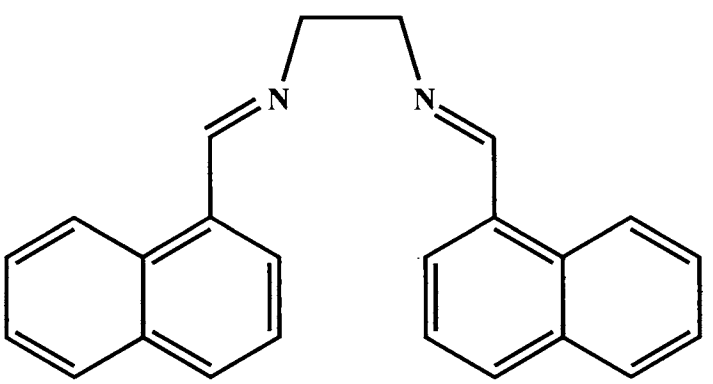

Figure 4.8 – Structure of the ionophore – NED

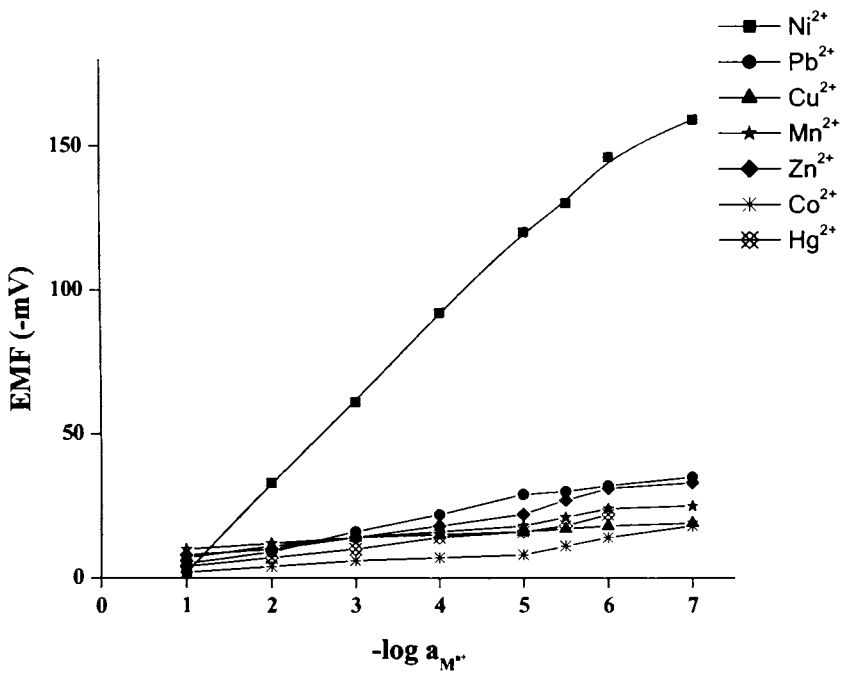

Figure 4.9 – Potential response of various sensors based on NED.

Conditions: Composition ratio 31% PVC:65% DOP:2% NaTPB:

2% NED

Internal solution – 1.0×10^{-1} M of each cation used;

conditioning in 1.0×10^{-1} M of corresponding cation salt solution for 24 h.

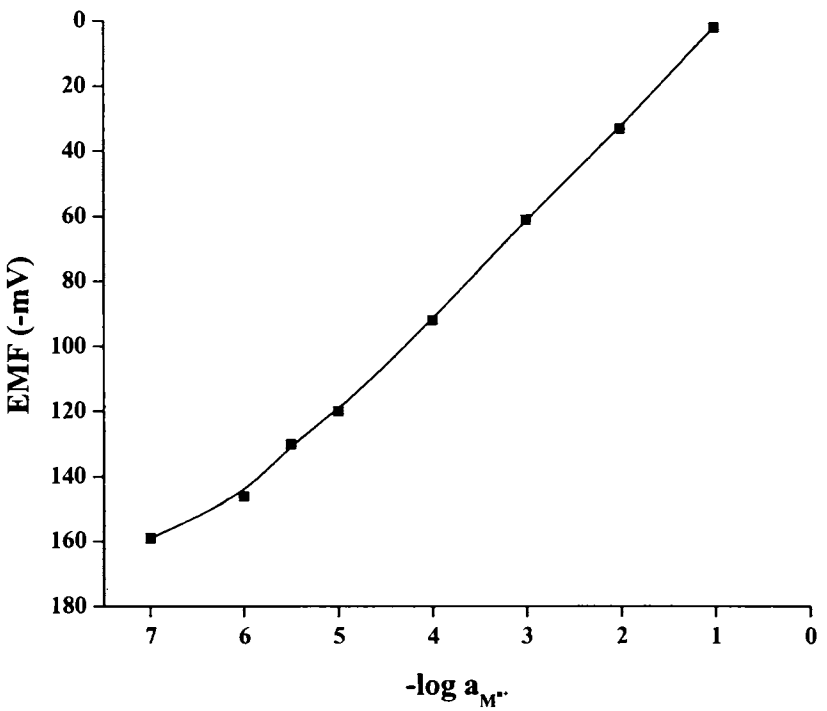

Figure 4.10 – Calibration plot of the sensor N_2 based on NED

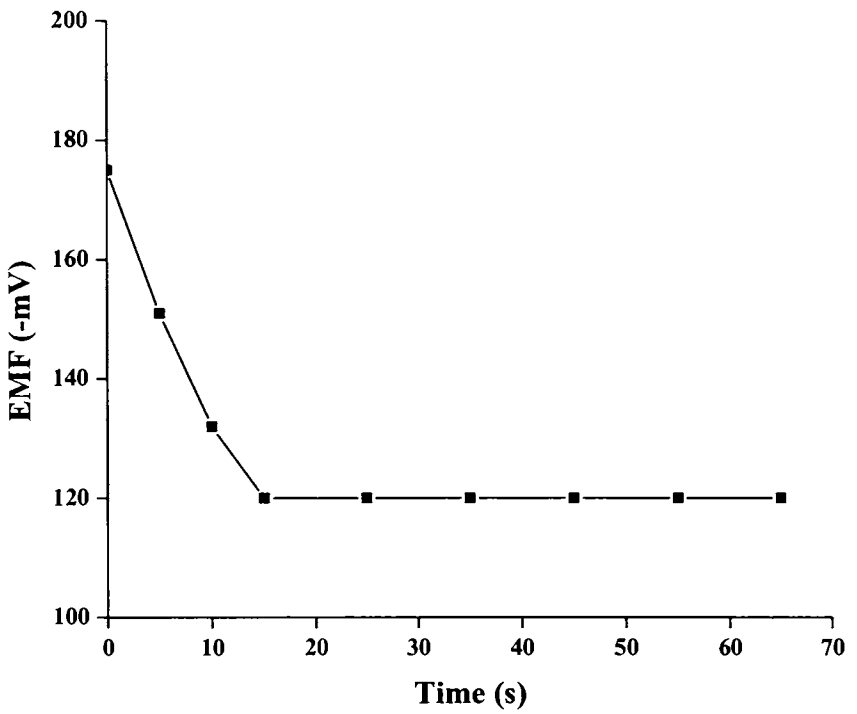

Figure 4.11 – Practical response time of the sensor N_2 from the moment of addition of Ni^{2+} (1.0×10^{-5} M) solution

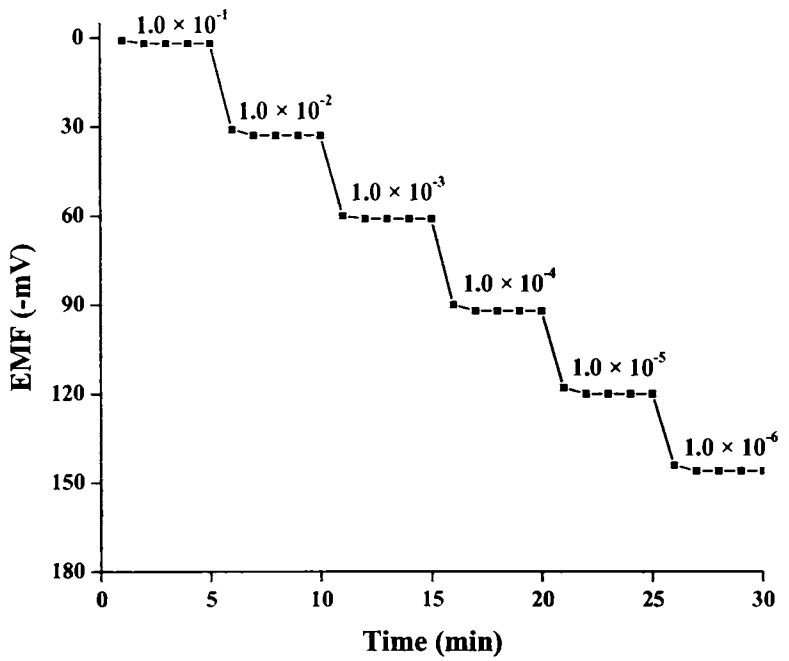

Figure 4.12 – Dynamic response time of the sensor N_2 for reversibility with step changes in concentration of Ni^{2+} (1.0×10^{-6} to 1.0×10^{-1} M)

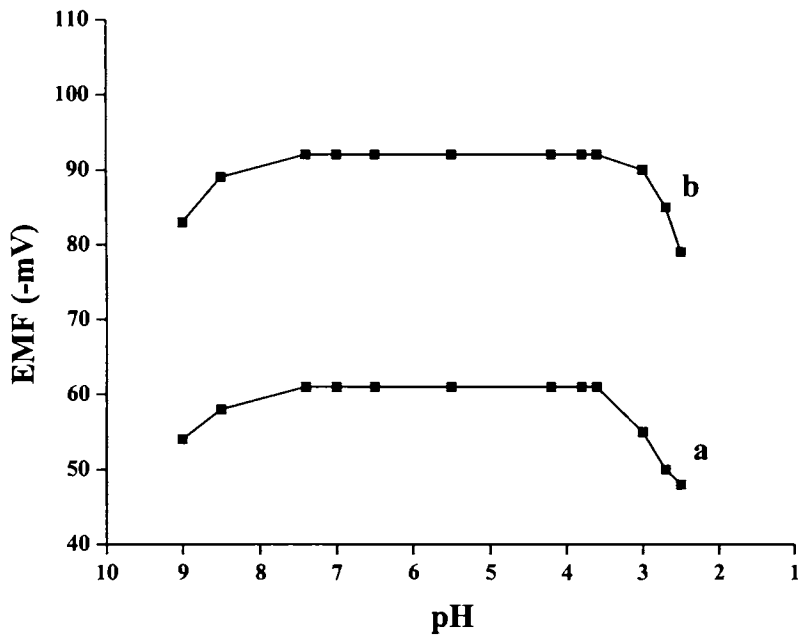

Figure 4.13 – Effect of pH on the cell potential of the sensor N_2 based on NED at 1.0×10^{-3} M (a) and 1.0×10^{-4} M (b)

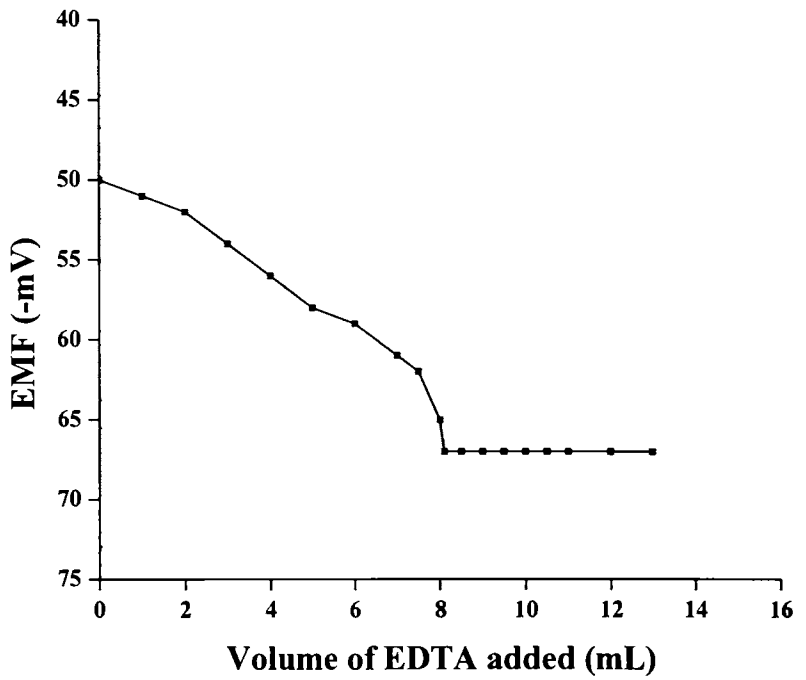

Figure 4.14 – Potentiometric titration curve of 20.0 mL of 4.0×10^{-3} M Ni^{2+} solution with 1.0×10^{-2} M EDTA using the sensor N_2 as an indicator electrode at pH 6.0.

Table 4.1 – Optimization of membrane ingredients for the sensor based on TED[a]

Sensor	% w/w composition of each membrane				Working concentration range (M)	Slope (mV decade^{-1})	Response time (s)
	PVC	TED	Plasticizer	NaTPB			
T_1	92	5	0	3	$1.0 \times 10^{-1} - 1.0 \times 10^{-5}$	20.3 (±0.2)	40
T_2	31	2	DBP, 64	3	$1.0 \times 10^{-1} - 2.6 \times 10^{-6}$	22.5 (±1.0)	11
T_3	31	5	DBP, 61	3	$1.0 \times 10^{-1} - 1.8 \times 10^{-6}$	29.5 (±1.0)	18
T_4	31	7	DBP, 59	3	$1.0 \times 10^{-1} - 5.7 \times 10^{-6}$	21.4 (±0.7)	25
T_5	31	5	DOP, 61	3	$1.0 \times 10^{-1} - 1.6 \times 10^{-5}$	19.8 (±0.8)	30
T_6	31	5	DOA, 61	3	$1.0 \times 10^{-1} - 7.2 \times 10^{-5}$	23.5 (±0.2)	30
T_7	31	5	DMS, 61	3	$1.0 \times 10^{-1} - 9.3 \times 10^{-4}$	12.8 (±0.5)	22
T_8	31	5	DBS, 61	3	$1.0 \times 10^{-1} - 1.0 \times 10^{-5}$	12.9 (±0.7)	20
T_9	31	5	DOS, 61	3	$1.0 \times 10^{-1} - 2.2 \times 10^{-5}$	13.0 (±0.4)	30

[a] Values in parentheses are RSDs based on three replicates.

Table 4.2 – Effect of partially non-aqueous medium on the working of the developed sensor, T_3

Non-aqueous content (% v/v)	Slope (mV decade^{-1})	Working concentration range (M)
0	29.5	$1.0 \times 10^{-1} - 1.8 \times 10^{-6}$
Ethanol		
10	29.1	$1.0 \times 10^{-1} - 3.4 \times 10^{-6}$
20	28.8	$1.0 \times 10^{-1} - 5.6 \times 10^{-6}$
30	28.2	$1.0 \times 10^{-1} - 6.2 \times 10^{-6}$
40	22.7	$1.0 \times 10^{-1} - 9.7 \times 10^{-6}$
Methanol		
10	29.3	$1.0 \times 10^{-1} - 2.8 \times 10^{-6}$
20	28.9	$1.0 \times 10^{-1} - 5.9 \times 10^{-6}$
30	28.3	$1.0 \times 10^{-1} - 8.7 \times 10^{-6}$
40	22.8	$1.0 \times 10^{-1} - 1.1 \times 10^{-5}$

Table 4.3 – Selectivity coefficients for the sensor T_3 using fixed interference method at 1.0×10^{-2} M concentration of interfering ion.

Interfering ion (X)	$K^{pot}_{Ni^{2+},X}$
Na^+	1.4×10^{-2}
K^+	1.7×10^{-2}
Mg^{2+}	4.2×10^{-3}
Ca^{2+}	2.5×10^{-3}
Ba^{2+}	1.9×10^{-3}
Sr^{2+}	2.4×10^{-3}
Cr^{3+}	5.3×10^{-3}
Mn^{2+}	7.9×10^{-3}
Co^{2+}	6.4×10^{-3}
Fe^{2+}	9.7×10^{-3}
Cu^{2+}	8.8×10^{-3}
Zn^{2+}	4.7×10^{-3}
Sn^{2+}	6.6×10^{-3}
Hg^{2+}	3.8×10^{-3}
Pb^{2+}	1.1×10^{-2}
Ag^+	1.3×10^{-2}
Cd^{2+}	5.0×10^{-3}

Table 4.4 – Determination of the Ni^{2+} content in real samples using the sensor T_3

Sample	Sensor T_3 (ppm)*	ICP-AES (ppm)
Nestle Milky Bar	1.19 ± 0.02	1.18
Cadbury Diary Milk	1.32 ± 0.01	1.30
Effluent sample	2.94 ± 0.02	2.93

* RSDs based on three replicates.

Table 4.5 – Optimization of membrane ingredients based on NED[a]

Sensor	% w/w composition of each membrane				Working concentration range (M)	Slope (mV decade^{-1})	Response time (s)
	PVC	NED	Plasticizer	NaTPB			
N_1	96	2	0	2	$1.0 \times 10^{-1} - 1.0 \times 10^{-5}$	21.7(±0.2)	65
N_2	31	2	DOP, 65	2	$1.0 \times 10^{-1} - 1.3 \times 10^{-6}$	29.9(±1.0)	15
N_3	31	5	DOP, 62	2	$1.0 \times 10^{-1} - 5.5 \times 10^{-6}$	28.2(±0.3)	20
N_4	31	7	DOP, 60	2	$1.0 \times 10^{-1} - 6.3 \times 10^{-6}$	27.6(±0.5)	20
N_5	31	2	DBP, 65	2	$1.0 \times 10^{-1} - 9.9 \times 10^{-5}$	17.5(±0.8)	40
N_6	31	2	DOA, 65	2	$1.0 \times 10^{-1} - 4.2 \times 10^{-5}$	20.7(±0.4)	40
N_7	31	2	DMS, 65	2	$1.0 \times 10^{-1} - 8.3 \times 10^{-4}$	15.8(±0.5)	30
N_8	31	2	DBS, 65	2	$1.0 \times 10^{-1} - 1.0 \times 10^{-4}$	14.9(±0.3)	25
N_9	31	2	DOS, 65	2	$1.0 \times 10^{-1} - 2.2 \times 10^{-4}$	12.3(±0.9)	30

[a] Values in parentheses are RSDs based on three replicates.

G9156

Table 4.6 – Effect of partially non-aqueous medium on the working of the developed sensor N_2

Non-aqueous content (% v/v)	Slope (mV decade^{-1})	Working concentration range (M)
0	29.9	$1.0 \times 10^{-1} - 1.3 \times 10^{-6}$
Ethanol		
10	29.3	$1.0 \times 10^{-1} - 5.2 \times 10^{-6}$
25	29.1	$1.0 \times 10^{-1} - 8.1 \times 10^{-6}$
30	23.5	$1.0 \times 10^{-1} - 5.0 \times 10^{-5}$
Methanol		
10	28.9	$1.0 \times 10^{-1} - 4.5 \times 10^{-6}$
25	28.6	$1.0 \times 10^{-1} - 9.9 \times 10^{-6}$
30	20.4	$1.0 \times 10^{-1} - 3.4 \times 10^{-5}$

Table 4.7 – Selectivity coefficients for the developed sensor N_2 using fixed interference method at 1.0×10^{-2} M concentration of interfering ion.

Interfering ion (X)	$K^{pot}_{Ni^{2+},X}$
Na^+	9.2×10^{-2}
K^+	8.4×10^{-3}
Mg^{2+}	3.1×10^{-3}
Ca^{2+}	5.5×10^{-3}
Ba^{2+}	9.1×10^{-3}
Sr^{2+}	3.7×10^{-3}
Cr^{3+}	2.8×10^{-3}
Mn^{2+}	5.4×10^{-3}
Co^{2+}	7.6×10^{-3}
Fe^{2+}	4.3×10^{-3}
Cu^{2+}	3.4×10^{-3}
Zn^{2+}	8.7×10^{-3}
Sn^{2+}	6.2×10^{-3}
Hg^{2+}	6.9×10^{-3}
Pb^{2+}	6.7×10^{-3}
Ag^+	8.9×10^{-3}
Cd^{2+}	2.9×10^{-3}

Table 4.8 – Determination of the Ni^{2+} content in real samples using the sensor N_2

Sample	Sensor N_2 (ppm)*	ICP-AES (ppm)
Chocolate sample	0.91 ± 0.02	0.92
Vanaspati	1.07 ± 0.01	1.09
Effluent sample	2.91 ± 0.03	2.93

* RSDs based on three replicates.

Table 4.9 – Response characteristics of the sensors T_3 and N_2

Parameter	Response characteristics	
	T_3	N_2
Working concentration range	$1.0 \times 10^{-1} - 5.0 \times 10^{-6}$ M	$1.0 \times 10^{-1} - 5.0 \times 10^{-6}$ M
Slope (mV decade^{-1})	29.5 ± 1.0	29.9 ± 1.0
Detection limit	1.8×10^{-6} M	1.3×10^{-6} M
Response time	18 s	15 s
pH range	3.2-7.9	3.6-7.4
Non aqueous tolerance limit	30%	25%
Shelf life	4 months	4 months

Table 4.10 – Comparison of characteristics of the sensors with some reported sensors

No.	Working concentration range (M)	Slope (mV decade^{-1})	pH range	Life time (months)	Ref. No.
1	$1.0 \times 10^{-1} - 1.0 \times 10^{-3}$	Non-Nernstian	NM*	NM	45
2	$1.0 \times 10^{-1} - 5.0 \times 10^{-5}$	Non-Nernstian	3.5-8.0	NM	50
3	$1.2 \times 10^{-2} - 6.3 \times 10^{-4}$	Near Nernstian	NM	NM	51
4	$1.0 \times 10^{-1} - 5.0 \times 10^{-5}$	Non-Nernstian	3.5-6.5	5-6	52
5	$1.0 \times 10^{-2} - 1.0 \times 10^{-8}$	Non-Nernstian	2.0-9.0	1	53
6	$1.0 \times 10^{-1} - 4.0 \times 10^{-5}$	Nernstian	3.0-7.5	2	54
7	$5.0 \times 10^{-2} - 1.0 \times 10^{-5}$	Nernstian	1.7-5.4	6	59
8	$5.5 \times 10^{-3} - 2.0 \times 10^{-6}$	Nernstian	4.0-8.0	1.5	61
9	$1.0 \times 10^{-2} - 5.0 \times 10^{-5}$	Nernstian	9.98	2	54
10	$1.0 \times 10^{-2} - 1.0 \times 10^{-7}$	Near Nernstian	4.0-7.0	3	53
11	$1.0 \times 10^{-1} - 2.0 \times 10^{-6}$	Non-Nernstian	2.0-7.0	6	72
12	$1.0 \times 10^{-2} - 5.0 \times 10^{-6}$	Nernstian	3.5-7.5	1	73
13	$1.0 \times 10^{1} - 1.0 \times 10^{-5}$	Nernstian	2.6-6.8	4	58
14	$1.0 \times 10^{-1} - 5.0 \times 10^{-6}$	Nernstian	3.2-7.9	4	$\mathbf{T_3}$
15	$1.0 \times 10^{-1} - 5.0 \times 10^{-6}$	Nernstian	3.6-7.4	4	$\mathbf{N_2}$

*NM – not mentioned

Chapter 5

SENSORS FOR COPPER

This chapter discusses the response characteristics of four sensors based on two different ionophores for the determination of copper ions. The membrane compositions have been optimized and response characteristics of the developed sensors have been studied in detail. The analytical applications of the developed sensors have also been discussed. The comparison between the sensors and to some of the reported sensors has been discussed in detail.

Copper was known to some of the oldest civilizations and has a history of use of at least 10,000 years old. It is a reddish-coloured metal with a high electrical and thermal conductivity. It occupies the same family of the periodic table as silver and gold, hence it shares many characteristics with these metals such as its malleability, ductility etc.

Copper is an essential element for human beings as it is required for several enzyme systems and biological electron transport[237]. Dietary sources of copper are nuts, seafood and the organs of animals mainly the liver part. The Recommended Dietary Allowance (RDA) for copper in normal healthy adults is 0.9 mg/day[238]. Deficiency of copper results in anemia but, the element is toxic at high concentrations and it is known to cause gastrointestinal problems, Wilson disease, hypoglycemia and dyslexia[239].

The toxicity is generally attributed to the aquo-complexed "free" copper ions rather than its organic or inorganic complexes[240]. The occurrence of copper in the environment is widespread as it is used in many industrial, agricultural and domestic purposes and because of its toxic effects, its monitoring is important. A number of methods, such as gravimetric detection[241], atomic absorption spectroscopy (AAS) usually coupled with electrothermal atomization[242,243], inductively coupled plasma-optical emission spectroscopy (ICP-OES)[244], chromatography[245] etc. are used for the determination of copper at low concentrations. However, these methods are not convenient for analysis as they generally require sample pre-treatment and also infrastructure backup.

This chapter presents the results of development of four sensors based on two different ionophores that have been used for the determination of copper ions.

5.1 Ionophores

The synthesis and characterization of the ionophores, 4-(2-hydroxybenzylideneamino)-N-(5-methyl-3-isoxazolyl) benzenesulphonamide (HIB) and N^1,N^2-bis(2-hydroxy-5-nitro benzylidene) propane-1,3-diamine (HPD), have been discussed under Section 2.2.4 and 2.2.5 respectively in Chapter 2.

5.2 Sensor based on HIB

The ionophore HIB blends well with graphite and was used in the fabrication of a CMCPE type of sensor. This type of sensor has the

advantage that it requires no internal solution. The structure of HIB is shown as Figure 5.1.

The preliminary investigations involved the recording of the potential responses of various sensors to different cations and this is depicted in Figure 5.2. It was found that the sensor responds most sensitively to copper ions and this may be due to the fast exchange kinetics at the membrane-sample interface.

5.2.1 Sensor membrane fabrication

The sensor was fabricated as detailed under Section 2.6.3 in Chapter 2. The graphite ionophore paste in tributyl phosphate was packed into the open end of the capillary tube. The composition ratio that gave the best response in terms of slope, concentration range and response time was found to be 95:5 (graphite:HIB) (% w/w). The sensor was conditioned by dipping it in a 1.0×10^{-1} M copper(II) nitrate solution for 2 h.

5.2.2 Potential measurement and calibration

Potentials were measured at 25±0.1 °C on a Systronics digital ion meter and on BAS Epsilon electrochemical workstation. An Ag | AgCl reference electrode was used in conjunction with the developed Cu^{2+} sensor. The cell assembly for potentiometric measurements can be represented as follows:

Ag | AgCl (3.0 M KCl) | test solution | CMCPE based on HIB.

The performance of the developed Cu^{2+} sensor was investigated by measuring the potential in Cu^{2+} solutions (pH maintained at 5.0 by adding buffer) prepared in the concentration range $1.0 \times 10^{-1} - 1.0 \times 10^{-6}$ M. The solutions were stirred and the stable potential reading was taken.

5.2.3 Optimization of amount of modifier

A set of six different have been fabricated by varying the ratio of graphite and the ionophore (modifier) and the results are consolidated in Table 5.1. A sensor without ionophore was first prepared and its effect was initially studied (sensor B_1). It was observed that the sensor B_2 with the composition ratio 95:5 (graphite:HIB) gave the best response in terms of response time, working concentration range and the Nernstian slope. On increasing the ionophore content, the response of the sensor seems to follow an irregular pattern which could probably be due to the decrease in conductance of the sensor material. Hence the sensor B_2 was used for further studies.

5.2.4 Working concentration range and slope

The plot of the EMF versus the pCu^{2+} gave the calibration graph of the sensor (Figure 5.3) and from the graph, the slope was calculated. The sensor B_2 gave a good working concentration range of $1.0 \times 10^{-1} - 5.0 \times 10^{-6}$ with a Nernstian slope of 29.4 (±0.6) mV $decade^{-1}$. The detection limit was calculated from the graph by the intersection of the two extrapolated linear segments of the calibration plot and was found to be 2.2×10^{-6} M.

5.2.5 Response time

The practical response time for the B_2 sensor was obtained from the plot of the changes in EMF from the moment of addition of 1.0×10^{-5} M Cu^{2+} solution with respect to time (Figure 5.4) and was found to be 21 s. The practical reversibility required for the Cu^{2+} sensor to reach a potential within ±1 mV of the copper ion solution with a 10-fold difference in concentration was plotted as potential versus time and is shown as Figure 5.5. The potentials were found to remain constant for about 3 min. The sensing behaviour of the membrane remained unchanged when potentials were recorded either from low to high concentrations or vice versa.

5.2.6 Effect of pH and non aqueous media

The behaviour of the sensor B_2 was studied for two fixed concentrations, 1.0×10^{-2} M and 1.0×10^{-3} M, over a pH range of 2.0-8.0. The pH was adjusted by introducing small drops of nitric acid (1.0 M) or sodium hydroxide (1.0 M). The results shown in Figure 5.6 indicate that the potential remained constant over a pH range of 4.0-7.0, beyond which the potentials changed considerably. The observed drift at higher pH may be due to the formation of some hydroxyl complexes of Cu^{2+} ion in solution[94]. At lower pH, the sensor may be responding to H^+ ions.

The performance of the sensor B_2 was also investigated in partially non-aqueous media using methanol-water and ethanol-water mixtures. The results obtained are compiled in Table 5.2 and it was seen that up to 20% non-aqueous content no significant change occurs in the working concentration range or slope. However, above 20% non-aqueous content the slope and working concentration range gets affected which may be attributed to leaching of the ligand into the sample solution.

5.2.7 Potentiometric selectivity

Potentiometric selectivity coefficients describe the preference of the sensor towards a particular ion in presence of foreign ions. The potential response of the developed Cu^{2+} sensor, (B_2) was investigated in presence of foreign ions by using the fixed interference method[227,35]. The selectivity coefficients were determined at 1.0×10^{-2} M concentration of foreign ions and was calculated using the following equation.

$$K_{A,B}^{pot} = a_A / (a_B)^{z_A / z_B}$$

The selectivity coefficient values shown in Table 5.3 indicate that the developed Cu^{2+} sensor (B_2) shows very good selectivity to Cu^{2+} ions in the presence of Na^+, K^+, Ag^+, Mg^{2+}, Ca^{2+}, Ba^{2+}, Mn^{2+}, Co^{2+}, Ni^{2+}, Zn^{2+}, Hg^{2+} and moderate selectivity in the presence of Cd^{2+}, Pb^{2+}, $Fe^{2+}$and Fe^{3+}.

5.2.8 Lifetime or Shelf life

The same surface of the Cu^{2+} sensor could be used repeatedly for a period of 3 weeks. During this period, the sensor showed no significant deviation on the optimized response characteristics. The response of the sensor can be restored by squeezing out a small amount of the paste, scrapping off the excess and polishing the new surface against a filter paper. The sensor was stored in 1.0×10^{-1} M copper(II) nitrate solution when not in use.

5.2.9 Analytical applications

The developed Cu^{2+} sensor was found to work well under laboratory conditions. It was successfully applied to the determination of copper in a

sample of industrial effluent (sample from electroplating unit). The sample solution was prepared as discussed under Section 2.5.3 in Chapter 2. With the use of the calibration curve of the sensor, the copper content in the sample solution was obtained. The results presented in Table 5.4 show that this method is comparable to the standard ICP-AES method[2].

The developed Cu^{2+} sensor was successfully applied as an indicator electrode in conjuction with Ag|AgCl in the potentiometric titration of Cu^{2+} solution (5.0×10^{-3} M) with EDTA solution (1.0×10^{-2} M) at pH 5.0 and the resulting titration curve is shown as Figure 5.7. The end point corresponds to the 1:1 stoichiometry of the Cu-EDTA complex.

5.3 Sensors based on HPD

This ionophore HPD has been used to fabricate all the three types of sensors – viz. the PVC membrane, CPE-PVC and CMCPE type. The structure of HPD is shown as Figure 5.8. Figure 5.9, Figure 5.10 and Figure 5.11 show the potential response of the three types of sensors towards different cations. It was found that the sensors showed a Nernstian response to copper ions. This may be attributed to the selective complexation behaviour of the ionophore for Cu^{2+} over other metal ions, as well as the rapid exchange kinetics of the resulting complex.

5.3.1 Sensor membrane fabrication

The general method of fabrication of PVC membrane, CPE-PVC type and CMCPE type of sensors has been discussed under Section 2.6 in Chapter 2.

For the PVC membrane solution, the best plasticizing agent was found to be dioctyl phthalate (DOP) and the anionic excluder added was sodium

tetraphenylborate (NaTPB). The composition ratio for the PVC plasticized membrane solution that gave the best response in terms of slope, concentration range and response time was found to be 31:63:2:4 (PVC:DOP:NaTPB:HPD) (% w/w).

For the fabrication of PVC membrane sensor, membranes were cut out and stuck on to the open end of a Pyrex glass tube and the tube was filled with an internal solution of 1.0×10^{-1} M $Cu(NO_3)_2$.

In the case of CPE-PVC type of sensor, graphite was made a paste using paraffin oil. The polished sensor filled with carbon paste was dipped in to the optimized PVC membrane solution repeatedly till a thin film was formed on the working surface of the sensor.

In the case of CMCPE type of sensor, the ionophore and graphite were made a paste using paraffin oil. The paste was then packed into the open end of the capillary glass tube as detailed in Chapter 2. The best composition ratio for CMCPE type of sensor was found to be 80:20 (graphite:HPD).

The sensors so fabricated were conditioned by dipping it in a 1.0×10^{-1} M copper(II) nitrate solution. The equilibration time was 24 h for the case of PVC membrane sensor, 30 h for CPE-PVC sensor and 3 h for CMCPE type of sensor.

5.3.2 Potential measurement and calibration

Potentials were measured at 25±0.1 °C on a Toshniwal digital ion meter and on BAS Epsilon electrochemical workstation. An Ag|AgCl reference electrode was used in conjunction with the developed Cu^{2+} sensor.

The cell assembly for potentiometric measurements for the three types of sensors can be represented as follows:

Ag | AgCl (3.0 M KCl) | Cu^{2+} (0.1 M) | PVC membrane based on HPD | test solution | Ag | AgCl (3.0 M KCl)

Ag | AgCl (3.0 M KCl) | test solution | CPE-PVC based on HPD or CMCPE based on HPD

The performance of the developed Cu^{2+} sensor was investigated by measuring the potential in Cu^{2+} solutions (pH maintained at 5.0 by adding buffer) prepared in the concentration range $1.0 \times 10^{-1} - 1.0 \times 10^{-8}$ M. The solutions were stirred and stable potential reading was taken.

5.3.3 Optimization of membrane composition

Optimization of the membrane ingredients in the PVC membrane solution is crucial as amount of ionophore, nature of the membrane solvent (plasticizer), plasticizer/PVC ratio and nature of the additives used in toto, influence sensitivity and selectivity of the sensors. Table 5.5 consolidates the results of seven different compositions of PVC membrane prepared based on HPD for the fabrication the PVC membrane sensor and CPE-PVC sensor. The PVC membrane without plasticizer was stiff and with unequal thickness and the sensor, Pa_I, gave a sub Nernstian slope but on addition of a plasticizing agent, the membrane surface became smooth and the sensor showed improved response characteristics. From the results, it was found that among the four different plasticizers used, DOP was the most effective solvent mediator in preparation of the PVC membrane whiles the others gave

Non Nernstian slopes. The amount of the ionophore was also found to affect the sensitivity of the sensors. 4% was found to be the optimum amount of ionophore and further addition of ionophore content results in a diminished response from the sensors which may be due to the saturation of the membrane. The optimization of the permselectivity of the PVC membrane is known to be highly dependent on the incorporation of additional membrane components. The presence of lipophilic negatively charged additives (anionic excluders) improves the potentiometric behaviour of the PVC membrane by reducing the ohmic resistance, improving the response and selectivity as well as sensitivity[213-226]. A 2% of NaTPB was the anionic excluder added.

This optimized PVC membrane solution was used for the fabrication of the CPE-PVC type sensor. Thus sensors Pa_3 and Pb_2 were found to be the best among the various sensors of different compositions and they wee used for further studies.

The weight ratio of graphite to ionophore was varied to arrive at an optimum composition for CMCPE type of sensor. Table 5.6 presents the results of the effect on the response of six different CMCPE type of sensor with changes in the composition ratio of graphite to ionophore. A sensor without ionophore Pc_1 was first prepared and it was observed that there was no response to copper ions. It was found that the sensor Pc_4 with the composition ratio 80:20 (graphite:HPD) was the best in terms of response time, working concentration range and the Nernstian slope. On increasing the ionophore content, nonlinearity in the response of the sensor was observed which could probably be due to the decrease in conductance of the sensor material. Hence, the sensor Pc_4 was used for further studies.

5.3.4 Working concentration range and slope

The calibration graph which is the plot of EMF versus pCu^{2+} for the sensors Pa_3, Pb_2 and Pc_4 are shown as Figure 5.12, Figure 5.13 and Figure 5.14 where Pa_3, Pb_2 and Pc_4 denote PVC membrane sensor, CPE-PVC type and CMCPE type of sensor respectively. The working concentration range for the sensors Pa_3, Pb_2 and Pc_4 was found to be $1.0 \times 10^{-1} - 5.0 \times 10^{-7}$ M, $1.0 \times 10^{-1} - 1.0 \times 10^{-7}$ M and $1.0 \times 10^{-1} - 5.0 \times 10^{-7}$ M respectively. The slope calculated from the calibration graph was found to be 29.1 (±1.0) mV $decade^{-1}$, 29.9 (±0.8) mV $decade^{-1}$ and 30.0 (±0.5) mV $decade^{-1}$ for the sensors Pa_3, Pb_2 and Pc_4 respectively proving a Nernstian behaviour. The detection limit was calculated from the graph by the intersection of the two extrapolated linear segments of the calibration plot and was found to be 2.3×10^{-7} M, 6.6×10^{-8} M and 1.4×10^{-7} M for the sensors Pa_3, Pb_2 and Pc_4 respectively.

5.3.5 Response time

The plot of the changes in EMF from the moment of addition of 1.0×10^{-5} M Cu^{2+} solution with respect to time for the sensors Pa_3, Pb_2 and Pc_4 is depicted as Figure 5.15, Figure 5.16 and Figure 5.17. The practical response time for the sensors Pa_3, Pb_2 and Pc_4 was obtained from the plot and was found to be 15 s, 20 s and 25 s respectively. The practical reversibility of the sensors Pa_3, Pb_2 and Pc_4 were evaluated by taking measurements for Cu^{2+} solutions with a 10-fold difference in concentration in the sequence high-to-low concentration and vice versa. The EMF versus time traces for the sensors Pa_3, Pb_2 and Pc_4 are shown as Figure 5.18, Figure 5.19 and Figure 5.20. The potentials remained constant for about 3 min in the case of Pb_2 and Pc_4 sensors and 5 min for the Pa_3 sensor. The sensing behaviour of the

membrane remained unchanged when potentials were recorded either from low to high concentrations or vice versa.

5.3.6 Effect of pH and non aqueous media

The influence of pH on the EMF response of the sensors Pa_3, Pb_2 and Pc_4 was studied for two fixed concentrations, 1.0×10^{-3} M and 1.0×10^{-4} M, over a pH range of 2.0-9.2. The pH was adjusted by introducing small drops of nitric acid (1.0 M) or sodium hydroxide (1.0 M). The results for the sensors Pa_3, Pb_2 and Pc_4 are shown in Figure 5.21, Figure 5.22 and Figure 5.23. It was found that the potential remained constant over a pH range of 3.0-7.8, 3.0-7.0 and 3.2-6.8 for the sensors Pa_3, Pb_2 and Pc_4 respectively. The observed drift in potentials at higher pH may be due to the formation of some hydroxyl complexes of Cu^{2+} ion in solution while at lower pH there may be some interference from H^+ ions.

The performance of the sensors Pa_3, Pb_2 and Pc_4 was also investigated in partially non-aqueous media using methanol-water and ethanol-water mixtures. The results obtained are compiled in Table 5.7 and it was seen that no significant change occurs in the slope for the sensors up to 30% of non-aqueous content in the case of PVC membrane sensor Pa_3, 25% for CPE-PVC type sensor Pb_2 and the tolerance level was 15% for CMCPE type sensor Pc_4. However, above the tolerance level the slopes get affected which may be attributed to leaching of the ligand into the sample solution.

5.3.7 Potentiometric selectivity

The selectivity is the most important characteristic of a sensor as it determines the extent of the utility of the sensor in real sample measurement.

The potential response of the sensors Pa_3, Pb_2 and Pc_4 were investigated in presence of foreign ions by using the fixed interference method[227,35]. The selectivity coefficients were determined at 1.0×10^{-2} M concentration of foreign ions and was calculated using the following equation.

$$K_{A,B}^{pot} = a_A / (a_B)^{z_A / z_B}$$

The selectivity coefficient values are consolidated in Table 5.8. and the values indicate that all the three sensors Pa_3, Pb_2 and Pc_4 shows very good selectivity to Cu^{2+} ions in the presence of Na^+, K^+, Ag^+, Mg^{2+}, Ca^{2+}, Ba^{2+}, Mn^{2+}, Co^{2+}, Ni^{2+}, Zn^{2+}, Cd^{2+} and Hg^{2+} but only moderate selectivity in the presence of Pb^{2+} and Fe^{2+}.

5.3.8 Lifetime or Shelf life

The operative life time for the sensors Pa_3, Pb_2 and Pc_4 was found to be 5 months, 2 months and 6 weeks respectively. The sensors were all kept immersed in 1.0×10^{-1} M copper(II) nitrate solution when not in use. The surface of CMCPE type sensor could be renewed by squeezing out a small amount of the paste, scrapping off the excess, polishing the new surface against a filter paper and equilibrating the sensor in the metal salt solution for 3h.

5.3.9 Analytical applications

The utility of the sensors Pa_3, Pb_2 and Pc_4 was further investigated in the determination of copper(II) in water sample collected from the nearby pond which is very close to an electroplating unit. The sample was prepared as explained under Section 2.5.3 in Chapter2. The results presented in Table 5.9 show that this method is comparable to the standard ICP-AES method[2].

The sensors Pa_3, Pb_2 and Pc_4 were successfully applied as an indicator electrode in conjuction with Ag|AgCl in the potentiometric titration of copper(II) nitrate solution at pH 5.0. The titration curves for the sensors Pa_3, Pb_2 and Pc_4 are depicted in Figure 5.24, Figure 5.25 and Figure 5.26 respectively. The titration plots obtained were all of the standard sigmoid shape and the end point corresponds to 1:1 stoichiometry of Cu-EDTA complex.

5.4 A comparative study among the sensors B_2, Pa_3, Pb_2 and Pc_4 and to some of the reported sensors

All the four sensors B_2, Pa_3, Pb_2 and Pc_4 are found to have very good response characteristics. Table 5.10 consolidates the response characteristics of the sensors B_2, Pa_3, Pb_2 and Pc_4. Between the two ionophores, HIB and HPD, the sensors based on HPD show better response characteristics in all respects. Among the different types of sensors fabricated based on HPD, the CPE-PVC type sensor is better in terms of working concentration range and detection limit. In terms of response time, CMCPE type of sensor Pc_4 gave the best result of 15 s. The PVC membrane sensor Pa_3 has the longest shelf life of 5 months but though the shelf life for the CMCPE type sensor Pc_4 is only 6 weeks, the surface could be renewed by cutting off a little of the paste, polishing it on a smooth surface and reconditioning it on 1.0×10^{-1} M of copper(II) nitrate solution. In terms of pH range, Pa_3 gave the widest range of pH. Table 5.11 lists the comparative study of the characteristics of developed sensors with some of the reported sensors for Cu^{2+}. It can be seen that the developed sensors, especially sensors Pa_3 and Pb_2, are superior in terms of working concentration range[84,88,90,98,105,108,112,115,119,123],

slope[84,88,90,98,105,108,112,115], life time[84,88,90,98,105,108,109] and pH range[88,90,98,108,119,123].

Figures

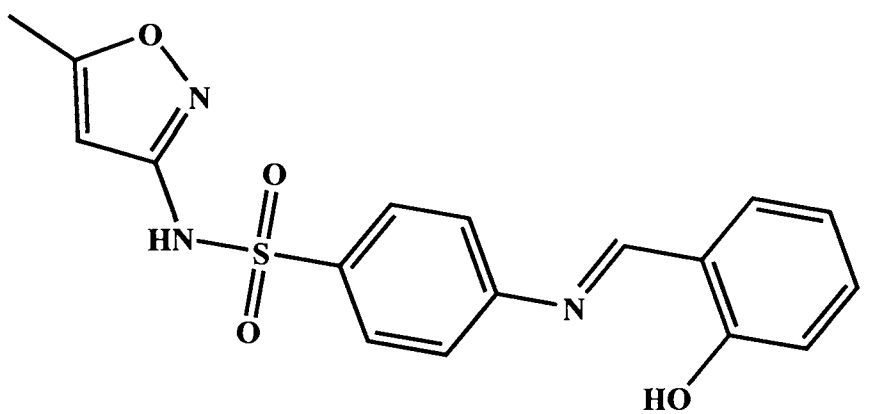

Figure 5.1 – Structure of the ionophore HIB

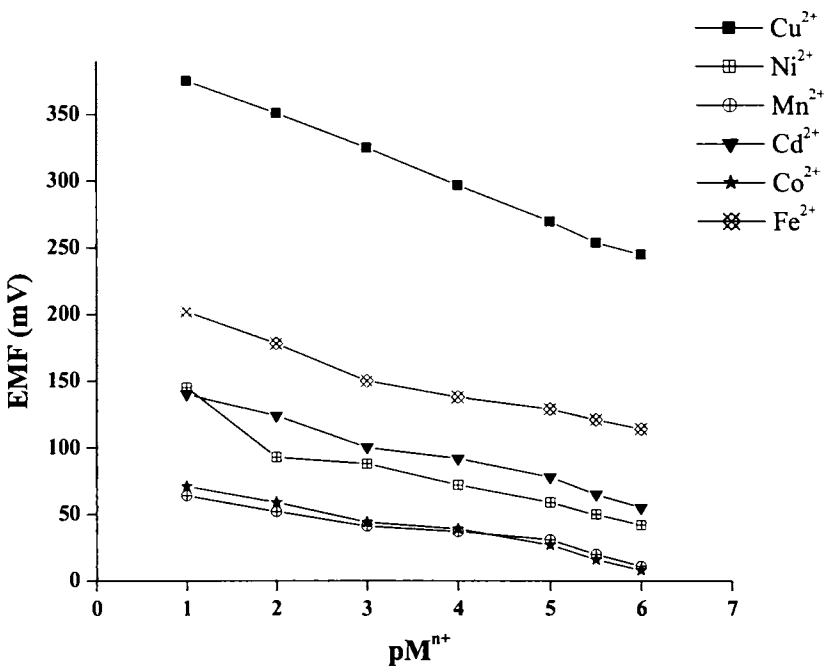

Figure 5.2 – Potential response of the various sensors based on HIB.
Conditions: composition ratio 5% HIB:95% graphite;
conditioned in 1.0×10^{-1} M of the corresponding cation solution for 2 h

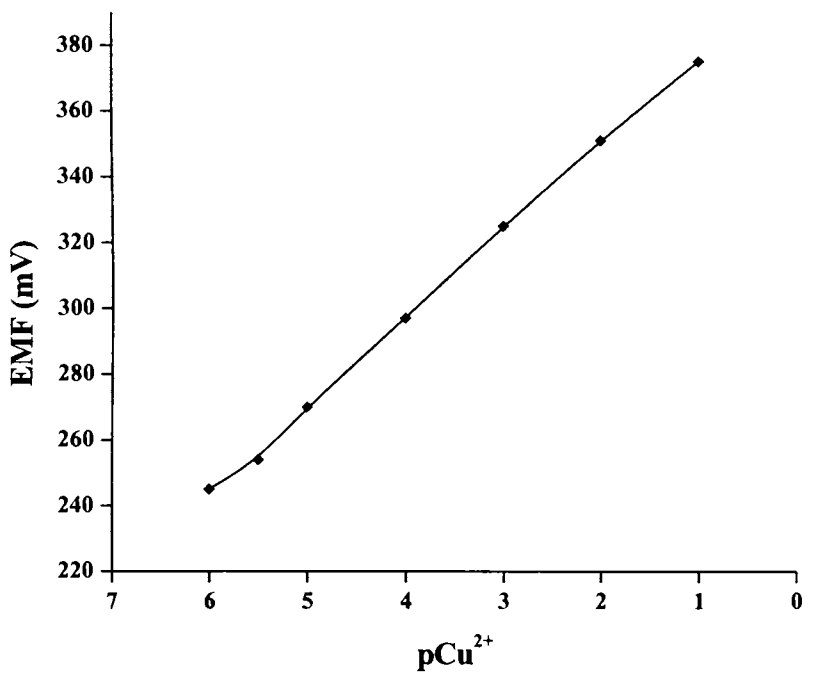

Figure 5.3 – Calibration graph of the sensor B_2 based on HIB

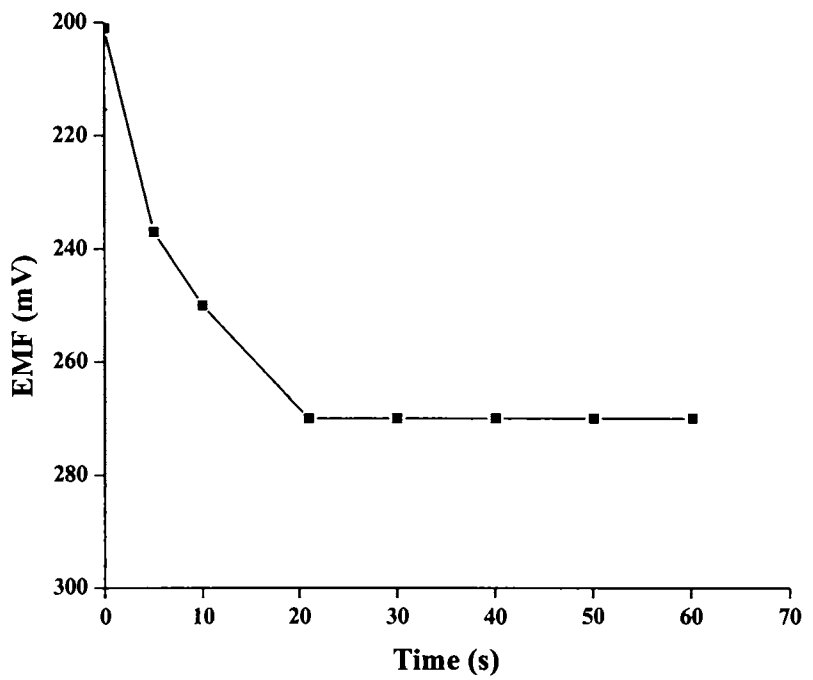

Figure 5.4 – Practical response time of the sensor B_2 from the moment of addition of Cu^{2+} (1.0×10^{-5} M) solution

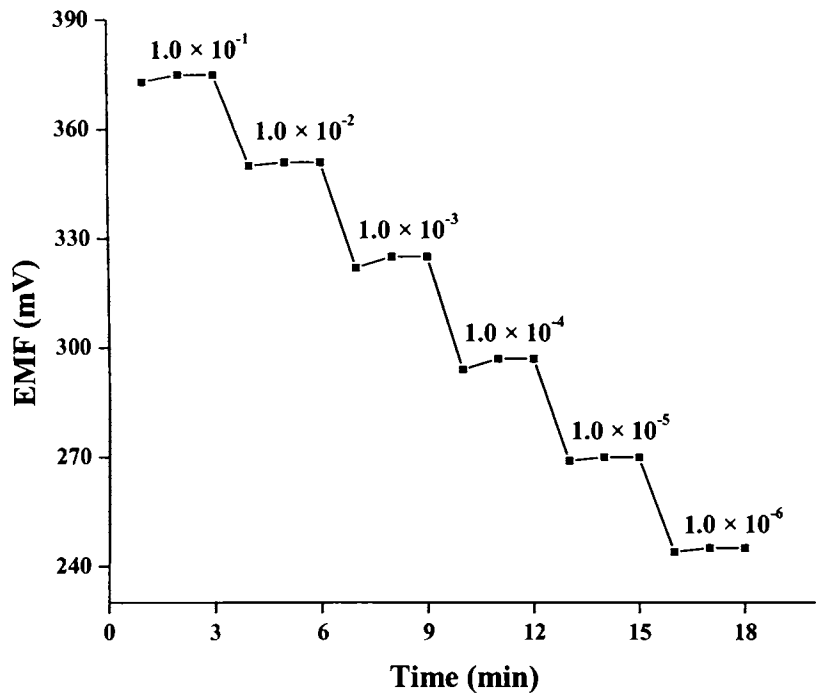

Figure 5.5 – Dynamic response time of the sensor B_2 for reversibility with step changes in concentration of Cu^{2+} (1.0×10^{-6} to 1.0×10^{-1} M)

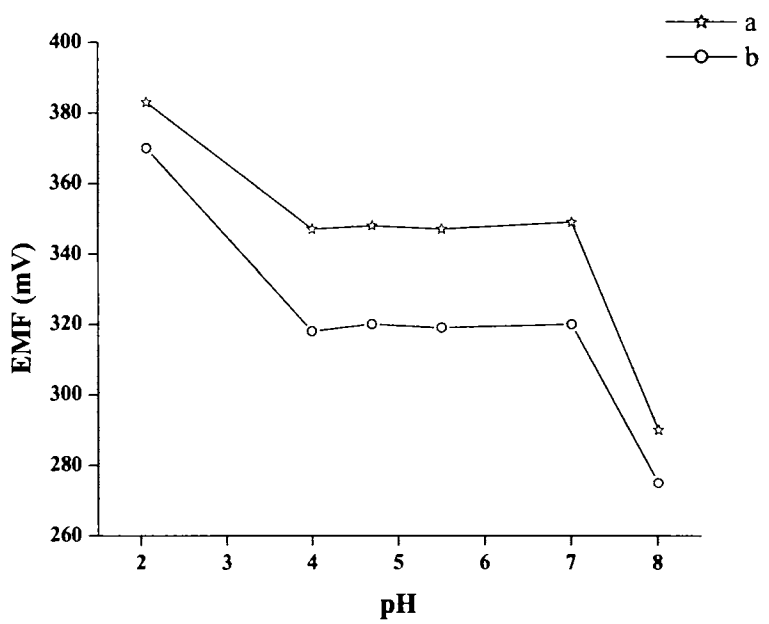

Figure 5.6 – Effect of pH on the cell potential of the sensor B_2 based on HIB at 1.0×10^{-2} M (a) and 1.0×10^{-3} M (b)

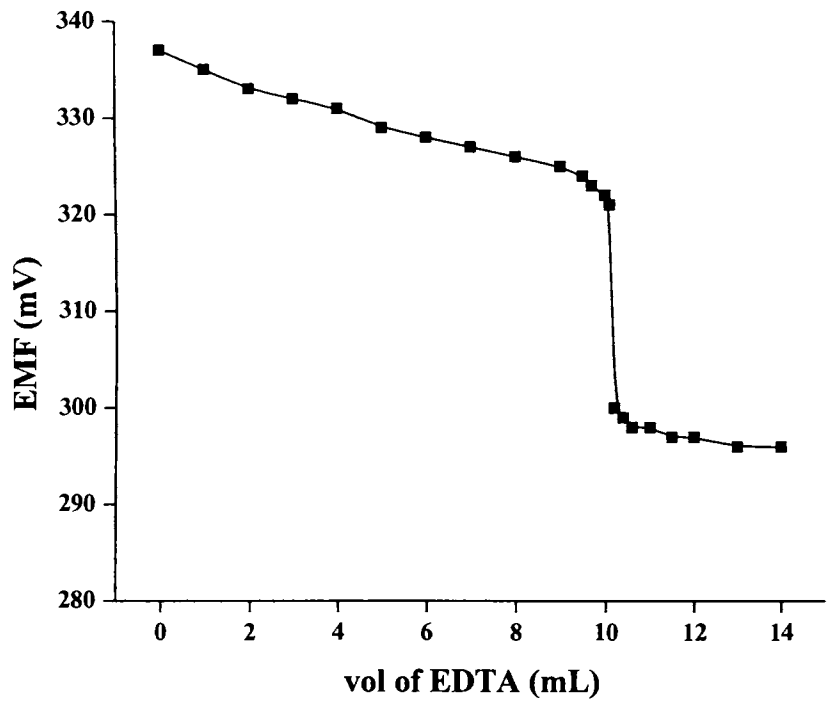

Figure 5.7 – Potentiometric titration curve of 20.0 mL of 5.0×10^{-3} M Cu^{2+} solution with 1.0×10^{-2} M EDTA using the sensor B_2 as an indicator electrode at pH 5.0.

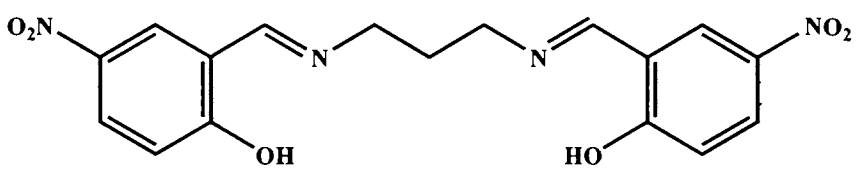

Figure 5.8 – Structure of the ionophore HPD

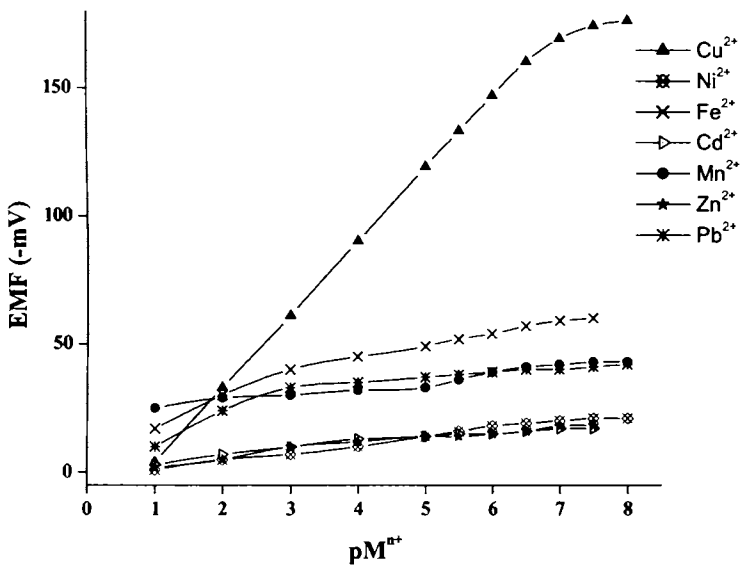

Figure 5.9- Potential response of the various PVC membrane sensors based on HPD.

Conditions: membrane composition ratio 31% PVC:63% DOP:2% NaTPB:4% HPD; internal solution 1.0×10^{-1} M of each cation used and conditioned in 1.0×10^{-1} M of the corresponding cation solution for 24 h

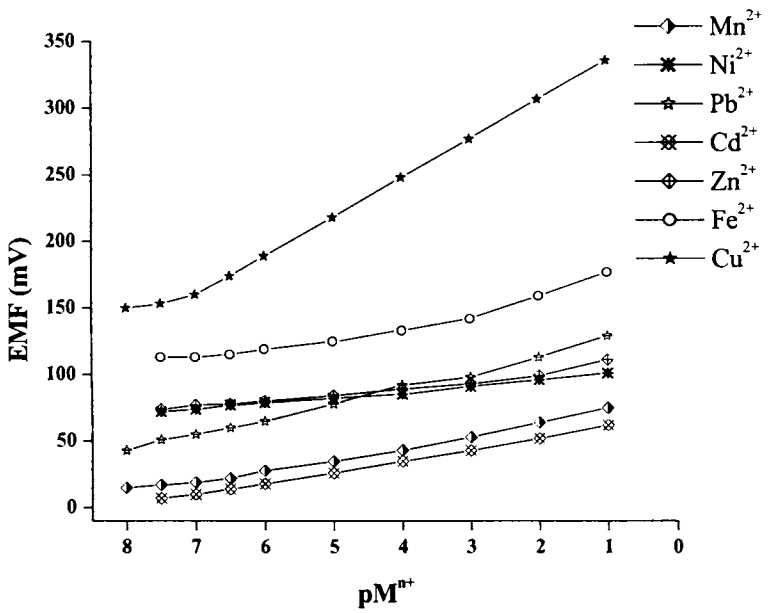

Figure 5.10- Potential response of the various CPE-PVC type sensors based on HPD.

Conditions: membrane composition ratio 31% PVC:63% DOP:2% NaTPB:4% HPD; conditioned in 1.0×10^{-1} M of the corresponding cation solution for 30 h

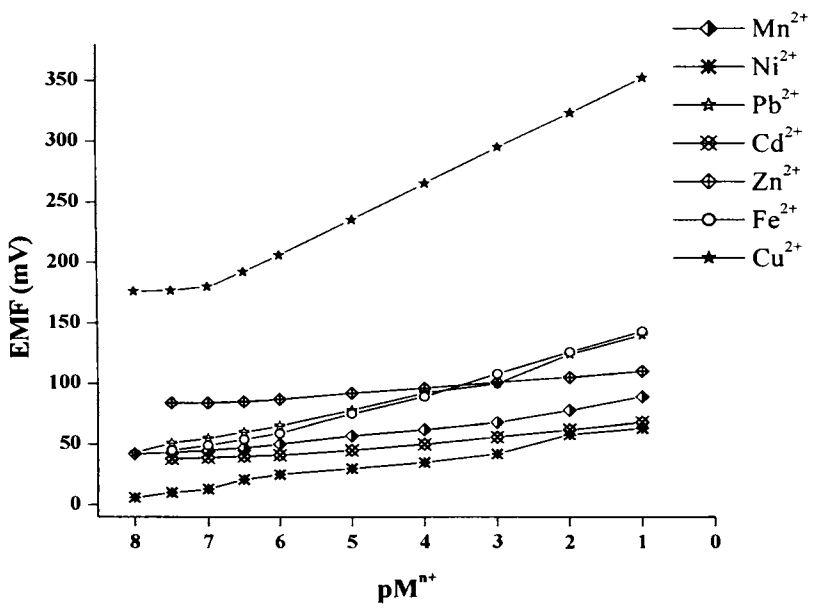

Figure 5.11 – Potential response of various CMCPE type sensors based on HPD.

Conditions: composition ratio 20% HPD:80% graphite; conditioned in 1.0×10^{-1} M of the corresponding cation solution for 3 h

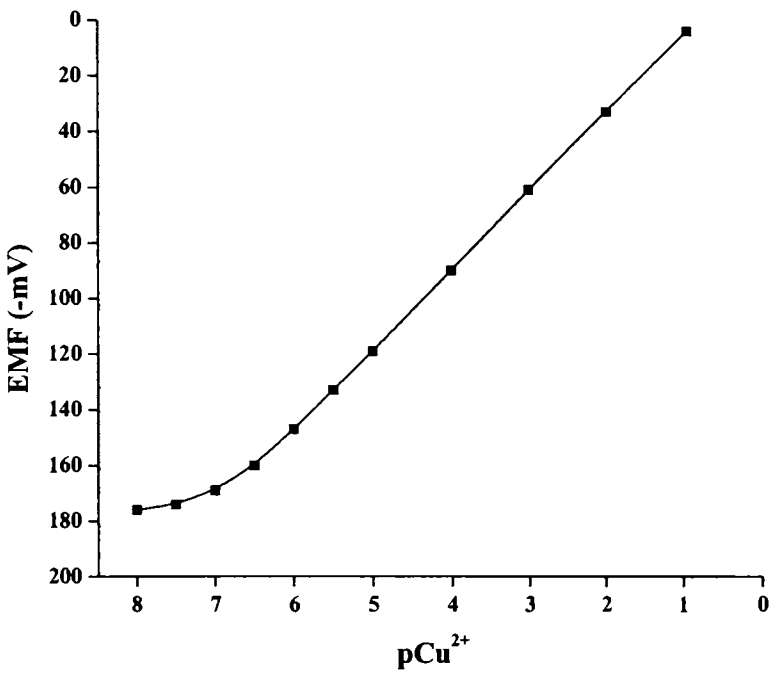

Figure 5.12 – Calibration graph of the PVC membrane sensor Pa_3 based on HPD

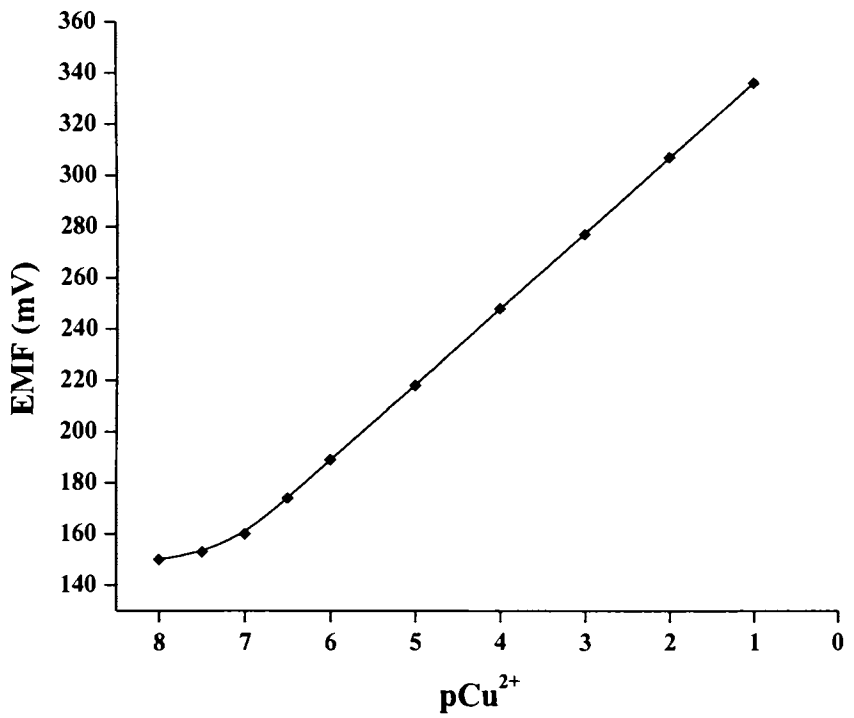

Figure 5.13 – Calibration graph of the CPE-PVC type sensor Pb_2 based on HPD

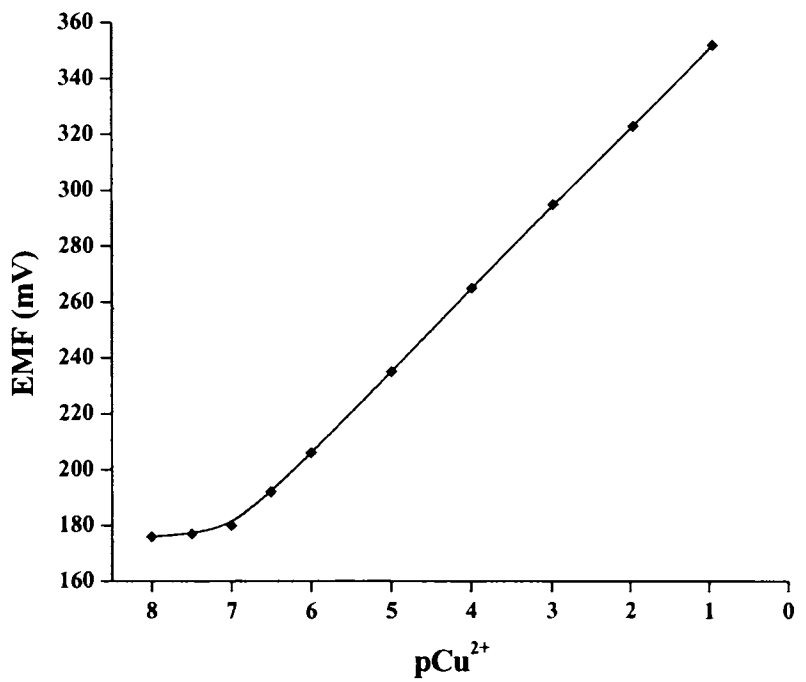

Figure 5.14 – Calibration graph of the CMCPE type sensor Pc_4 based on HPD

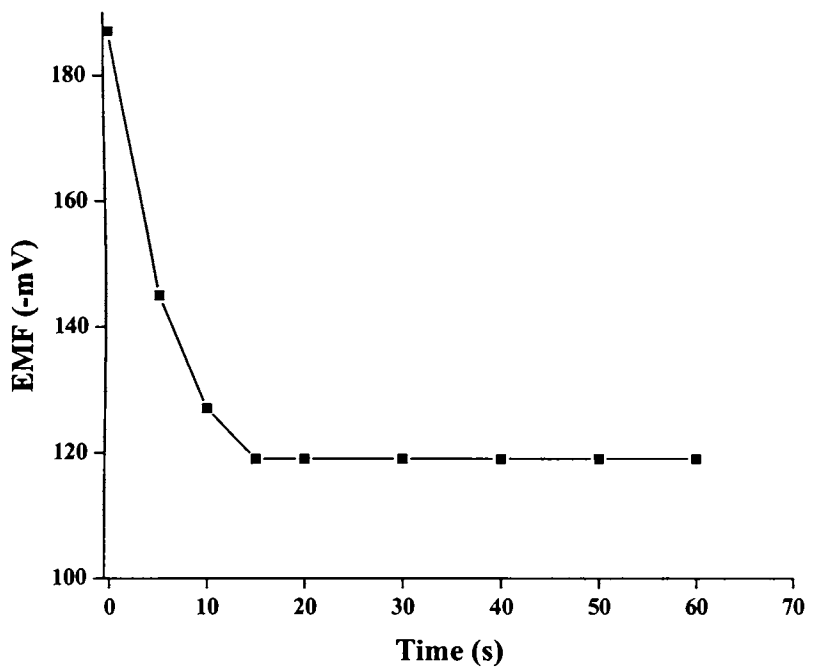

Figure 5.15 – Practical response time of the PVC membrane sensor Pa_3 based on HPD from the moment of addition of Cu^{2+} (1.0×10^{-5} M) solution

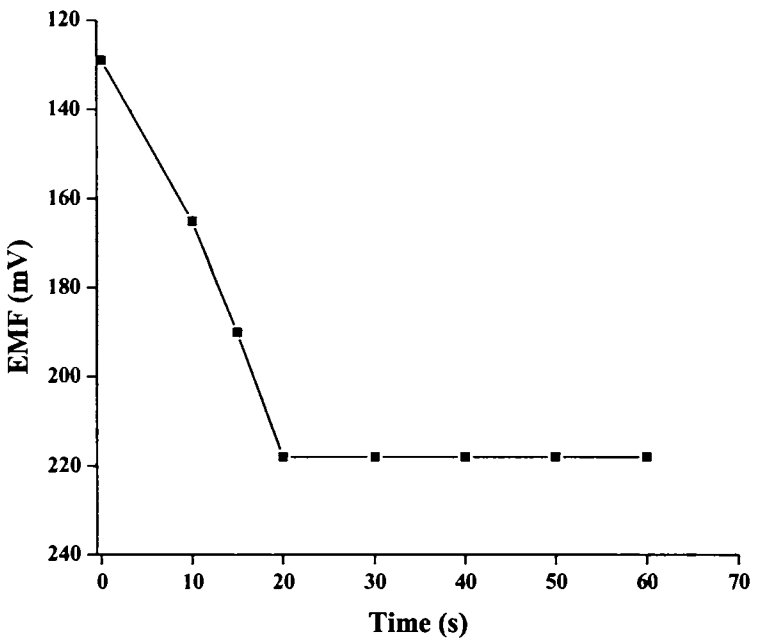

Figure 5.16 – Practical response time of the CPE-PVC type sensor Pb_2 based on HPD from the moment of addition of Cu^{2+} (1.0×10^{-5} M) solution

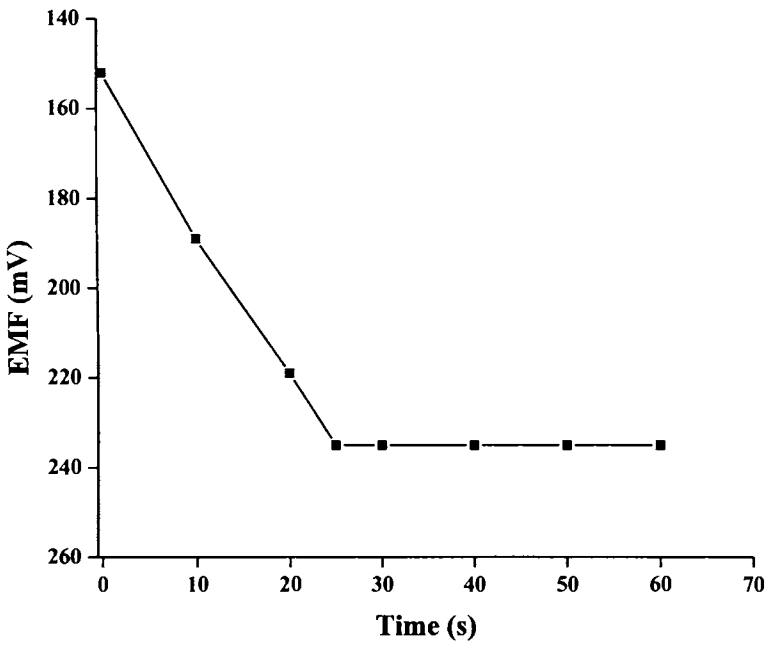

Figure 5.17 – Practical response time of the CMCPE type sensor Pc_4 based on HPD from the moment of addition of Cu^{2+} (1.0×10^{-5} M) solution

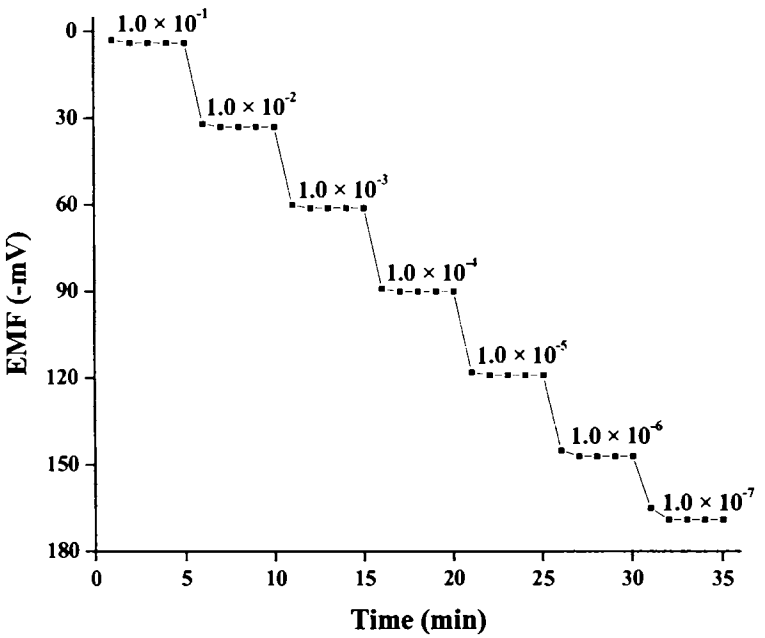

Figure 5.18 – Dynamic response time of the PVC membrane sensor Pa_3 based on HPD for reversibility with step changes in concentration of Cu^{2+} (1.0×10^{-7} to 1.0×10^{-1} M)

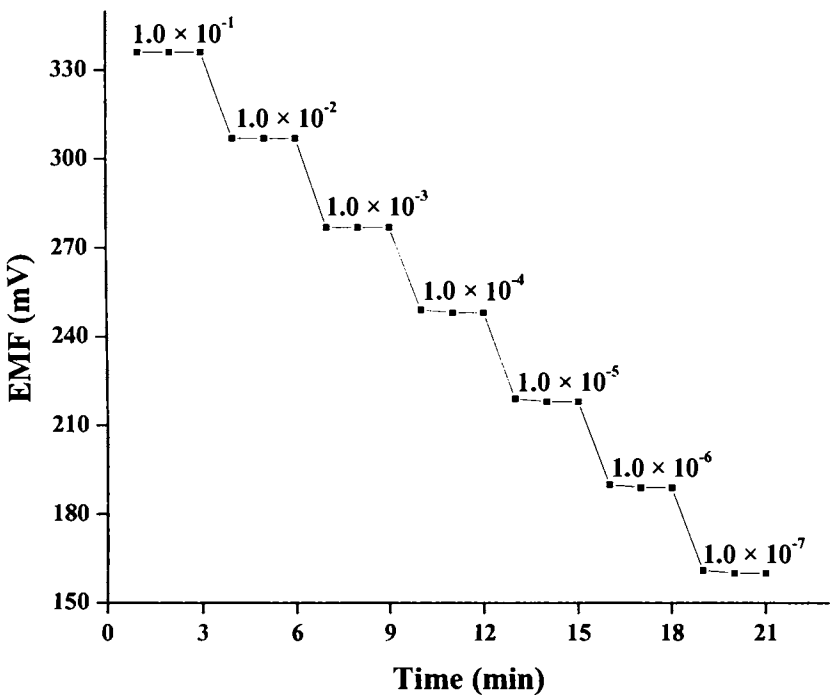

Figure 5.19 – Dynamic response time of the CPE-PVC type sensor Pb_2 based on HPD for reversibility with step changes in concentration of Cu^{2+} (1.0×10^{-7} to 1.0×10^{-1} M)

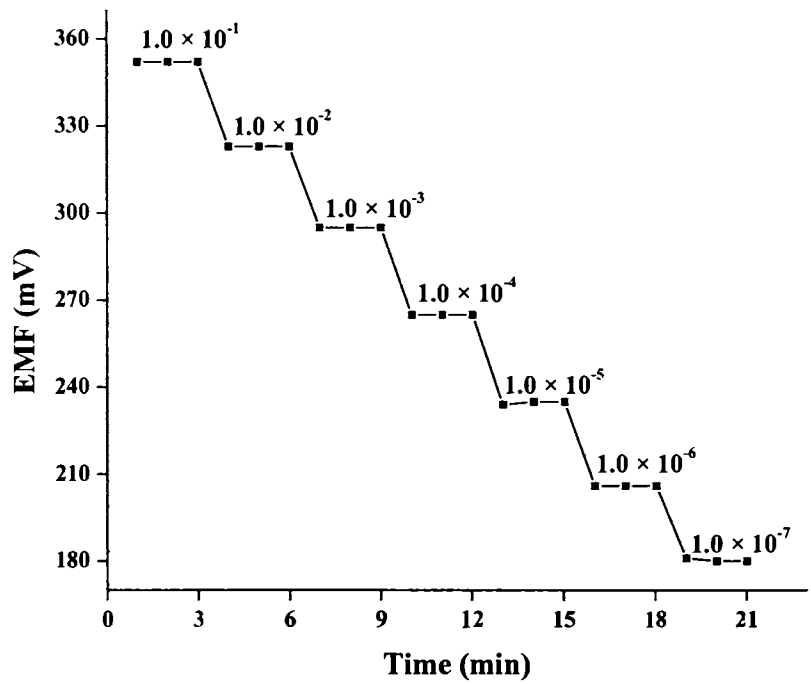

Figure 5.20 – Dynamic response time of the CMCPE type sensor Pc_4 based on HPD for reversibility with step changes in concentration of Cu^{2+} (1.0×10^{-7} to 1.0×10^{-1} M)

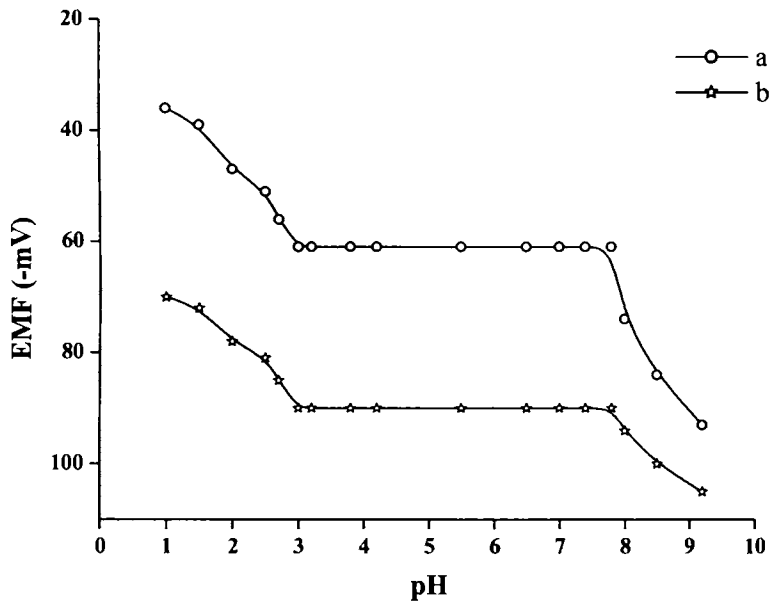

Figure 5.21 – Effect of pH on the cell potential of the PVC membrane sensor Pa_3 based on HPD at 1.0×10^{-3} M (a) and 1.0×10^{-4} M (b)

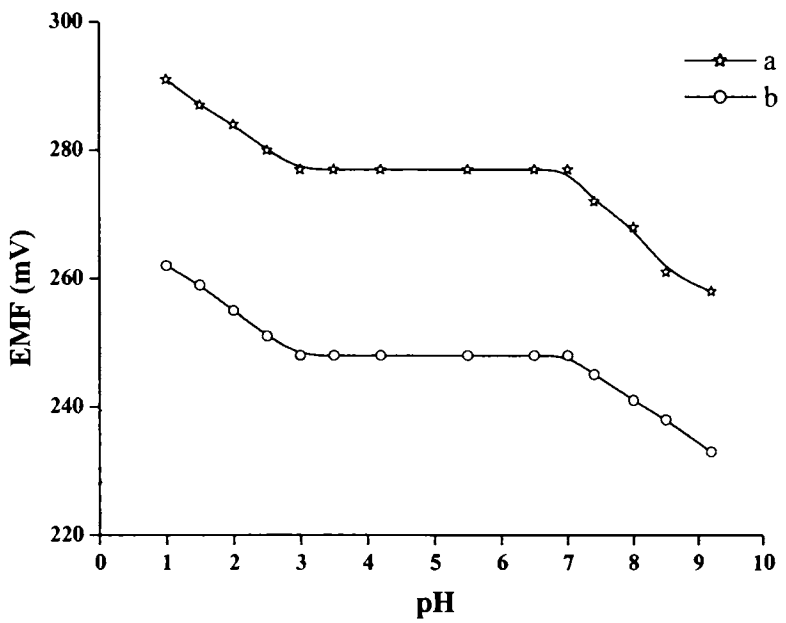

Figure 5.22 – Effect of pH on the cell potential of the CPE-PVC type sensor Pb_2 based on HPD at 1.0×10^{-3} M (a) and 1.0×10^{-4} M (b)

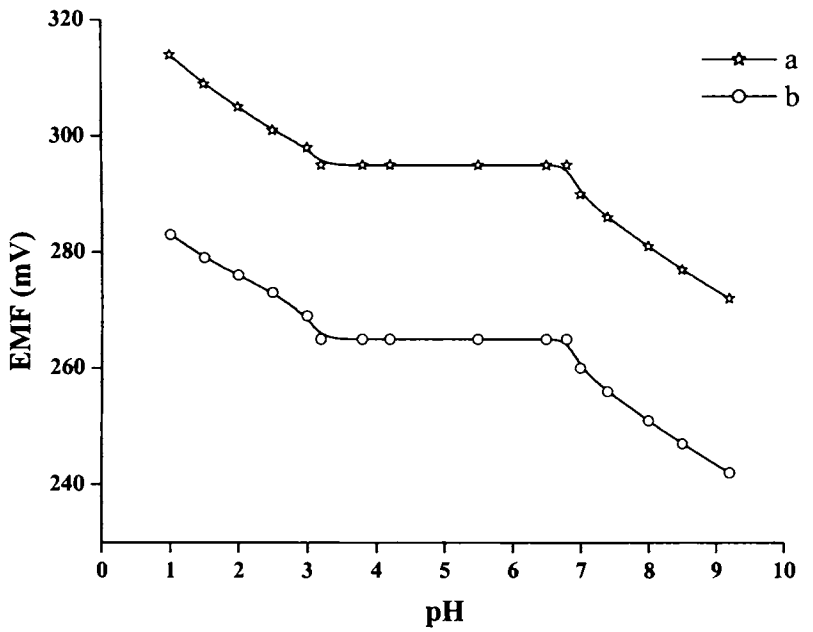

Figure 5.23 – Effect of pH on the cell potential of the CMCPE type sensor Pc_4 based on HPD at 1.0×10^{-3} M (a) and 1.0×10^{-4} M (b)

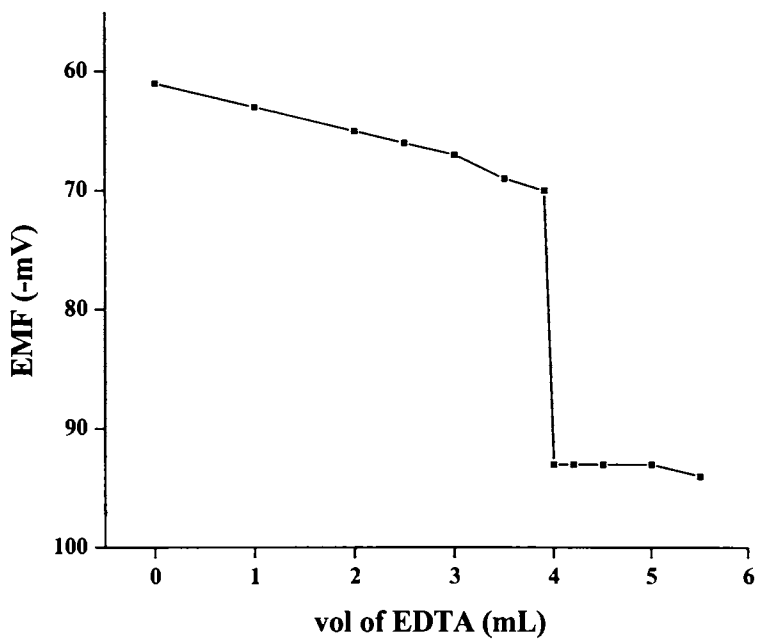

Figure 5.24 – Potentiometric titration curve of 40.0 mL of 1.0×10^{-3} M Cu^{2+} solution with 1.0×10^{-2} M EDTA using the PVC membrane sensor Pa_3 as an indicator electrode at pH 5.0.

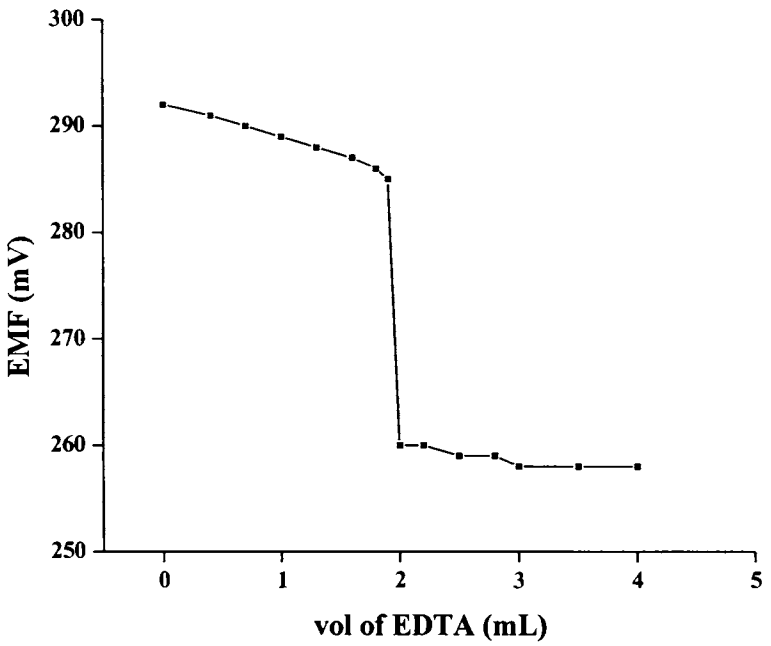

Figure 5.25 – Potentiometric titration curve of 20.0 mL of 5.0×10^{-3} M Cu^{2+} solution with 5.0×10^{-2} M EDTA using the CPE-PVC type sensor Pb_2 as an indicator electrode at pH 5.0.

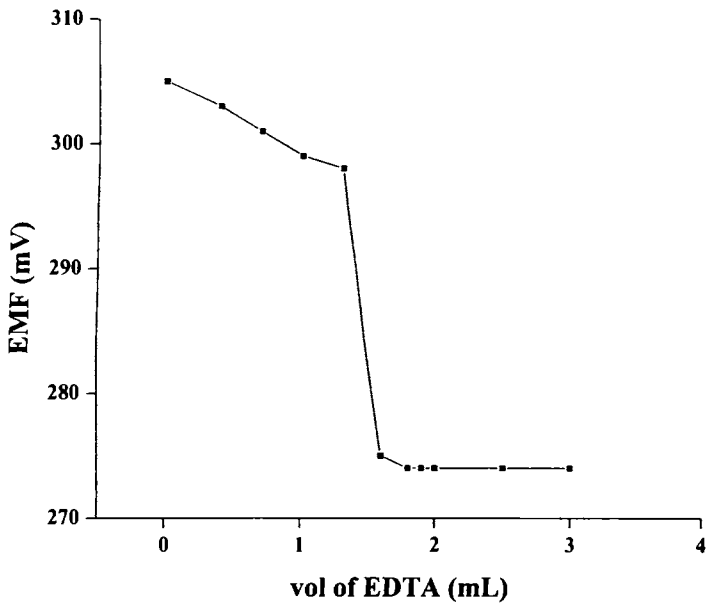

Figure 5.26 – Potentiometric titration curve of 20.0 mL of 4.0×10^{-3} M Cu^{2+} solution with 5.0×10^{-2} M EDTA using the CMCPE type sensor Pc_4 as an indicator electrode at pH 5.0.

Table 5.1 – Optimization of the ionophore composition for the CMCPE type of sensor based on HIB[a]

Sensor	Ionophore	Graphite	Working concentration range (M)	Slope (mV decade^{-1})	Response time (s)
B_1	0	100	$1.0 \times 10^{-1} - 9.9 \times 10^{-4}$	2.2(±0.2)	90
B_2	5	95	$1.0 \times 10^{-1} - 2.2 \times 10^{-6}$	29.4(±0.6)	21
B_3	10	90	$1.0 \times 10^{-1} - 6.3 \times 10^{-6}$	30.4(±0.9)	35
B_4	20	80	$1.0 \times 10^{-1} - 4.9 \times 10^{-5}$	22.9(±0.4)	28
B_5	30	70	$1.0 \times 10^{-2} - 3.6 \times 10^{-5}$	23.5(±0.1)	32
B_6	50	50	$1.0 \times 10^{-1} - 9.1 \times 10^{-4}$	26.9(±0.2)	39

[a] Values in parentheses are RSDs based on three replicates.

Table 5.2 – Effect of partially non-aqueous medium on the working of the developed sensor, B_2

Non-aqueous content (% v/v)	Slope (mV decade^{-1})	Working concentration range (M)
0	29.4	$1.0 \times 10^{-1} - 2.2 \times 10^{-6}$
Ethanol		
10	29.3	$1.0 \times 10^{-1} - 5.4 \times 10^{-6}$
20	29.2	$1.0 \times 10^{-1} - 5.6 \times 10^{-6}$
25	28.0	$1.0 \times 10^{-1} - 9.3 \times 10^{-5}$
Methanol		
10	29.3	$1.0 \times 10^{-1} - 5.1 \times 10^{-6}$
20	29.1	$1.0 \times 10^{-1} - 4.8 \times 10^{-6}$
25	28.1	$1.0 \times 10^{-1} - 9.4 \times 10^{-5}$

Table 5.3 – Selectivity coefficients for the developed sensor B_2 using fixed interference method at 1.0×10^{-2} M concentration of interfering ion.

Interfering ion (X)	$K^{pot}_{Cu^{2+},X}$
Na^+	4.6×10^{-3}
K^+	9.2×10^{-4}
Ag^+	3.0×10^{-3}
Mg^{2+}	4.6×10^{-3}
Ca^{2+}	3.3×10^{-3}
Ba^{2+}	5.1×10^{-3}
Mn^{2+}	8.1×10^{-3}
Co^{2+}	3.4×10^{-3}
Ni^{2+}	4.3×10^{-3}
Zn^{2+}	8.8×10^{-3}
Cd^{2+}	1.3×10^{-1}
Hg^{2+}	4.5×10^{-3}
Pb^{2+}	2.8×10^{-1}
Fe^{2+}	5.6×10^{-1}
Fe^{3+}	3.1×10^{-1}

Table 5.4 – Determination of the Cu^{2+} content in waste sample from electroplating unit

Sample	Developed sensor* ppm	ICP-AES ppm
Effluent sample	5.79 ± 0.02	5.81

* RSDs based on three replicates

Table 5.5 – Optimization of the PVC membrane ingredients for the PVC membrane (Pa) and CPE-PVC type (Pb) of sensors based on HPD[a]

Sensor	% w/w composition of each membrane				Working concentration range (M)	Slope (mV decade^{-1})	Response time (s)
	PVC	HPD	Plasticizer	NaTPB			
Pa_1	94	4	0	2	$1.0 \times 10^{-1} - 2.5 \times 10^{-6}$	25.2(±0.8)	50
Pa_2	31	2	DOP, 65	2	$1.0 \times 10^{-1} - 9.4 \times 10^{-7}$	27.8(±1.1)	32
Pa_3	31	4	DOP, 63	2	$1.0 \times 10^{-1} - 2.3 \times 10^{-7}$	29.1(±1.0)	25
Pa_4	31	6	DOP, 61	2	$1.0 \times 10^{-1} - 1.1 \times 10^{-6}$	27.9(±0.2)	22
Pa_5	31	4	DBP, 63	2	$1.0 \times 10^{-1} - 5.2 \times 10^{-6}$	23.7(±0.7)	28
Pa_6	31	4	DOA, 63	2	$1.0 \times 10^{-1} - 2.7 \times 10^{-5}$	22.9(±0.3)	45
Pa_7	31	4	DOS, 63	2	$1.0 \times 10^{-1} - 7.1 \times 10^{-6}$	19.3(±0.5)	25
Pb_1	0	0	0	0	$1.0 \times 10^{-1} - 1.0 \times 10^{-4}$	~0.0	200
Pb_2	31	4	DOP, 63	2	$1.0 \times 10^{-1} - 6.6 \times 10^{-8}$	29.9(±0.8)	20

[a] Values in parentheses are RSDs based on three replicates.

Table 5.6 – Optimization of the ionophore composition for the CMCPE type of sensor based on HPD[a]

Sensor	Ionophore	Graphite	Working concentration range (M)	Slope (mV decade^{-1})	Response time (s)
Pc_1	0	100	$1.0 \times 10^{-2} - 1.0 \times 10^{-4}$	1.6(±0.2)	120
Pc_2	5	95	$1.0 \times 10^{-1} - 4.4 \times 10^{-5}$	22.9(±0.7)	65
Pc_3	10	90	$1.0 \times 10^{-1} - 5.8 \times 10^{-6}$	27.3(±0.4)	50
Pc_4	20	80	$1.0 \times 10^{-1} - 1.4 \times 10^{-7}$	30.0(±0.5)	15
Pc_5	30	70	$1.0 \times 10^{-2} - 2.9 \times 10^{-5}$	26.8(±0.6)	25
Pc_6	50	50	$1.0 \times 10^{-3} - 7.6 \times 10^{-4}$	35.1(±0.4)	40

[a] Values in parentheses are RSDs based on three replicates.

Table 5.7 – Effect of partially non-aqueous medium on the slope of the sensors Pa_3, Pb_2 and Pc_4

Non-aqueous content (% v/v)	Slope (mV decade^{-1})		
	Pa_3	Pb_2	Pc_4
0	29.1	29.9	30.0
Ethanol			
10	29.1	29.7	29.7
15	29.0	29.3	29.1
25	28.7	28.9	28.1
30	28.4	27.3	26.5
40	27.2	26.1	24.7
Methanol			
10	29.0	29.8	29.8
15	28.8	29.5	29.1
25	28.5	29.0	28.3
30	28.3	28.1	26.4
40	27.4	26.3	24.1

Table 5.8 – Selectivity coefficients for the sensors Pa_3, Pb_2 and Pc_4 using fixed interference method at 1.0×10^{-2} M concentration of interfering ion.

Interfering ion (X)	Pa_3	Pb_2	Pc_4
Na^+	0.4×10^{-2}	1.8×10^{-2}	2.1×10^{-2}
K^+	8.1×10^{-3}	7.4×10^{-3}	8.5×10^{-3}
Ag^+	2.1×10^{-3}	3.2×10^{-3}	3.7×10^{-3}
Mg^{2+}	2.5×10^{-3}	1.9×10^{-3}	1.4×10^{-3}
Ca^{2+}	7.2×10^{-4}	9.0×10^{-4}	7.9×10^{-4}
Ba^{2+}	7.3×10^{-3}	6.8×10^{-3}	5.9×10^{-3}
Mn^{2+}	7.7×10^{-3}	9.4×10^{-3}	6.7×10^{-3}
Co^{2+}	7.4×10^{-3}	8.1×10^{-3}	5.9×10^{-3}
Ni^{2+}	9.9×10^{-3}	7.4×10^{-3}	7.9×10^{-3}
Zn^{2+}	4.9×10^{-4}	3.5×10^{-4}	4.7×10^{-4}
Cd^{2+}	9.3×10^{-4}	8.8×10^{-4}	8.1×10^{-4}
Hg^{2+}	1.5×10^{-3}	1.0×10^{-3}	2.3×10^{-3}
Pb^{2+}	1.2×10^{-1}	3.9×10^{-1}	2.4×10^{-1}
Fe^{2+}	6.0×10^{-1}	5.1×10^{-1}	5.8×10^{-1}

Table 5.7 – Effect of partially non-aqueous medium on the slope of the sensors Pa_3, Pb_2 and Pc_4

Non-aqueous content (% v/v)	Slope (mV decade^{-1})		
	Pa_3	Pb_2	Pc_4
0	29.1	29.9	30.0
Ethanol			
10	29.1	29.7	29.7
15	29.0	29.3	29.1
25	28.7	28.9	28.1
30	28.4	27.3	26.5
40	27.2	26.1	24.7
Methanol			
10	29.0	29.8	29.8
15	28.8	29.5	29.1
25	28.5	29.0	28.3
30	28.3	28.1	26.4
40	27.4	26.3	24.1

Table 5.8 – Selectivity coefficients for the sensors Pa_3, Pb_2 and Pc_4 using fixed interference method at 1.0×10^{-2} M concentration of interfering ion.

Interfering ion (X)	Pa_3	Pb_2	Pc_4
Na^+	0.4×10^{-2}	1.8×10^{-2}	2.1×10^{-2}
K^+	8.1×10^{-3}	7.4×10^{-3}	8.5×10^{-3}
Ag^+	2.1×10^{-3}	3.2×10^{-3}	3.7×10^{-3}
Mg^{2+}	2.5×10^{-3}	1.9×10^{-3}	1.4×10^{-3}
Ca^{2+}	7.2×10^{-4}	9.0×10^{-4}	7.9×10^{-4}
Ba^{2+}	7.3×10^{-3}	6.8×10^{-3}	5.9×10^{-3}
Mn^{2+}	7.7×10^{-3}	9.4×10^{-3}	6.7×10^{-3}
Co^{2+}	7.4×10^{-3}	8.1×10^{-3}	5.9×10^{-3}
Ni^{2+}	9.9×10^{-3}	7.4×10^{-3}	7.9×10^{-3}
Zn^{2+}	4.9×10^{-4}	3.5×10^{-4}	4.7×10^{-4}
Cd^{2+}	9.3×10^{-4}	8.8×10^{-4}	8.1×10^{-4}
Hg^{2+}	1.5×10^{-3}	1.0×10^{-3}	2.3×10^{-3}
Pb^{2+}	1.2×10^{-1}	3.9×10^{-1}	2.4×10^{-1}
Fe^{2+}	6.0×10^{-1}	5.1×10^{-1}	5.8×10^{-1}

Table 5.9 – Determination of the Cu^{2+} content in water sample from a nearby pond

Sample	Pa_3* ppm	Pb_2* ppm	Pc_4* ppm	ICP-AES ppm
Water sample	2.00 ± 0.01	2.02 ± 0.02	2.01 ± 0.04	1.94

* RSDs based on three replicates.

Table 5.10 – Response characteristics of the sensors B_2, Pa_3, Pb_2 and Pc_4

Parameter	Response characteristics			
	B_2	Pa_3	Pb_2	Pc_4
Working concentration range (M)	1.0×10^{-1} – 5.0×10^{-6}	1.0×10^{-1} – 5.0×10^{-7}	1.0×10^{-1} – 1.0×10^{-7}	1.0×10^{-1} – 5.0×10^{-7}
Slope (mV decade^{-1})	29.4 ± 0.6	29.1 ± 1.0	29.9 ± 0.8	30.0 ± 0.5
Detection limit (M)	2.2×10^{-6}	2.3×10^{-7}	6.6×10^{-8}	1.4×10^{-7}
Response time	21 s	25 s	20 s	15 s
pH range	4.0-7.0	3.0-7.8	3.0-7.0	3.0-6.8
Non aqueous tolerance limit	20%	30%	25%	15%
Shelf life	3 weeks	5 months	2 months	1.5 months

Table 5.11 –Comparison of characteristics of the sensor with some reported sensors

No.	Working concentration range (M)	Slope (mV decade^{-1})	pH range	Lifetime	Ref. No.
1	$1.0 \times 10^{-1} - 1.0 \times 10^{-5}$	Non-Nernstian	2.0-5.4	NM*	84
2	$1.0 \times 10^{-2.5} - 1.0 \times 10^{-4.5}$	Near Nernstian	6.0-7.2	NM	98
3	$1.0 \times 10^{-2} - 5.0 \times 10^{-5}$	Near Nernstian	3.7-5.6	NM	108
4	$1.0 \times 10^{-1} - 3.2 \times 10^{-5}$	Near Nernstian	3.5-6.0	3 months	90
5	$1.0 \times 10^{-1} - 6.0 \times 10^{-6}$	Near Nernstian	4.0-7.5	6 months	115
6	$1.0 \times 10^{-2} - 1.0 \times 10^{-5}$	Near Nernstian	NM	NM	88
7	$1.0 \times 10^{-1} - 1.0 \times 10^{-6}$	Near Nernstian	3.0-6.5	2 months	105
8	$1.0 \times 10^{-1} - 7.9 \times 10^{-6}$	Nernstian	2.1-6.3	6 months	112
9	$1.0 \times 10^{-1} - 5.0 \times 10^{-6}$	Nernstian	1.9-5.2	>4months	116
10	$1.0 \times 10^{-1} - 1.0 \times 10^{-5}$	Nernstian	3.5-6.5	9 weeks	119
11	$1.0 \times 10^{-2} - 3.0 \times 10^{-6}$	Nernstian	3.9-6.4	7 months	123
12	$1.0 \times 10^{-1} - 5.0 \times 10^{-6}$	Nernstian	4.0-7.0	3 weeks	**B_2**
13	$1.0 \times 10^{-1} - 5.0 \times 10^{-7}$	Nernstian	3.0-7.8	5 months	**Pa_3**
14	$1.0 \times 10^{-1} - 1.0 \times 10^{-7}$	Nernstian	3.0-7.0	2 months	**Pb_2**
15	$1.0 \times 10^{-1} - 5.0 \times 10^{-7}$	Nernstian	3.2-6.8	6 weeks	**Pc_4**

*NM – not mentioned

Chapter 6

SENSORS FOR MERCURY

This chapter details the response characteristics of three types of sensors based on a Schiff base ionophore for the determination of mercury ions. The different response parameters of the developed sensors have been discussed in detail. The analytical applications of the developed sensors have been illustrated in the form of potentiometric titration plots. Also their applicability in the determination of mercury ions have been tested in water samples by the standard addition method. The comparison of the developed sensors with other reported sensors has been discussed as a separate section.

Mercury, also known as quicksilver, is one of the five elements that is a liquid at room temperature. Mercury is used primarily for the manufacture of industrial chemicals and for electrical and electronic applications. It is used in some thermometers, electrodes, mercury switches, batteries, catalysts, insecticides, dental amalgam, mercury vapour lamps, barometers and liquid mirror telescopes. Doctors used mercuric chloride as a disinfectant.

The worst industrial disaster in history was caused by the dumping of mercury compounds into Minamata Bay, Japan. The Chisso Corporation, a fertilizer and later petrochemical company, was found responsible for

Department of Applied Chemistry,
CUSAT

polluting the bay from 1932–1968. It is estimated that over 3,000 people suffered various deformities, severe mercury poisoning symptoms or death from what became known as Minamata disease. The symptoms of mercury poisoning include tremors, emotional lability, insomnia, dementia and hallucinations.

Thus, it is very necessary to monitor the mercury levels in our environment. The common methods for the purpose that are being adopted are complexometry[246], spectrophotometry[247,248], flame and atomic absorption spectroscopy[249,250], inductively coupled plasma[251], fluorimetry[252,253], X-Ray fluorescence[254] and voltammetry[255]. But the potentiometric technique has advantages such as high selectivity, sensitivity, good precision, simplicity and low cost. As part of the present investigations, a Schiff base has been used as the ionophore in the fabrication of a PVC membrane, CPE-PVC type and CMCPE type of sensors, for the determination of mercury(II).

6.1 Ionophore

The synthesis and characterization of the ionophore, 1-(2-hydroxy-5-nitrobenzylidene) thiosemicarbazide (HTS), has been discussed under Section 2.2.6 in Chapter 2.

6.2 Sensors based on HTS

The ionophore, HTS, has been used to fabricate the three types of sensors – viz. the PVC membrane, CPE-PVC and CMCPE type. The structure of HTS is shown as Figure 6.1.

Figure 6.2, Figure 6.3 and Figure 6.4 show the potential response of the three types of sensors towards different cations. It was found that the sensors showed a Nernstian response to mercury ions. This may be attributed to the

selective complexation behaviour of the ionophore for Hg^{2+} over other metal ions, as well as the rapid exchange kinetics of the resulting complex.

6.2.1 Sensor membrane fabrication

The general method of fabrication of the PVC membrane, CPE-PVC type and CMCPE type of sensors has been discussed under Section 2.6 in Chapter 2.

In the case of PVC membrane sensor and CPE-PVC type of sensor, the composition ratio for the membrane that gave the best response in terms of slope, concentration range and response time was found to be 33:60:2:5 (PVC:DMS:NaTPB:HTS) (% w/w) where the plasticizer used was dimethyl sebacate (DMS) and the anionic excluder was sodium tetraphenylborate (NaTPB).

For the fabrication of PVC membrane sensor, membranes were cut out and stuck on to the open end of a Pyrex glass tube and it was filled with an internal solution of 1.0×10^{-1} M $Hg(NO_3)_2$.

In the case of CPE-PVC type of sensor, graphite was made a paste using paraffin oil. The polished sensor filled with carbon paste was dipped in to the optimized PVC membrane solution repeatedly till a thin film was formed on the working surface of the sensor.

In the case of CMCPE type of sensor, the ionophore and graphite were made a paste using paraffin oil and this paste was packed into the capillary glass tube as detailed in Chapter 2. The best composition ratio for CMCPE type of sensor was found to be 85:15 (graphite:HTS).

The three types of sensors were conditioned by dipping it in a 1.0×10^{-1} M mercury(II) nitrate solution. The equilibration time was 2 days for the

case of PVC membrane sensor and CPE-PVC sensor and just 24 h conditioning time was required for CMCPE type of sensor.

6.2.2 Potential measurement and calibration

Potentials were measured at 25±0.1 °C on a Toshniwal digital ion meter and on BAS Epsilon electrochemical workstation. An Hg | HgCl reference electrode was used in conjunction with the developed Hg^{2+} sensor. The cell assembly for potentiometric measurements for the three types of sensors can be represented as follows:

Hg | HgCl (sat. KCl) | Hg^{2+} (0.1 M) | PVC membrane based on HTS | test solution | Hg | HgCl (sat. KCl)

Hg | Hg_2Cl_2 (sat. KCl) | test solution | CPE-PVC based on HTS or CMCPE based on HTS

The performance of the developed Hg^{2+} sensor was investigated by measuring the potential in Hg^{2+} solutions (pH maintained at 3.0 using buffer) prepared in the concentration range $1.0 \times 10^{-1} - 1.0 \times 10^{-6}$ M. The solutions were stirred and the stable potential reading was taken.

6.2.3 Optimization of membrane composition

Besides the critical role of the ionophore, some other important features of the PVC membrane such as amount of ionophore, nature of the membrane solvent (plasticizer), plasticizer/PVC ratio and nature of the additives used influence sensitivity and selectivity of the sensors. Table 6.1 consolidates the results of seven different compositions of PVC membrane

solution prepared based on HTS. The PVC membrane without plasticizer was stiff and with unequal thickness and the sensor, Ha_1, gave a sub Nernstian slope but on addition of a plasticizing agent, the membrane surface became smooth and the sensor showed improved response characteristics. From the results, it was found that among the four different plasticizers used, DMS was the most effective solvent mediator in preparation of the PVC membrane while the others gave Non Nernstian slopes. The amount of the ionophore was also found to affect the sensitivity of the sensors. 5% was found to be the optimum amount of ionophore and further addition of ionophore content results in a diminished response from the sensors which may be due to the saturation of the membrane. The optimization of the permselectivity of the PVC membrane is known to be highly dependent on the incorporation of additional membrane components. The presence of lipophilic negatively charged additives (anionic excluders) improves the potentiometric behaviour of the PVC membrane by reducing the ohmic resistance and improving the response, selectivity as well as sensitivity[213-226]. A 2% of NaTPB was the anionic excluder added.

This optimized PVC membrane solution was used for the fabrication of the CPE-PVC type sensor. Thus sensors Ha_3 and Hb_2 (PVC membrane sensor and CPE-PVC type sensor), were found to be the best among the various sensors of different compositions studied.

The weight ratio of graphite to ionophore was varied to arrive at an optimum composition for CMCPE type of sensor. Table 6.2 presents the results of the effect on the response of the CMCPE type of sensor with changes in the composition ratio of graphite to ionophore. A sensor without ionophore Hc_1 was first prepared and it was observed that there was no response to mercury ions. It was found that the sensor Hc_4 with the

composition ratio 85:15 (graphite:HTS) was the best in terms of response time, working concentration range and the Nernstian slope. On increasing the ionophore content, nonlinearity in the response of the sensor was observed which may be attributed to the decrease in conductance of the sensor material. Hence this sensor (Hc_4) was used for further studies.

6.2.4 Working concentration range and slope

The calibration plot of the EMF versus pHg^{2+} for the sensors Ha_3, Hb_2 and Hc_4 are shown as Figure 6.5, Figure 6.6 and Figure 6.7 where Ha_3, Hb_2 and Hc_4 denote PVC membrane sensor, CPE-PVC type and CMCPE type of sensors respectively. The working concentration range for the sensors Ha_3, Hb_2 and Hc_4 was found to be $1.0 \times 10^{-1} - 1.0 \times 10^{-6}$ M. The slope calculated from the calibration graph was found to be 29.2 (±0.2) mV $decade^{-1}$, 28.7 (±0.8) mV $decade^{-1}$ and 29.6 (±0.3) mV $decade^{-1}$ for the sensors Ha_3, Hb_2 and Hc_4 respectively. The detection limit was calculated from the graph by the intersection of the two extrapolated linear segments of the calibration plot and was found to be 9.0×10^{-7} M, 8.8×10^{-7} M and 5.9×10^{-7} M for the sensors Ha_3, Hb_2 and Hc_4 respectively.

6.2.5 Response time

The plot of the changes in EMF from the moment of addition of 1.0×10^{-5} M Hg^{2+}solution with respect to time for the sensors Ha_3, Hb_2 and Hc_4 is depicted as Figure 6.8, Figure 6.9 and Figure 6.10. The practical response time for the sensors Ha_3, Hb_2 and Hc_4 was obtained from the plot and was found to be 24 s, 12 s and 30 s respectively. The practical reversibility of the sensors Ha_3, Hb_2 and Hc_4 were evaluated by taking measurements for Hg^{2+} solutions with a 10-fold difference in concentration in the sequence high-to-

low concentration and vice versa. The EMF versus time traces for the sensors Ha_3, Hb_2 and Hc_4 are shown as Figure 6.11, Figure 6.12 and Figure 6.13. The potentials remained constant for about 4 min in the case of Ha_2 and Hb_4 sensors and 2 min for Hc_3 sensor. The sensing behaviour of the membrane remained unchanged when potentials were recorded either from low to high concentrations or vice versa.

6.2.6 Effect of pH and non aqueous media

The influence of pH on the EMF response of the sensors Ha_3, Hb_2 and Hc_4 was studied for two fixed concentrations, 1.0×10^{-3} M and 1.0×10^{-4} M, over a pH range of 1.0-7.0. The pH was adjusted by introducing small drops of nitric acid (1.0 M) or sodium hydroxide (1.0 M). The results for the sensors Ha_3, Hb_2 and Hc_4 are shown in Figure 6.14, Figure 6.15 and Figure 6.16. It was found that the potential remained constant over a pH range of 1.0-4.0, 1.0-3.8 and 1.0-3.9 for the sensors Ha_3, Hb_2 and Hc_4 respectively. The observed drift in potentials at higher pH may be due to the formation of some hydroxyl complexes of Hg^{2+} ion in solution.

The performance of the sensors Ha_3, Hb_2 and Hc_4 was also investigated in partially non-aqueous media using methanol-water and ethanol-water mixtures. The results obtained are compiled in Table 6.3 and it was seen that no significant change occurs in the slope for the sensors up to 20% of non-aqueous content in the case of PVC membrane sensor Ha_3 and CPE-PVC type sensor Hb_2; and the tolerance level was 10% for CMCPE type sensor Hc_4. However, above the tolerance level of the sensors Ha_3, Hb_2 and Hc_4, the slopes gets affected which may be attributed to leaching of the ligand into the sample solution.

6.2.7 Potentiometric selectivity

The selectivity is the most important characteristic of a sensor as it determines the extent of the utility of the sensor in real sample measurement. The potential response of the sensors Ha_3, Hb_2 and Hc_4 were investigated in presence of foreign ions by using the fixed interference method[227,35]. The selectivity coefficients were determined at 1.0×10^{-2} M concentration of foreign ions and was calculated using the following equation.

$$K_{A,B}^{pot} = a_A / (a_B)^{z_A / z_B}$$

The selectivity coefficient values are consolidated in Table 6.4. and the values indicate that all the three sensors Ha_3, Hb_2 and Hc_4 show very good selectivity to Hg^{2+} ions in the presence of the following cations – Na^+, K^+, Mg^{2+}, Ca^{2+}, Ba^{2+}, NH_4^+, Mn^{2+}, Co^{2+}, Ni^{2+}, Zn^{2+}, Cu^{2+}, Cd^{2+}, Pb^{2+} and Fe^{3+} but only moderate selectivity in the presence of Ag^+.

6.2.8 Lifetime or Shelf life

The operative life time for the sensors Ha_3, Hb_2 and Hc_4 was found to be 4 months, 3 months and 5 weeks respectively. The sensors were all kept immersed in 1.0×10^{-1} M mercury(II) nitrate solution when not in use. And as explained in the previous chapters for CMCPE sensors, the surface could be renewed.

6.2.9 Analytical applications

The practical utility of the sensors Ha_3, Hb_2 and Hc_4 was further investigated in the determination of mercury(II) in different water samples containing added Hg^{2+} ions collected from the nearby pond. The preparation of the two different concentrations for each sample has been discussed under

Section 2.5.5 in Chapter 2. The results presented in Table 6.5 show that the results of determination of mercury(II) from different water samples is quantitative.

The sensors Ha_3, Hb_2 and Hc_4 were successfully applied as an indicator electrode in conjuction with Ag|AgCl in the potentiometric titration of mercury(II) nitrate solution at pH 3.0. The titration curves for the sensors Ha_3, Hb_2 and Hc_4 are depicted in Figure 6.17, Figure 6.18 and Figure 6.19 respectively. The titration plots obtained were all of the standard sigmoid shape and the end point corresponds to 1:1 stoichiometry of Hg-EDTA complex.

6.3 A comparative study among the sensors Ha_3, Hb_2 and Hc_4 and to some of the reported sensors

All the three sensors Ha_3, Hb_2 and Hc_4 are found to have very good response characteristics. Table 6.6 consolidates the response characteristics of the sensors Ha_3, Hb_2 and Hc_4. Among the different types of sensors fabricated, the PVC membrane sensor (Ha_3) is better in terms of pH range, slope and non aqueous tolerance limit. In terms of response time, sensor Hb_2 gave the best result of 12 s but its slope was slightly near Nernstian. The detection limit of the sensor Hc_4 was the lowest. The sensor Ha_3 has the longest shelf life of 4 months but though the shelf life for the CMCPE type sensor Hc_4 was only 5 weeks, the surface could be renewed by cutting off a little of the paste, polishing it on a smooth surface and reconditioning it on 1.0×10^{-1} M of mercury(II) nitrate solution. Table 6.7 lists the comparative study of the characteristics of developed sensors with some of the reported sensors for Hg^{2+}. It can be seen that the developed sensors are superior in

terms of working concentration range[139,140,147,149], slope[147,149], life time[139,140,147,149-151,156] and pH range[149,151,156].

Figures

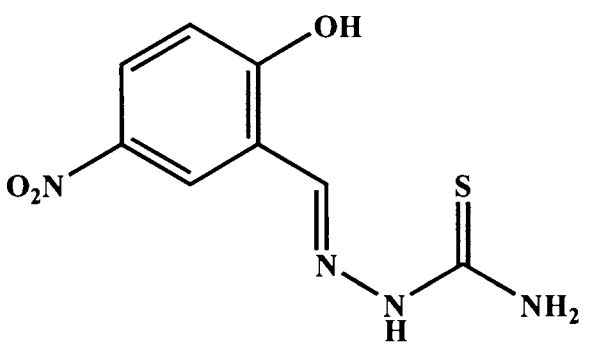

Figure 6.1 – Structure of the ionophore HTS

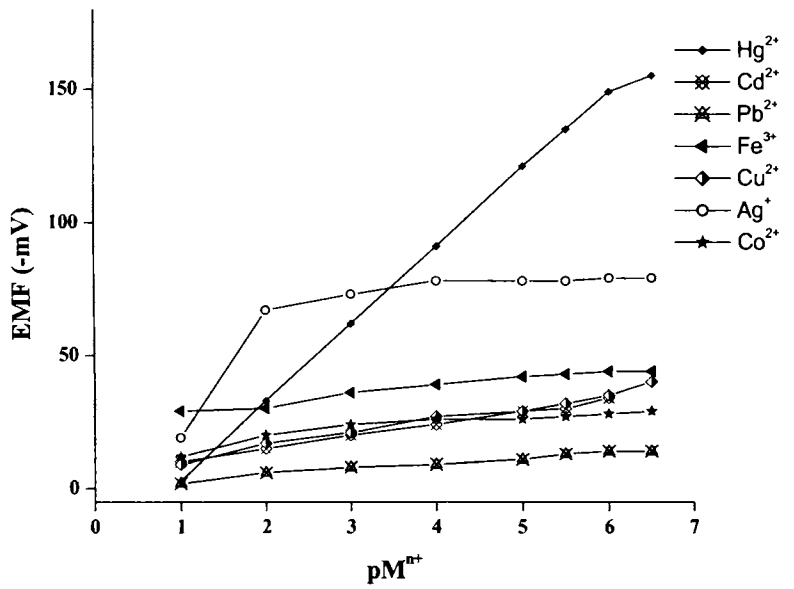

Figure 6.2 - Potential response of the various PVC membrane sensors based on HTS.

Conditions: membrane composition ratio 33% PVC:60% DMS:2% NaTPB:5% HTS; internal solution 1.0×10^{-1} M of each cation used and conditioned in 1.0×10^{-1} M of the corresponding cation solution for 2 days

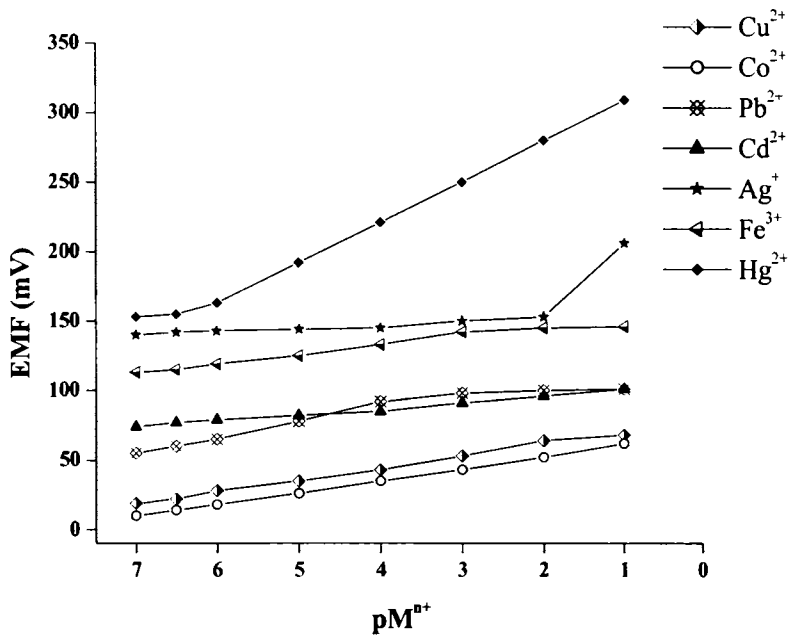

Figure 6.3 - Potential response of the various CPE-PVC type sensors based on HTS.

Conditions: membrane composition ratio 33% PVC:60% DMS:2% NaTPB:5% HTS; conditioned in 1.0×10^{-1} M of the corresponding cation solution for 2 days

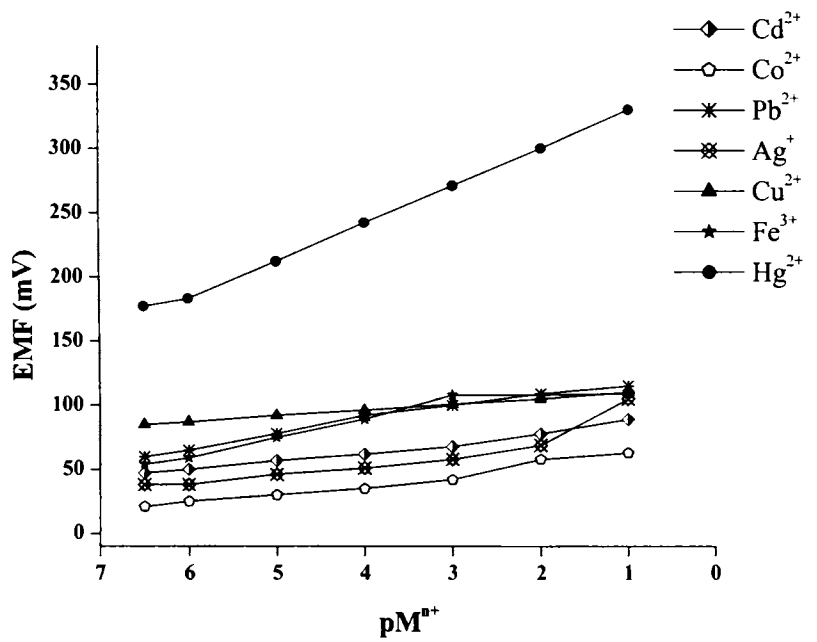

Figure 6.4 - Potential response of various CMCPE type sensors based on HTS.

Conditions: composition ratio 15% HTS:85% graphite; conditioned in 1.0×10^{-1} M of the corresponding cation solution for 24 h

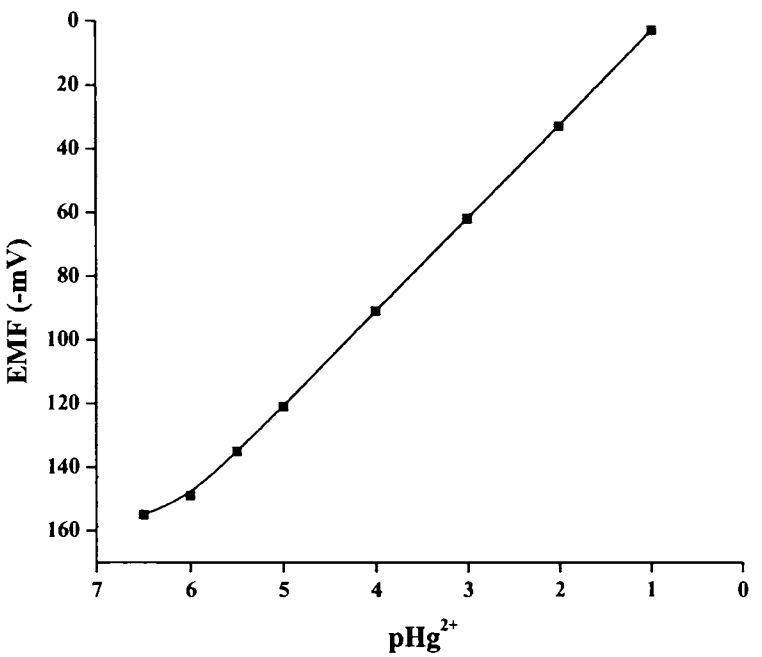

Figure 6.5 - Calibration graph of the PVC membrane sensor Ha_3 based on HTS

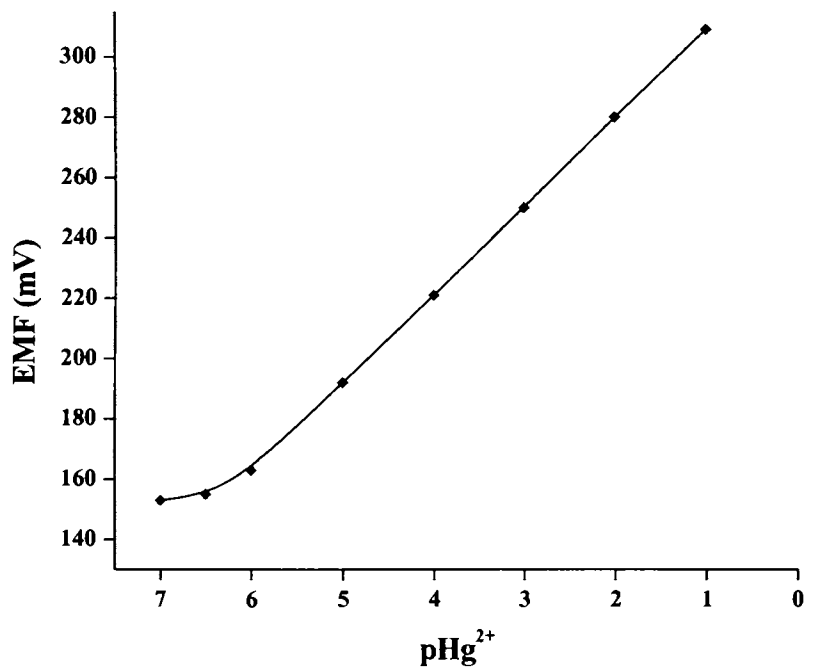

Figure 6.6 - Calibration graph of the CPE-PVC type sensor Hb_2 based on HTS

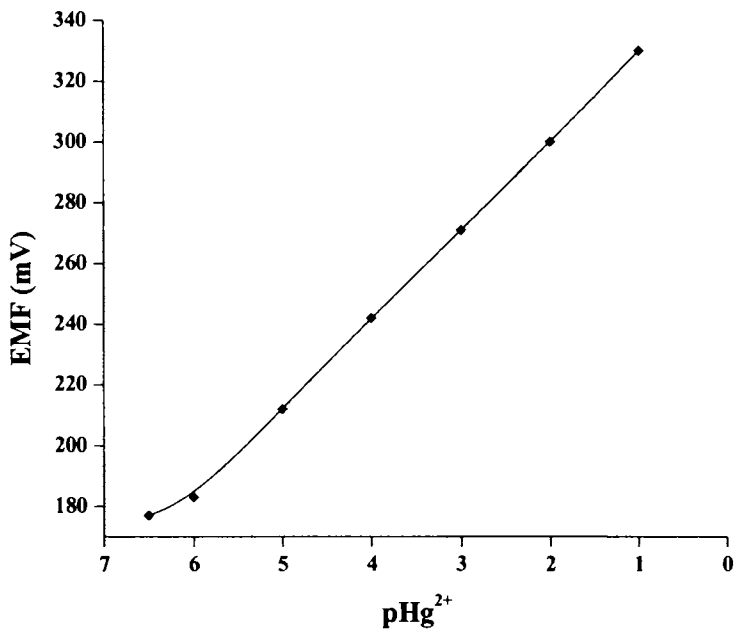

Figure 6.7 - Calibration graph of the CMCPE type sensor Hc_4 based on HTS

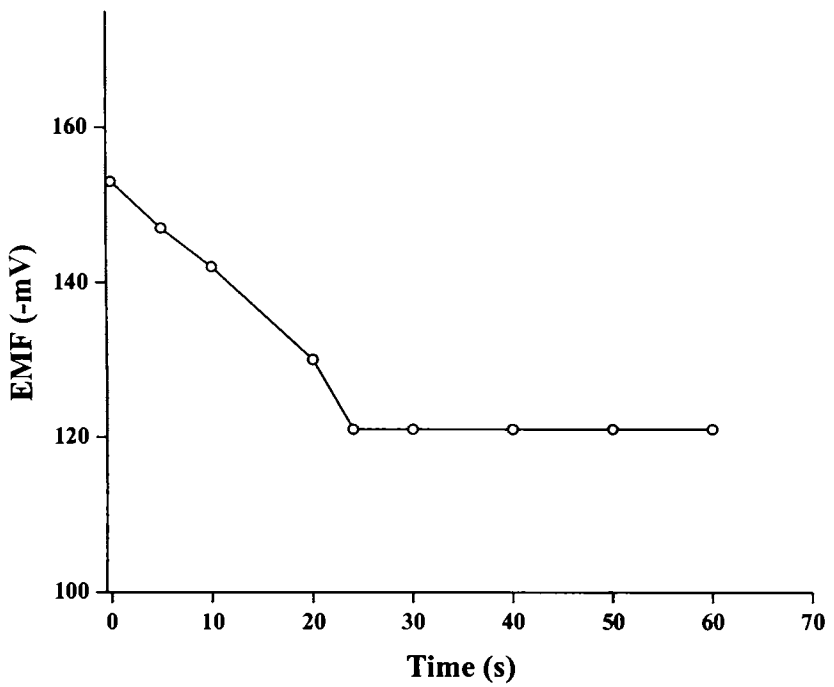

Figure 6.8 – Practical response time of the PVC membrane sensor Ha_3 based on HTS from the moment of addition of Hg^{2+} (1.0×10^{-5} M) solution

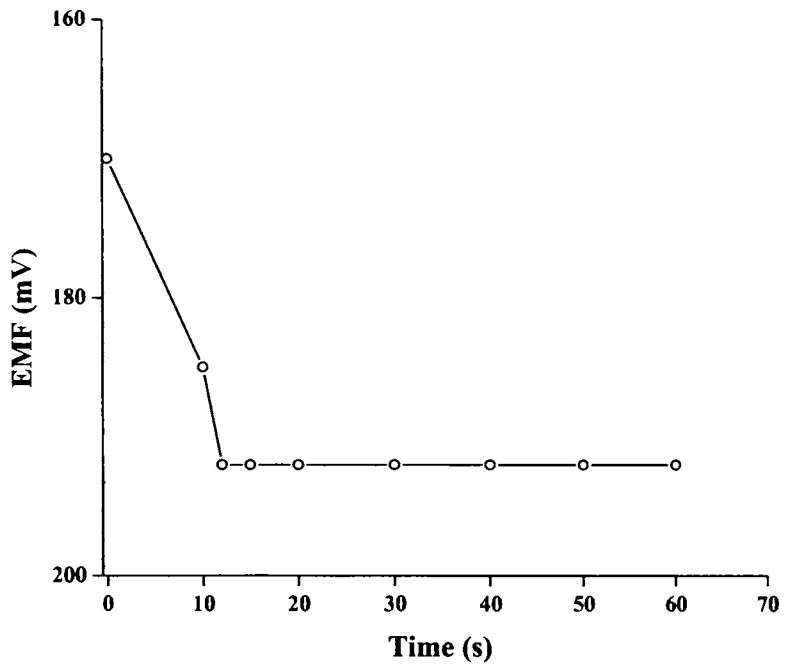

Figure 6.9 – Practical response time of the CPE-PVC type sensor Hb_2 based on HTS from the moment of addition of Hg^{2+} (1.0×10^{-5} M) solution

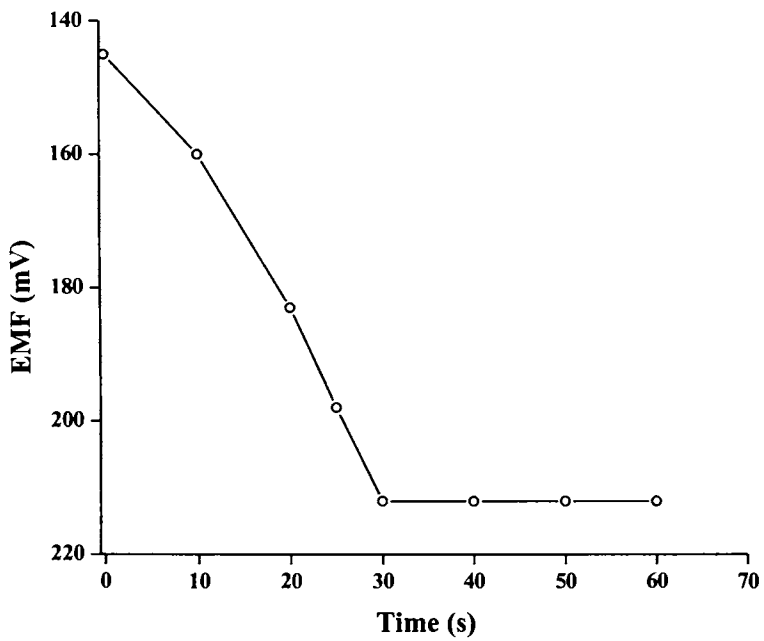

Figure 6.10 – Practical response time of the CMCPE type sensor Hc_4 based on HTS from the moment of addition of Hg^{2+} (1.0×10^{-5} M) solution

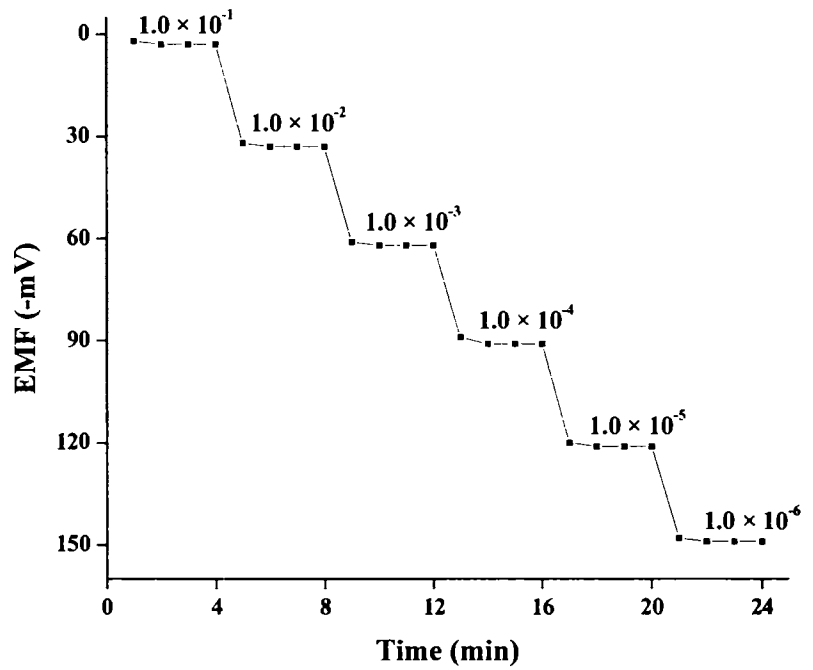

Figure 6.11 - Dynamic response time of the PVC membrane sensor Ha_3 based on HTS for reversibility with step changes in concentration of Hg^{2+} (1.0×10^{-6} to 1.0×10^{-1} M)

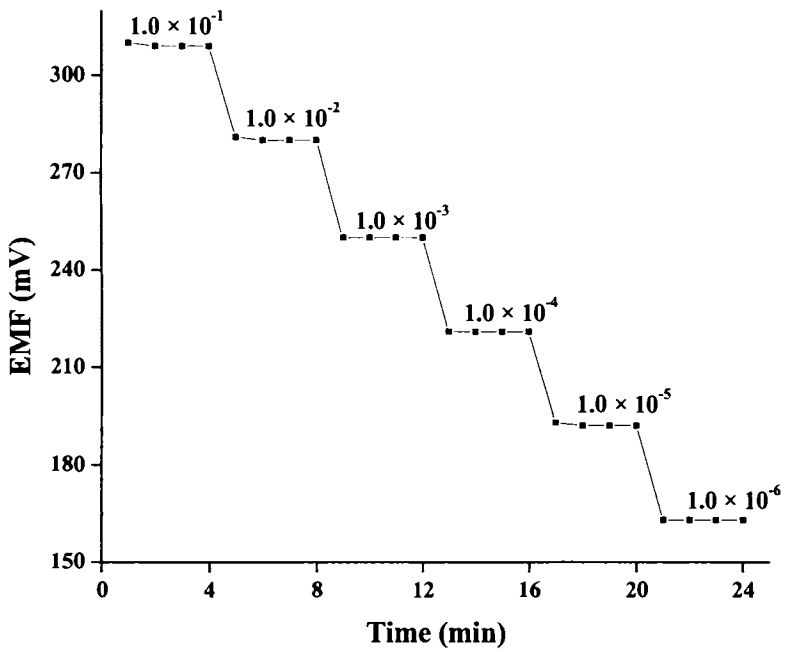

Figure 6.12 - Dynamic response time of the CPE-PVC type sensor Hb_2 based on HTS for reversibility with step changes in concentration of Hg^{2+} (1.0×10^{-6} to 1.0×10^{-1} M)

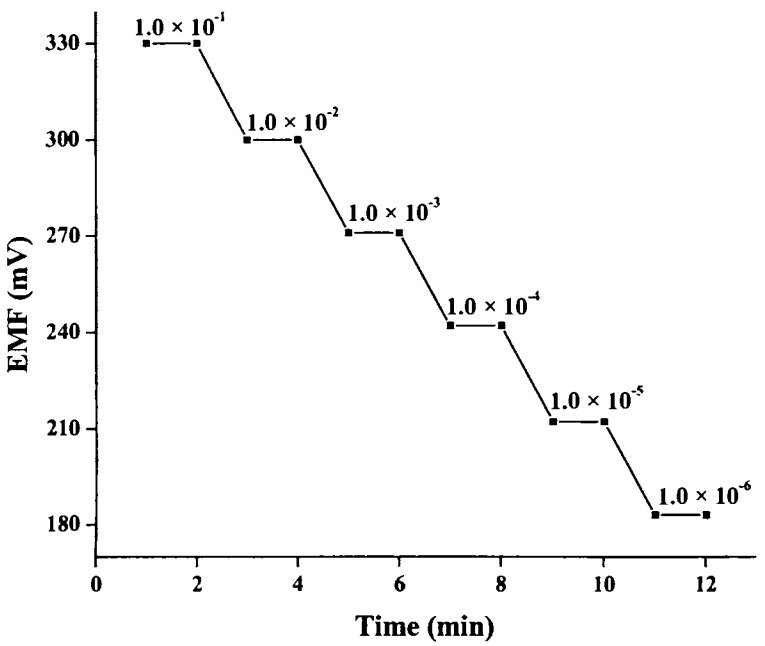

Figure 6.13 - Dynamic response time of the CMCPE type sensor Hc_4 based on HTS for reversibility with step changes in concentration of Hg^{2+} (1.0×10^{-6} to 1.0×10^{-1} M)

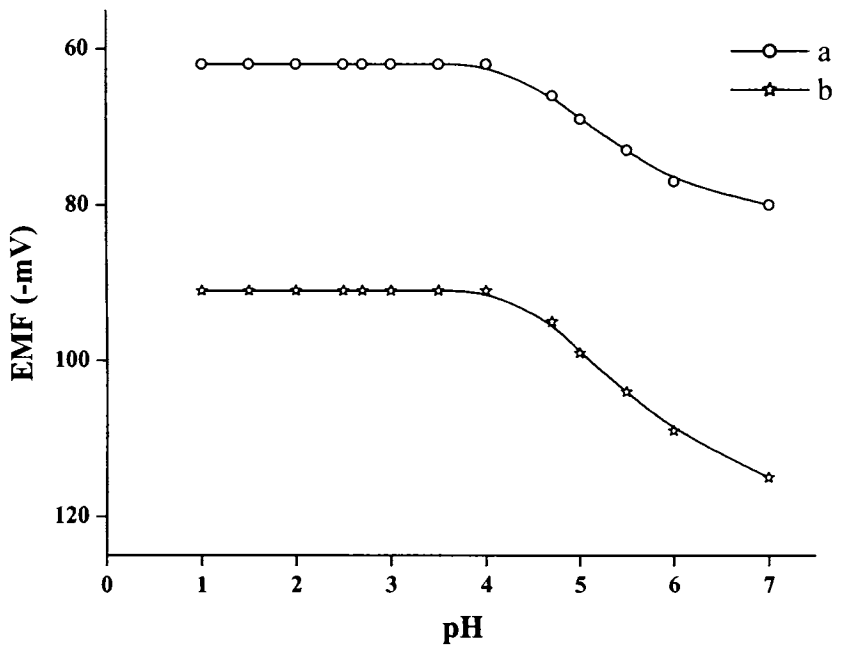

Figure 6.14 – Effect of pH on the cell potential of the PVC membrane sensor Ha_3 based on HTS at 1.0×10^{-3} M (a) and 1.0×10^{-4} M (b)

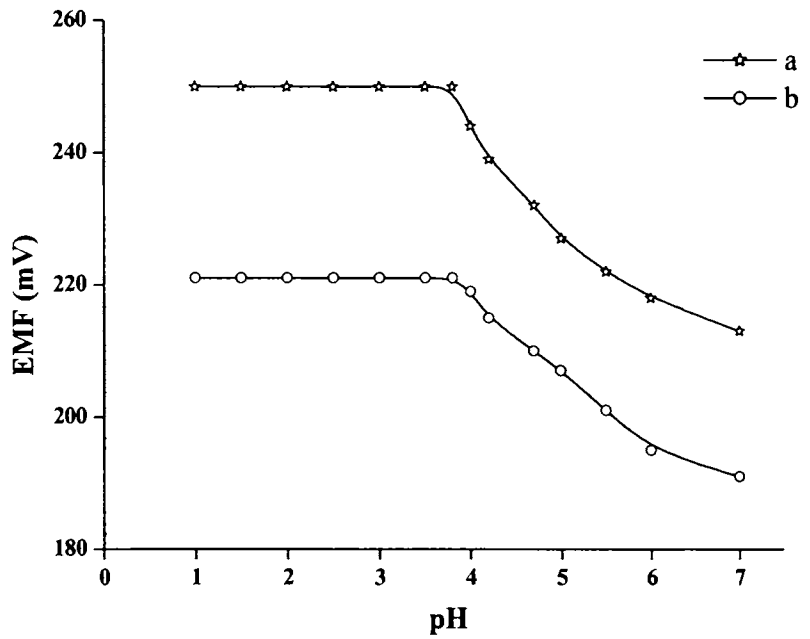

Figure 6.15 – Effect of pH on the cell potential of the CPE-PVC type sensor Hb_2 based on HTS at 1.0×10^{-3} M (a) and 1.0×10^{-4} M (b)

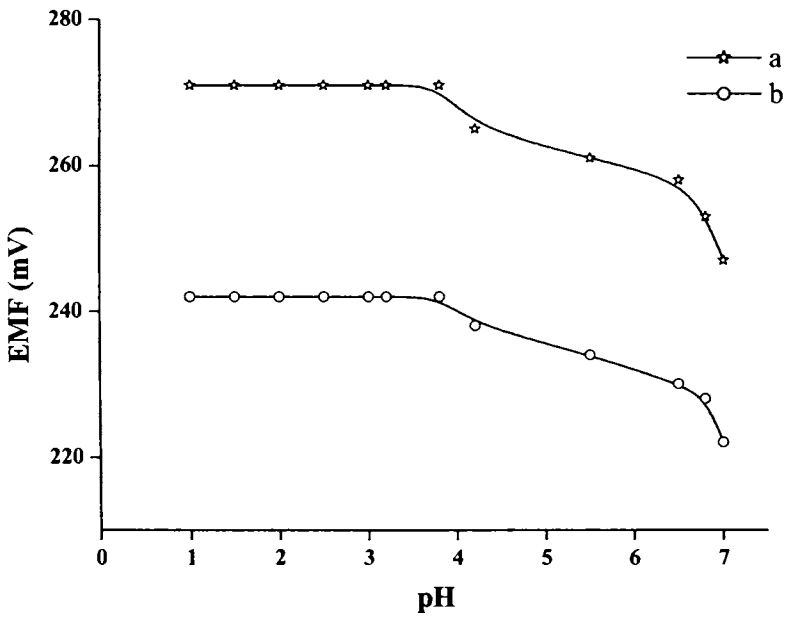

Figure 6.16 – Effect of pH on the cell potential of the CMCPE type sensor Hc_4 based on HTS at 1.0×10^{-3} M (a) and 1.0×10^{-4} M (b)

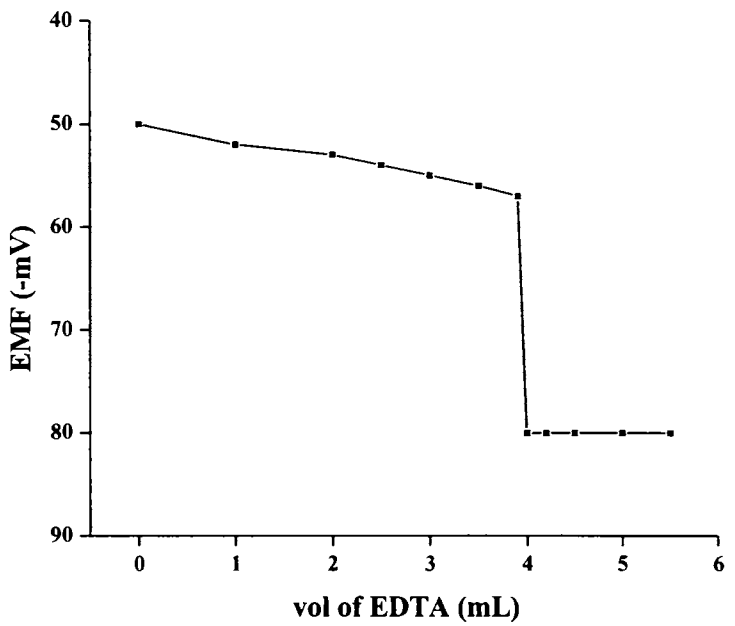

Figure 6.17 – Potentiometric titration curve of 10.0 mL of 4.0×10^{-3} M Hg^{2+} solution with 1.0×10^{-2} M EDTA using the PVC membrane sensor Ha_3 as an indicator electrode at pH 3.0.

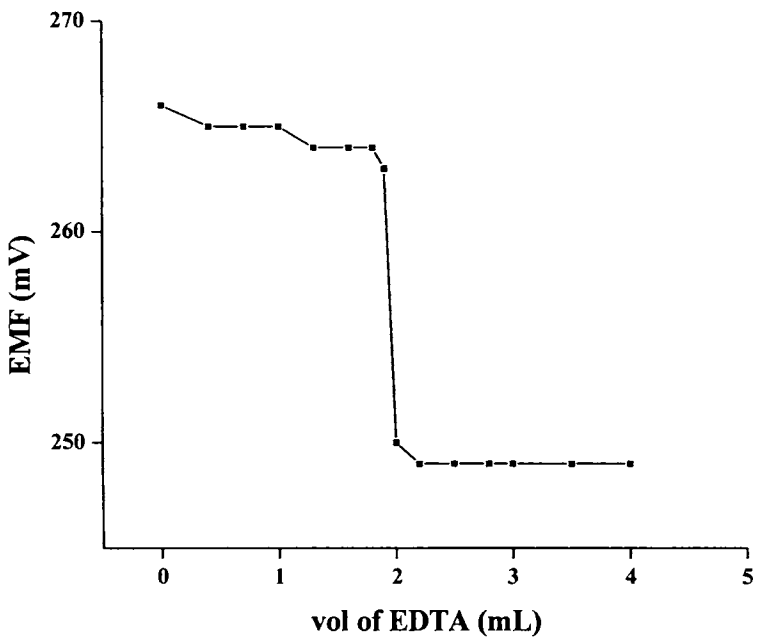

Figure 6.18 – Potentiometric titration curve of 20.0 mL of 5.0×10^{-3} M Hg^{2+} solution with 5.0×10^{-2} M EDTA using the CPE-PVC type sensor Hb_2 as an indicator electrode at pH 3.0.

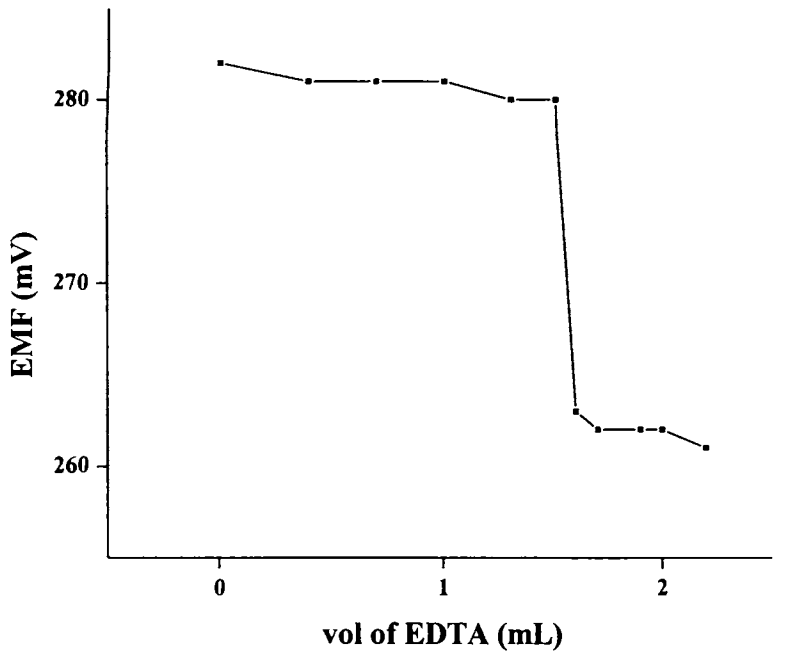

Figure 6.19 – Potentiometric titration curve of 20.0 mL of 4.0×10^{-3} M Hg^{2+} solution with 5.0×10^{-2} M EDTA using the CMCPE type sensor Hc_4 as an indicator electrode at pH 3.0.

Table 6.1 - Optimization of the PVC membrane ingredients for the PVC membrane (Ha) and CPE-PVC type (HTb) of sensors based on HTS[a]

Sensor	% w/w composition of each membrane				Working concentration range (M)	Slope (mV decade^{-1})	Response time (s)
	PVC	HTS	Plasticizer	NaTPB			
Ha_1	93	5	0	2	$1.0 \times 10^{-1} - 1.0 \times 10^{-5}$	24.3(±0.6)	60
Ha_2	33	2	DMS, 63	2	$1.0 \times 10^{-1} - 5.0 \times 10^{-6}$	27.7(±1.0)	25
Ha_3	33	5	DMS, 60	2	$1.0 \times 10^{-1} - 9.0 \times 10^{-7}$	29.2(±0.2)	24
Ha_4	33	7	DMS, 58	2	$1.0 \times 10^{-1} - 4.5 \times 10^{-6}$	28.0(±0.1)	22
Ha_5	33	5	DOS, 60	2	$1.0 \times 10^{-1} - 1.9 \times 10^{-6}$	21.3(±0.5)	30
Ha_6	33	5	DOA, 60	2	$1.0 \times 10^{-1} - 3.8 \times 10^{-4}$	19.4(±1.0)	35
Ha_7	33	5	DOP, 60	2	$1.0 \times 10^{-1} - 8.6 \times 10^{-5}$	17.8(±1.0)	42
Hb_1	0	0	0	0	$1.0 \times 10^{-1} - 1.0 \times 10^{-4}$	~0.0	75
Hb_2	33	5	DMS, 60	2	$1.0 \times 10^{-1} - 8.8 \times 10^{-7}$	28.7(±0.8)	12

[a] Values in parentheses are RSDs based on three replicates

Table 6.2 - Optimization of the ionophore composition for the CMCPE type of sensor based on HTS[a]

Sensor	Ionophore	Graphite	Working concentration range (M)	Slope (mV decade^{-1})	Response time (s)
Hc_1	0	100	1.0×10^{-1} - 1.0×10^{-4}	1.2(±1.0)	100
Hc_2	5	95	1.0×10^{-1} - 7.9×10^{-5}	21.4(±0.3)	60
Hc_3	10	90	1.0×10^{-1} - 2.1×10^{-6}	28.1(±0.7)	46
Hc_4	15	85	1.0×10^{-1} - 5.9×10^{-7}	29.6(±0.3)	30
Hc_5	20	80	1.0×10^{-1} - 5.0×10^{-6}	32.0(±0.2)	31
Hc_6	30	70	1.0×10^{-2} - 1.0×10^{-5}	38.5(±0.5)	45
Hc_7	50	50	1.0×10^{-2} - 1.0×10^{-5}	27.7(±0.3)	63

[a] Values in parentheses are RSDs based on three replicates.

Table 6.3 – Effect of partially non-aqueous medium on the slope of the sensors Ha_3, Hb_2 and Hc_4

Non-aqueous content (% v/v)	Slope (mV decade^{-1})		
	Ha_3	Hb_2	Hc_4
0	29.2	28.7	29.6
Ethanol			
5	29.2	28.6	29.6
10	29.1	28.0	29.4
20	29.0	28.0	27.8
30	28.1	27.1	26.2
40	26.7	25.8	24.1
Methanol			
5	29.2	28.7	29.5
10	29.2	28.1	29.2
20	29.0	28.0	27.3
30	28.2	27.3	25.2
40	26.5	25.5	23.6

Table 6.4 – Selectivity coefficients for the sensors Ha_3, Hb_2 and Hc_4 using fixed interference method at 1.0×10^{-2} M concentration of interfering ion.

Interfering ion (X)	Ha_3	Hb_2	Hc_4
Na^+	5.4×10^{-2}	4.8×10^{-2}	7.1×10^{-2}
K^+	3.1×10^{-3}	6.4×10^{-3}	5.5×10^{-3}
Ag^+	9.5×10^{-1}	8.3×10^{-1}	9.1×10^{-1}
Mg^{2+}	5.5×10^{-3}	5.9×10^{-3}	5.4×10^{-3}
Ca^{2+}	2.2×10^{-3}	3.2×10^{-3}	2.9×10^{-3}
Ba^{2+}	4.2×10^{-3}	4.9×10^{-3}	3.1×10^{-3}
Mn^{2+}	6.3×10^{-3}	6.9×10^{-3}	7.4×10^{-3}
Co^{2+}	7.4×10^{-2}	8.1×10^{-2}	5.9×10^{-2}
Ni^{2+}	3.7×10^{-3}	4.2×10^{-3}	4.1×10^{-3}
Zn^{2+}	4.2×10^{-3}	5.1×10^{-3}	5.2×10^{-3}
Cd^{2+}	9.3×10^{-3}	8.2×10^{-3}	8.9×10^{-3}
Cu^{2+}	4.5×10^{-3}	3.9×10^{-3}	5.3×10^{-3}
Pb^{2+}	1.2×10^{-2}	3.9×10^{-2}	2.4×10^{-2}
Fe^{3+}	1.6×10^{-2}	1.1×10^{-2}	3.0×10^{-2}

Table 6.5 - Recovery of mercury ions from two different water samples

Sensor	Tap Water Hg(II) (ppm)			Well Water Hg(II) (ppm)		
	Added	Found*	Recovery (%)	Added	Found*	Recove (%)
Ha_3	50.00	49.97 ± 0.01	99.9	100.00	99.92 ± 0.02	99.9
Hb_2	50.00	48.87 ± 0.03	97.7	100.00	98.33 ± 0.02	98.3
Hc_4	50.00	50.11± 0.01	100.2	100.00	100.72 ± 0.01	100.7

*RSDs based on three replicates.

Table 6.6 – Response characteristics of the sensors Ha_3, Hb_2 and Hc_4

Parameter	Response characteristics		
	Ha_3	Hb_2	Hc_4
Working concentration range (M)	1.0×10^{-1} – 1.0×10^{-6}	1.0×10^{-1} – 1.0×10^{-6}	1.0×10^{-1} – 1.0×10^{-6}
Slope (mV decade^{-1})	29.2 ± 0.2	28.7 ± 0.8	29.6 ± 0.3
Detection limit (M)	9.0×10^{-7}	8.8×10^{-7}	5.9×10^{-7}
Response time	24 s	12 s	30 s
pH range	1.0-4.0	1.0-3.8	1.0-3.9
Non aqueous tolerance limit	20%	20%	10%
Shelf life	4 months	3 months	5 weeks

Table 6.7 -Comparison of characteristics of the sensor with some reported sensors

No.	Working concentration range (M)	Slope (mV decade^{-1})	pH range	Lifetime	Ref. No.
1	$1.0 \times 10^{-3} - 4.0 \times 10^{-6}$	Nernstian	0.5-2.5	3 months	139
2	$1.0 \times 10^{-2} - 8.0 \times 10^{-6}$	Nernstian	0.5-2.5	3 months	140
3	$3.0 \times 10^{-2} - 2.0 \times 10^{-7}$	Nernstian	1.0-4.0	2 months	150
4	$5.0 \times 10^{-2} - 7.0 \times 10^{-7}$	Nernstian	1.0-3.5	3 months	151
5	$1.0 \times 10^{-3} - 6.0 \times 10^{-6}$	Near Nernstian	4.0-9.0	4 weeks	147
6	$1.0 \times 10^{-1} - 5.0 \times 10^{-5}$	Near Nernstian	1.3-4.0	3 months	149
7	$1.0 \times 10^{-1} - 1.0 \times 10^{-6}$	Nernstian	4.0-9.0	3 months	156
8	$1.0 \times 10^{-1} - 1.0 \times 10^{-6}$	Nernstian	1.0-4.0	4 months	**Ha_3**
9	$1.0 \times 10^{-1} - 1.0 \times 10^{-6}$	Near Nernstian	1.0-3.8	3 months	**Hb_2**
10	$1.0 \times 10^{-1} - 1.0 \times 10^{-6}$	Nernstian	1.0-3.9	5 weeks	**Hc_4**

Chapter 7

SENSORS FOR LEAD

This chapter describes the fabrication of three types of sensors based on a simple schiff base as ionophore. Optimization of the membrane composition and the response characteristics of the developed sensors have been discussed. The application of the developed sensors as an indicator electrode in potentiometric titration and in the direct determination of lead in battery waste has also been described.

Lead is a bluish white metal when freshly cut, but tarnishes to dull grey when exposed to air. It is soft, heavy and has poor electrical conductivity. It is highly resistant to corrosion and thus, is used to contain corrosive liquids like sulphuric acid. It finds use in building construction, lead-acid batteries, bullets, solder, pewter, fusible alloys and as a petrol additive. The earliest pencils were actually made of lead and though they are still called 'pencil lead', they now contain graphite.

Lead is a poisonous metal and it is cycled in the environment through the biogeochemical cycle. Lead acetate (known as *sugar of lead*) was used by the Roman Empire as a sweetener for wine; and that is believed to be the cause of the dementia which affected many Roman Emperors. The metal is highly toxic and it adversely affects the nervous, reproductive, immune, cardiovascular systems as well as developmental processes in children[256,257].

Spectrophotometric methods, atomic absorption spectroscopy (AAS), inductively coupled plasma-atomic emission spectroscopy or the inductively coupled plasma-mass spectroscopy (ICP-MS) techniques are among the most common methods employed for the determination of lead in solutions[258,259]. However, potentiometric sensors are better suited as they offer advantages such as high selectivity, sensitivity, good precision, simplicity and low cost. As part of the present investigations, a Schiff base has been used as the ionophore in the fabrication of a PVC membrane, CPE-PVC type and CMCPE type of sensors.

7.1 Ionophore

The synthesis and characterization of the ionophore, N^1,N^2-bis(2-hydroxy-5-nitro benzylidene) benzene-1,2-diamine (HBD), has been discussed under Section 2.2.7 in Chapter 2.

7.2 Sensors based on HBD

The PVC membrane, CPE-PVC and CMCPE type of sensors were fabricated using HBD as ionophore. The structure of HBD is shown as Figure 7.1. Figure 7.2, Figure 7.3 and Figure 7.4 show the potential response of the three types of sensors towards different cations and it was found that the sensors showed a Nernstian response to lead ions. This may be attributed to the selective affinity of the ionophore to Pb^{2+} over other metal ions, as well as the rapid exchange kinetics of the resulting complex.

7.2.1 Sensor membrane fabrication

The general method of fabrication of the PVC membrane, CPE-PVC type and CMCPE type of sensors has been discussed under Section 2.6 in Chapter 2.

For the PVC plasticized solution, the composition ratio of 30:65:2:3 (PVC:DOP:NaTPB:HBD) (% w/w) was found to give the best response in terms of slope, concentration range and response time with dioctyl phthalate (DOP) as the plasticizing agent and sodium tetaphenylborate (NaTPB) as anionic excluder.

For the fabrication of PVC membrane sensor, disc shaped membranes were cut out and stuck on to the open end of a Pyrex glass tube. The tube was filled with an internal solution of 1.0×10^{-1} M $Pb(NO_3)_2$.

The fabrication of CPE-PVC type of sensor initially involves the preparation of the carbon paste. The carbon paste was packed in to the sensor body and then polished. The open end packed with carbon paste, was dipped in to the optimized PVC membrane solution repeatedly till a thin film was formed on the working surface of the sensor.

The CMCPE type of sensor was fabricated by packing the paste of ionophore and graphite in paraffin oil into the open end of the capillary tube. The best composition ratio for CMCPE type of sensor was found to be 90:10 (graphite:HBD).

The three types of sensors were conditioned by dipping it in a 1.0×10^{-1} M lead(II) nitrate solution. The equilibration time was 2 days for the case of PVC membrane sensor and CPE-PVC sensor and 6 h in the case of CMCPE type of sensor.

7.2.2 Potential measurement and calibration

Potentials were measured at 25±0.1 °C on a Toshniwal digital ion meter and on BAS Epsilon electrochemical workstation. An $Hg \mid Hg_2Cl_2$ reference electrode was used in conjunction with the developed Pb^{2+} sensor. The cell assembly for potentiometric measurements for the three types of sensors can be represented as follows:

$Hg \mid Hg_2Cl_2$ (sat. KCl) $\mid$ Pb^{2+} (0.1 M) $\mid$ PVC membrane based on HBD $\mid$ test solution $\mid$ $Hg \mid Hg_2Cl_2$ (sat. KCl)

$Hg \mid Hg_2Cl_2$ (sat. KCl) $\mid$ test solution $\mid$ CPE-PVC based on HBD or CMCPE based on HBD

The performance of the developed Pb^{2+} sensor was investigated by measuring the potential in Pb^{2+} solutions (pH maintained at 5.0 using buffer solution) prepared in the concentration range $1.0 \times 10^{-1} - 1.0 \times 10^{-8}$ M. The solutions were stirred and stable potential reading was taken.

7.2.3 Optimization of membrane composition

The sensitivity and selectivity of the PVC membrane is largely influenced by the amount of ionophore, nature of the membrane solvent (plasticizer), plasticizer/PVC ratio and nature of the additives used. A set of seven different compositions of PVC membrane solution was prepared for the fabrication the PVC membrane sensor and CPE-PVC sensor. Initially a membrane without plasticizer was prepared and the sensor, Da_1, gave a sub Nernstian slope but on addition of a plasticizing agent, the membrane surface became smooth and the sensor showed improved response characteristics.

Among the four different plasticizers used, DOP was found to be the most effective solvent mediator in the preparation of the PVC membrane while others gave a Non Nernstian response. The amount of the ionophore was also found to affect the sensitivity of the sensors. 3% was found to be the optimum amount of ionophore and further addition of ionophore content results in a diminished response from the sensors which may be due to the saturation of the membrane. The optimization of the permselectivity of the PVC membrane is known to be highly dependent on the incorporation of additional membrane components. The presence of lipophilic negatively charged additives (anionic excluders) improves the potentiometric behaviour of the PVC membrane by reducing the ohmic resistance and improving the response and selectivity as well as sensitivity[213-226]. Thus the optimum amount of anionic excluder incorporated in the membrane ingredients was 2% of NaTPB.

This optimized PVC membrane solution was used for the fabrication of the CPE-PVC type sensor. Thus sensors Da_3 and Db_2 were found to be the best among the sensors fabricated with varying compositions.

The weight ratio of graphite to ionophore was varied to arrive at an optimum composition for CMCPE type of sensor. Table 7.2 presents the results of the effect on the response of CMCPE type of sensor with changes in the composition ratio of graphite to ionophore. A sensor without ionophore Dc_1 was first prepared and it was observed that there was no response to lead ions. It was found that the sensor Dc_3 with the composition ratio 90:10 (graphite:HBD) was the best in terms of response time, working concentration range and the Nernstian slope and this sensor was used for further studies. On increasing the ionophore content, nonlinearity in the

response of the sensor was observed which can be attributed to the decrease in conductance of the sensor material.

7.2.4 Working concentration range and slope

The plot of EMF versus pPb^{2+} for the sensors Da_3, Db_2 and Dc_3 are shown as Figure 7.5, Figure 7.6 and Figure 7.7 where Da_3, Db_2 and Dc_3 denote PVC membrane sensor, CPE-PVC type and CMCPE type of sensor respectively. The working concentration range for the sensors Da_3, Db_2 and Dc_3 was found to be $1.0 \times 10^{-1} - 5.0 \times 10^{-7}$ M, $1.0 \times 10^{-1} - 1.0 \times 10^{-7}$ M and $1.0 \times 10^{-1} - 1.0 \times 10^{-7}$ M respectively. The slope calculated from the calibration graph was found to be 29.7 (±0.6) mV $decade^{-1}$, 29.8 (±0.9) mV $decade^{-1}$ and 30.2 (±0.5) mV $decade^{-1}$ for the sensors Da_3, Db_2 and Dc_3 respectively. The detection limit was calculated from the graph by the intersection of the two extrapolated linear segments of the calibration plot and was found to be 1.8×10^{-7} M, 8.8×10^{-8} M and 5.9×10^{-8} M for the sensors Da_3, Db_2 and Dc_3 respectively. The sensing behaviour of the membrane remained unchanged when potentials were recorded either from low to high concentrations or vice versa.

7.2.5 Response time

Figure 7.8, Figure 7.9 and Figure 7.10 depicts the traces of the changes in EMF from the moment of addition of 1.0×10^{-5} M Pb^{2+} solution with respect to time for the sensors Da_3, Db_2 and Dc_3. Practical response time for the sensors Da_3, Db_2 and Dc_3 was obtained from the plot and was found to be 10 s, 22 s and 27 s respectively. Practical reversibility of the sensors Da_3, Db_2 and Dc_3 were evaluated by taking measurements for Pb^{2+} solutions with a 10-fold difference in concentration in the sequence high-to-low

concentration and vice versa. The EMF versus time traces for the sensors Da_3, Db_2 and Dc_3 are shown as Figure 7.11, Figure 7.12 and Figure 7.13. The potentials remained constant for about 5 min in the case of Da_3 sensor and 3 min for the Db_2 and Dc_3 sensors. The sensing behaviour of the membrane remained unchanged when potentials were recorded either from low to high concentrations or vice versa.

7.2.6 Effect of pH and non aqueous media

The influence of pH on the EMF response of the sensors Da_3, Db_2 and Dc_3 was studied for two fixed concentrations, 1.0×10^{-3} M and 1.0×10^{-4} M, over a pH range of 2.0-9.2. The pH was adjusted by introducing small drops of nitric acid (1.0 M) or sodium hydroxide (1.0 M). The results for the sensors Da_3, Db_2 and Dc_3 are shown in Figure 7.14, Figure 7.15 and Figure 7.16. It was found that the potential remained constant over a pH range of 2.0-6.8, 3.0-6.5 and 3.0-7.0 for the sensors Da_3, Db_2 and Dc_3 respectively. The observed drift in potentials at higher pH may be due to the formation of some hydroxyl complexes of Pb^{2+} ion in solution while at lower pH there may be interferences from H^+ ions.

The performance of the sensors Da_3, Db_2 and Dc_3 was also investigated in partially non-aqueous media using methanol-water and ethanol-water mixtures. The results obtained are compiled in Table 7.3 and it was seen that no significant change occurs in the slope for the sensors up to 25% of non-aqueous content in the case of PVC membrane sensor Da_3, 20% in the case of CPE-PVC type sensor Db_2 and the tolerance level was 10% for the CMCPE type sensor Dc_3. However, above the tolerance level, the slopes get affected, which may be attributed to leaching of the ligand into the sample solution.

7.2.7 Potentiometric selectivity

The potentiometric selectivity coefficients of the sensors Da_3, Db_2 and Dc_3 towards different cations were determined by the fixed interference method[227,35]. The selectivity coefficients were determined at 1.0×10^{-2} M concentration of foreign ions and was calculated using the following equation.

$$K_{A,B}^{pot} = a_A / (a_B)^{z_A / z_B}$$

The selectivity coefficient values are consolidated in Table 7.4. and the values indicate that all the three sensors Da_3, Db_2 and Dc_3 show very good selectivity to Pb^{2+} ions in the presence of Na^+, K^+, Mg^{2+}, Ca^{2+}, Ba^{2+}, NH_4^+, Mn^{2+}, Co^{2+}, Ni^{2+}, Zn^{2+}, Cu^{2+}, Hg^{2+} and Fe^{3+}, but only moderate selectivity in the presence of Ag^+ and Cd^{2+}.

7.2.8 Lifetime or Shelf life

The operative life time for the sensors Da_3, Db_2 and Dc_3 was found to be 6 months, 3.5 months and 4 weeks respectively. The sensors were all kept immersed in 1.0×10^{-1} M lead(II) nitrate solution when not in use. And as explained in the previous chapters for CMCPE sensors, the surface could be renewed.

7.2.9 Analytical applications

The utility of the sensors Da_3, Db_2 and Dc_3 was further investigated in the determination of lead(II) in 'Eveready' battery waste. The sample was prepared as discussed under Section 2.5.3 in Chapter 2. The results presented in Table 7.5 show that this method is comparable to the standard ICP-AES method[2].

The sensors Da_3, Db_2 and Dc_3 were successfully applied as an indicator electrode in conjuction with $Hg|Hg_2Cl_2$ (sat.) in the potentiometric titration of lead(II) nitrate solution. The titration curves for the sensors Da_3, Db_2 and Dc_3 are depicted in Figure 7.17, Figure 7.18 and Figure 7.19 respectively. The titration plots obtained were all of the standard sigmoid shape and the end point corresponds to 1:1 stoichiometry of Pb-EDTA complex.

7.3 A comparative study among the sensors Da_3, Db_2 and Dc_3 and to some of the reported sensors

All the three sensors Da_3, Db_2 and Dc_3 were found to have very good response characteristics. Table 7.6 consolidates the response characteristics of the sensors Da_3, Db_2 and Dc_3. Among the different types of sensors fabricated based on HBD, the CMCPE type sensor is better in terms of working concentration range and detection limit. The PVC membrane sensor Da_3 was found to have a fast response time of 10 s and also a tolerance of 25% non aqueous content with the longest shelf life of 6 months. The shelf life for the CMCPE type sensor Dc_3 was only 6 weeks but it had an advantage that the surface could be renewed by cutting off a little of the paste, polishing it on a smooth surface and reconditioning it on 1.0×10^{-1} M of lead(II) nitrate solution. In terms of pH range, Dc_3 gave the widest range of pH. Table 7.7 lists the comparative study of the characteristics of developed sensors with some of the reported sensors for Pb^{2+}. It can be seen that the developed sensors, especially sensor Da_3 and Db_2, are superior in terms of working concentration range[164,180,184,188,190,191,193,194,197,199,201], life time[164,180,184,188,190,191,193,194,197,199] and pH range[188,190,191,201] when compared with the performance of the sensors already reported.

Figures

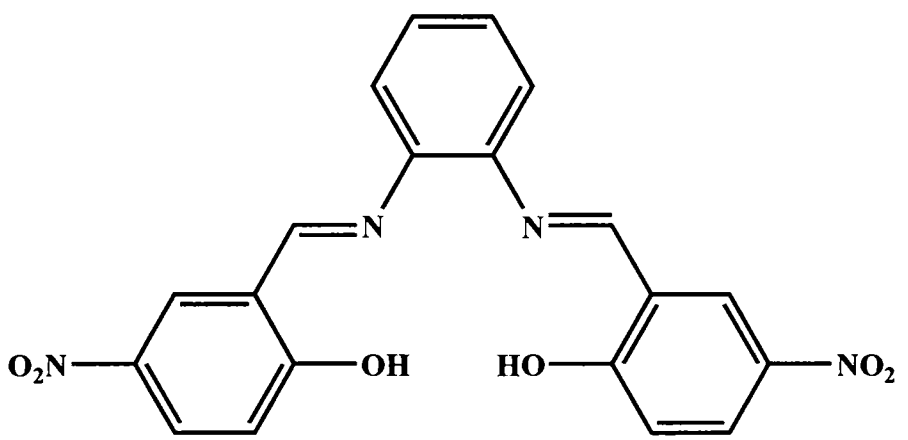

Figure 7.1 – Structure of the ionophore HBD

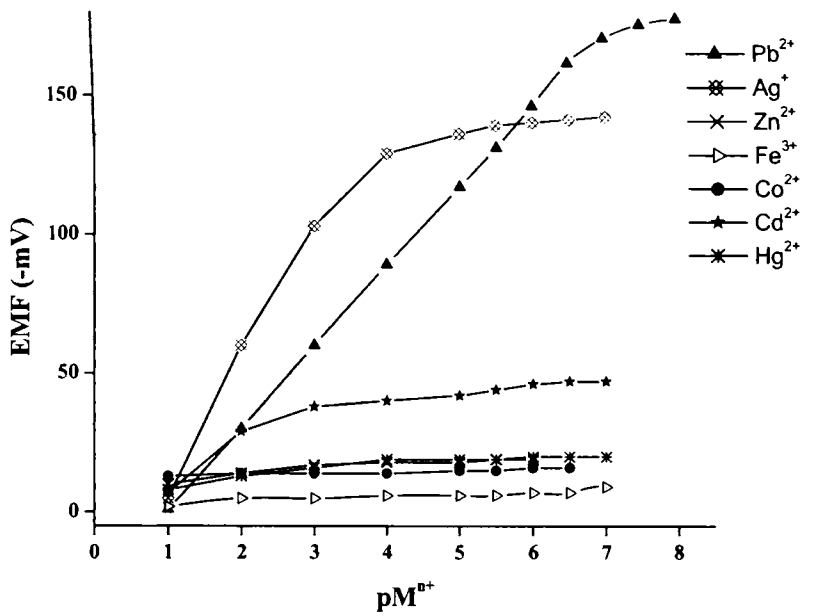

Figure 7.2- Potential response of the various PVC membrane sensors based on HBD.

Conditions: membrane composition ratio 30% PVC:65% DOP:2% NaTPB:3% HBD; internal solution 1.0×10^{-1} M of each cation used and conditioned in 1.0×10^{-1} M of the corresponding cation solution for 2 days

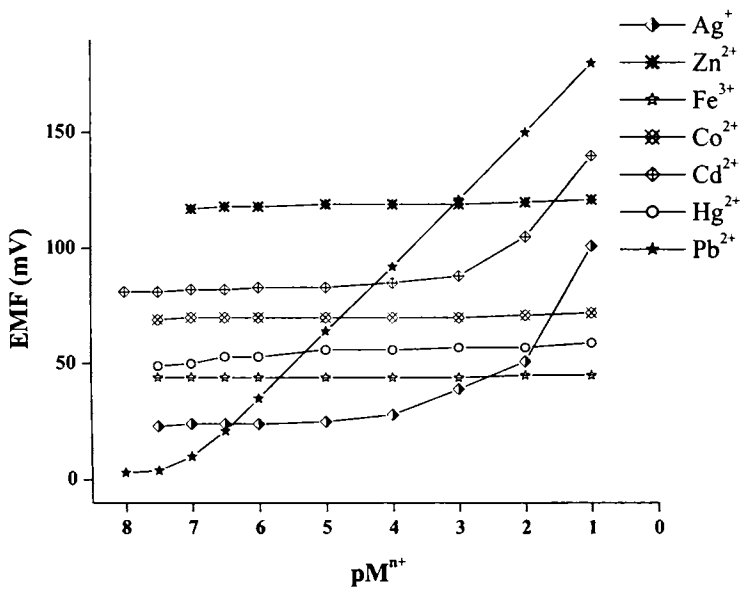

Figure 7.3- Potential response of the various CPE-PVC type sensors based on HBD.

Conditions: membrane composition ratio 30% PVC:65% DOP:2% NaTPB:3% HBD; conditioned in 1.0×10^{-1} M of the corresponding cation solution for 2 days

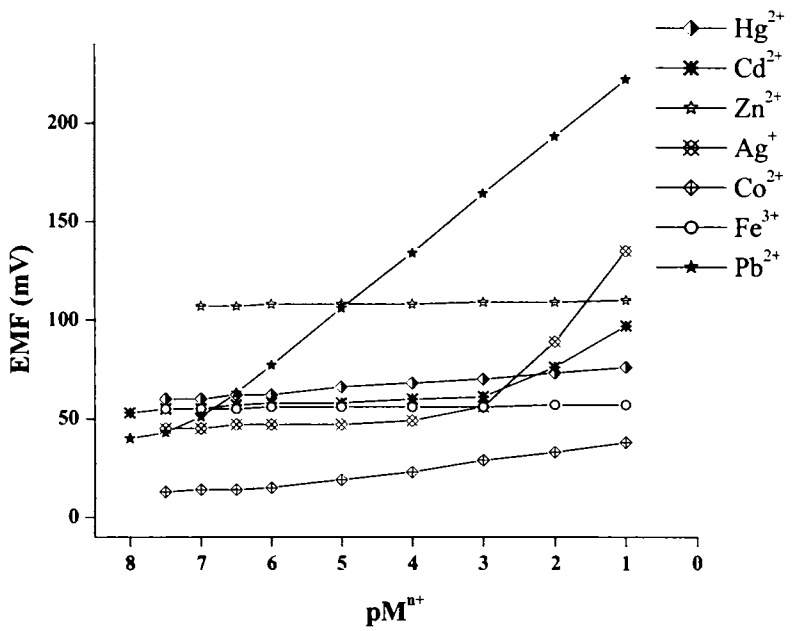

Figure 7.4 - Potential response of various CMCPE type sensors based on HBD.

Conditions: composition ratio 10% HBD:90% graphite; conditioned in 1.0×10^{-1} M of the corresponding cation solution for 6 h

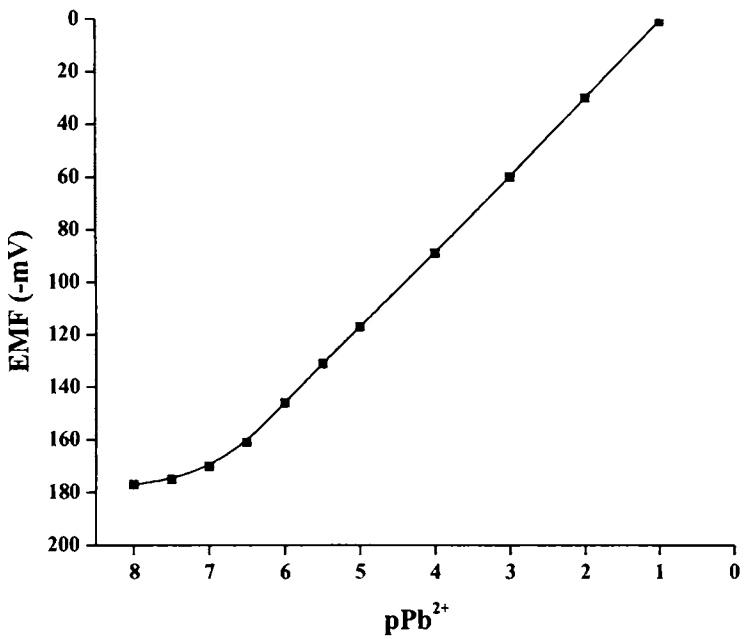

Figure 7.5 - Calibration graph of the PVC membrane sensor Da_3 based on HBD

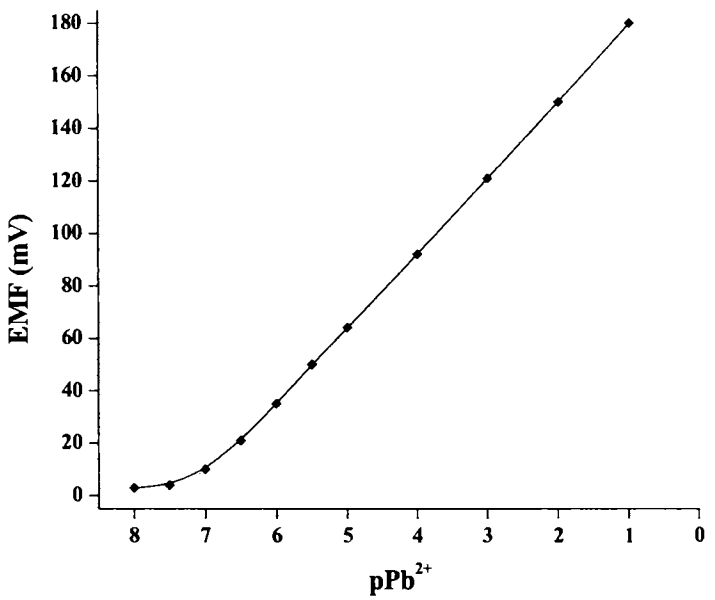

Figure 7.6 - Calibration graph of the CPE-PVC type sensor Db_2 based on HBD

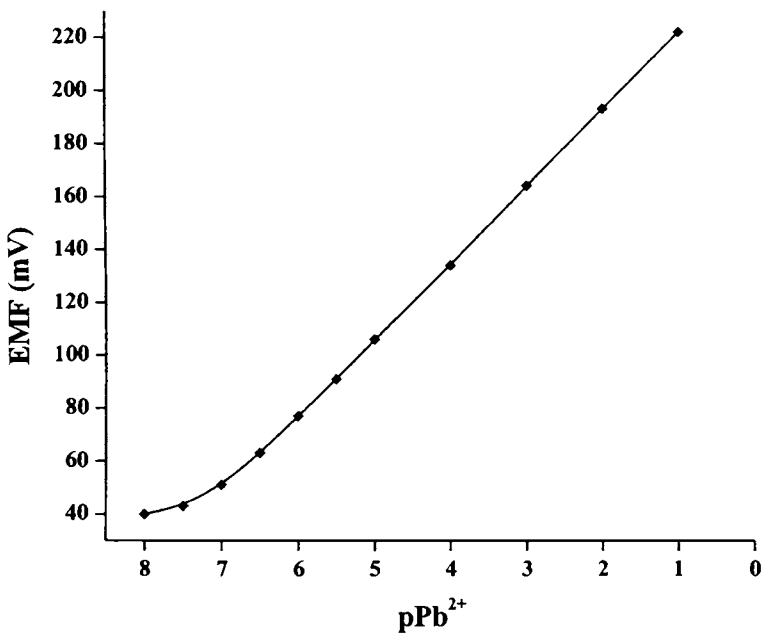

Figure 7.7 - Calibration graph of the CMCPE type sensor Dc_3 based on HBD

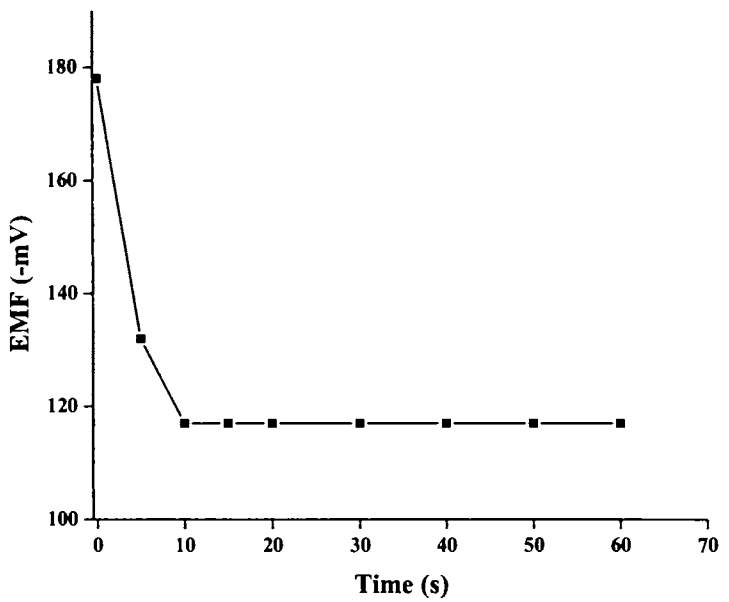

Figure 7.8 – Practical response time of the PVC membrane sensor Da_3 based on HBD from the moment of addition of Pb^{2+} (1.0×10^{-5} M) solution

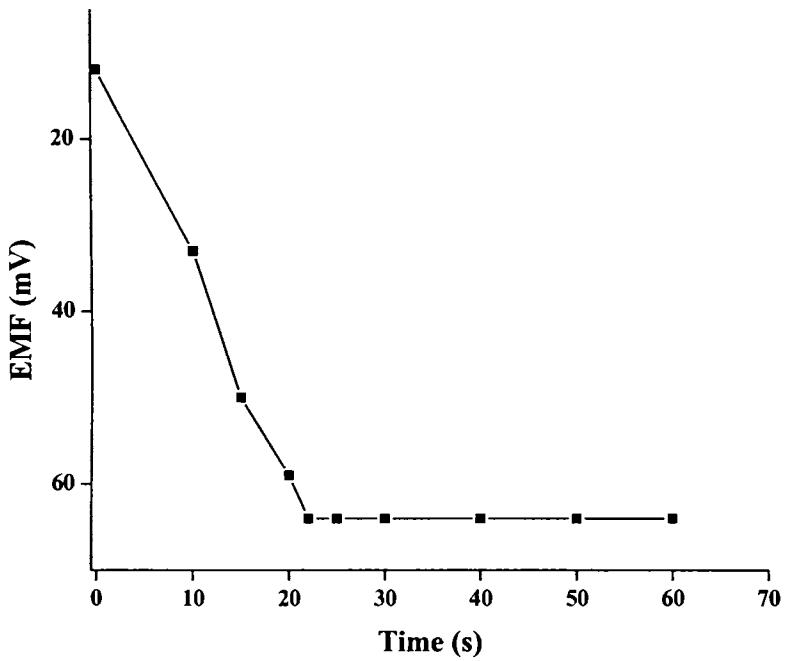

Figure 7.9 – Practical response time of the CPE-PVC type sensor Db_2 based on HBD from the moment of addition of Pb^{2+} (1.0×10^{-5} M) solution

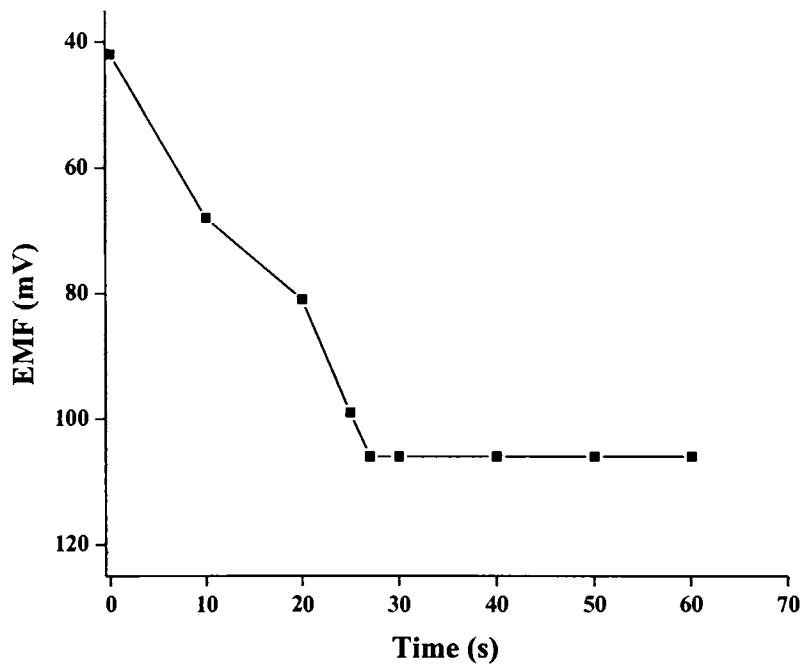

Figure 7.10 – Practical response time of the CMCPE type sensor Dc_3 based on HBD from the moment of addition of Pb^{2+} (1.0×10^{-5} M) solution

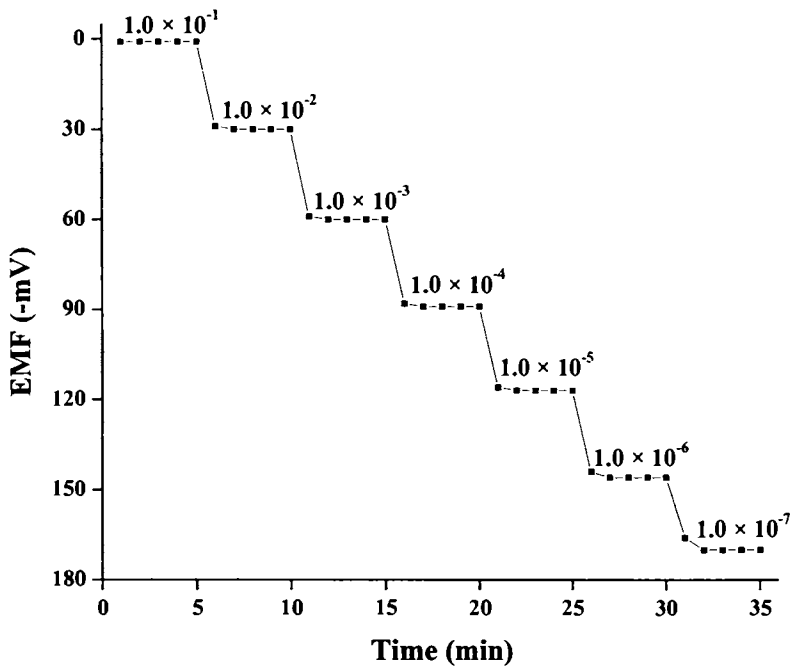

Figure 7.11 - Dynamic response time of the PVC membrane sensor Da_3 based on HBD for reversibility with step changes in concentration of Pb^{2+} (1.0×10^{-7} to 1.0×10^{-1} M)

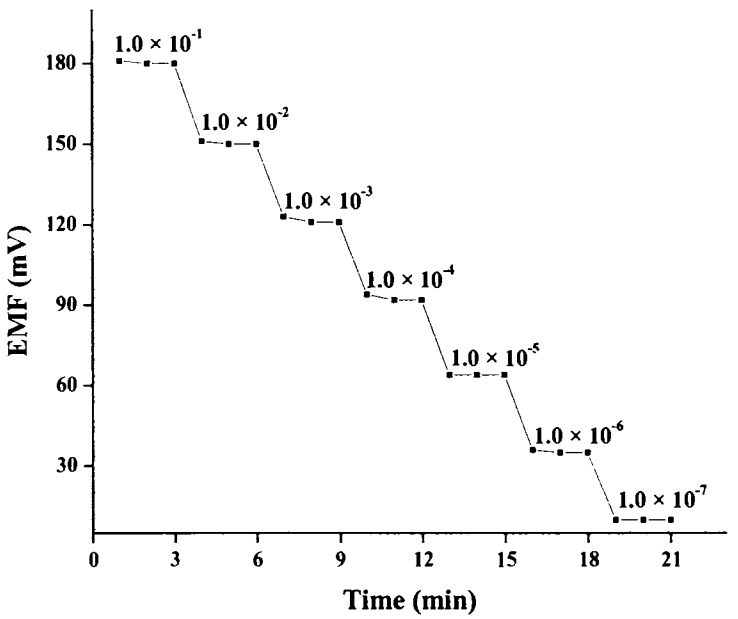

Figure 7.12 - Dynamic response time of the CPE-PVC type sensor Db_2 based on HBD for reversibility with step changes in concentration of Pb^{2+} (1.0×10^{-7} to 1.0×10^{-1} M)

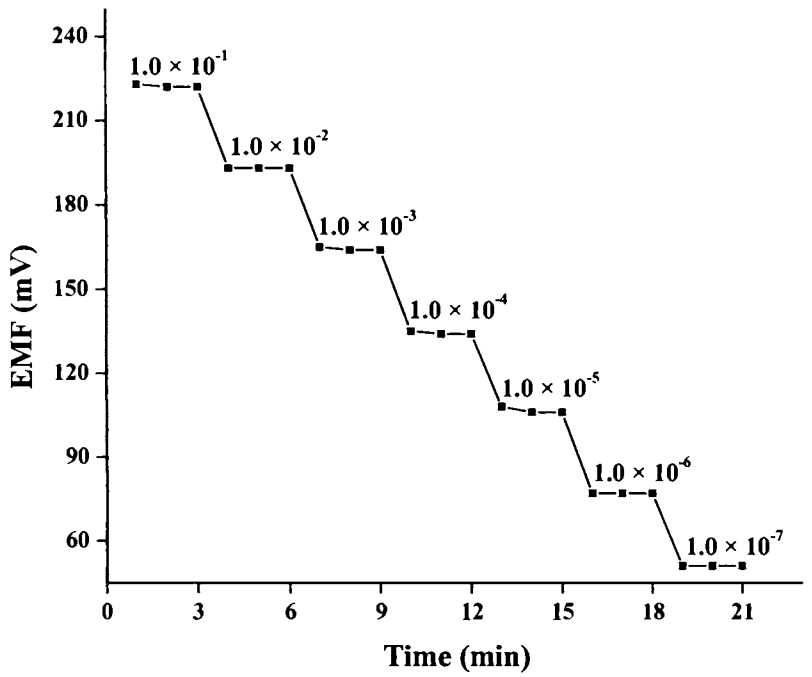

Figure 7.13 - Dynamic response time of the CMCPE type sensor Dc_3 based on HBD for reversibility with step changes in concentration of Pb^{2+} (1.0×10^{-7} to 1.0×10^{-1} M)

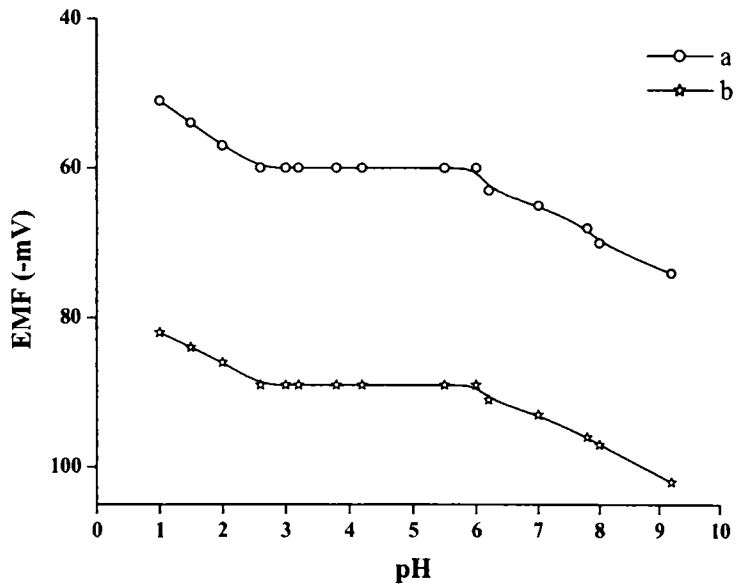

Figure 7.14 – Effect of pH on the cell potential of the PVC membrane sensor Da_3 based on HBD at 1.0×10^{-3} M (a) and 1.0×10^{-4} M (b)

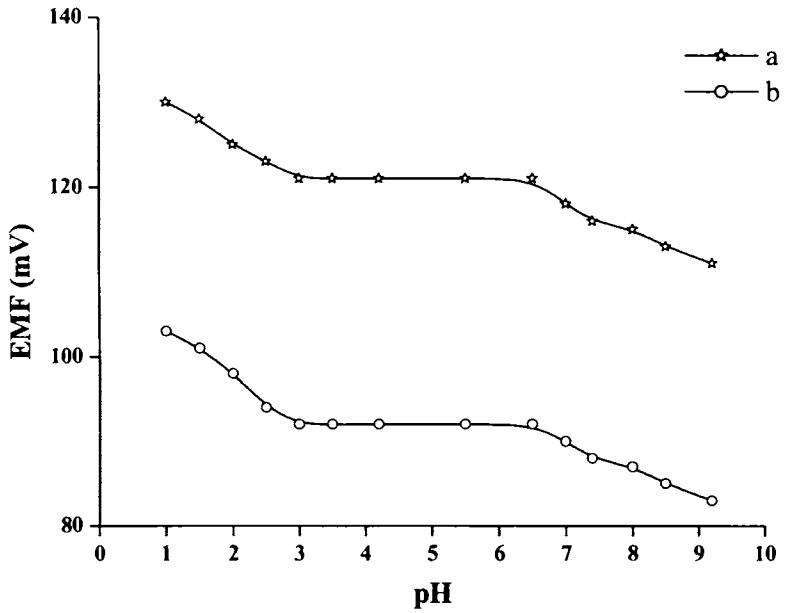

Figure 7.15 – Effect of pH on the cell potential of the CPE-PVC type sensor Db_2 based on HBD at 1.0×10^{-3} M (a) and 1.0×10^{-4} M (b)

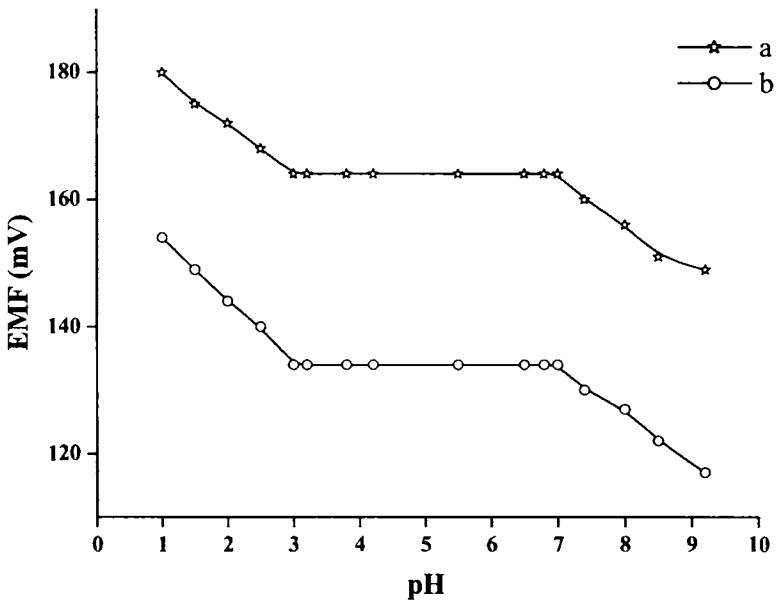

Figure 7.16 – Effect of pH on the cell potential of the CMCPE type sensor Dc_3 based on HBD at 1.0×10^{-3} M (a) and 1.0×10^{-4} M (b)

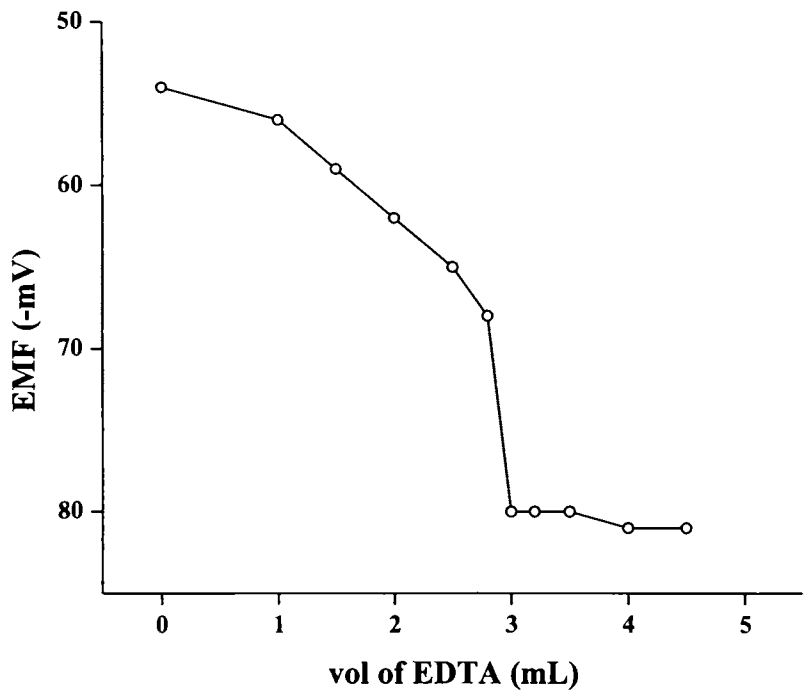

Figure 7.17 – Potentiometric titration curve of 10.0 mL of 3.0×10^{-3} M Pb^{2+} solution with 1.0×10^{-2} M EDTA using the PVC membrane sensor Da_3 as an indicator electrode at pH 5.0.

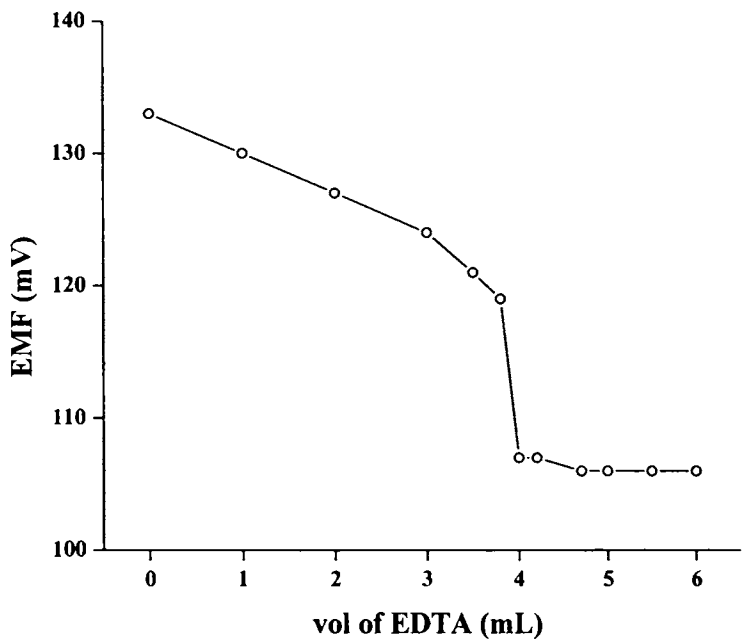

Figure 7.18 – Potentiometric titration curve of 10.0 mL of 4.0×10^{-3} M Pb^{2+} solution with 1.0×10^{-2} M EDTA using the CPE-PVC type sensor Db_2 as an indicator electrode at pH 5.0.

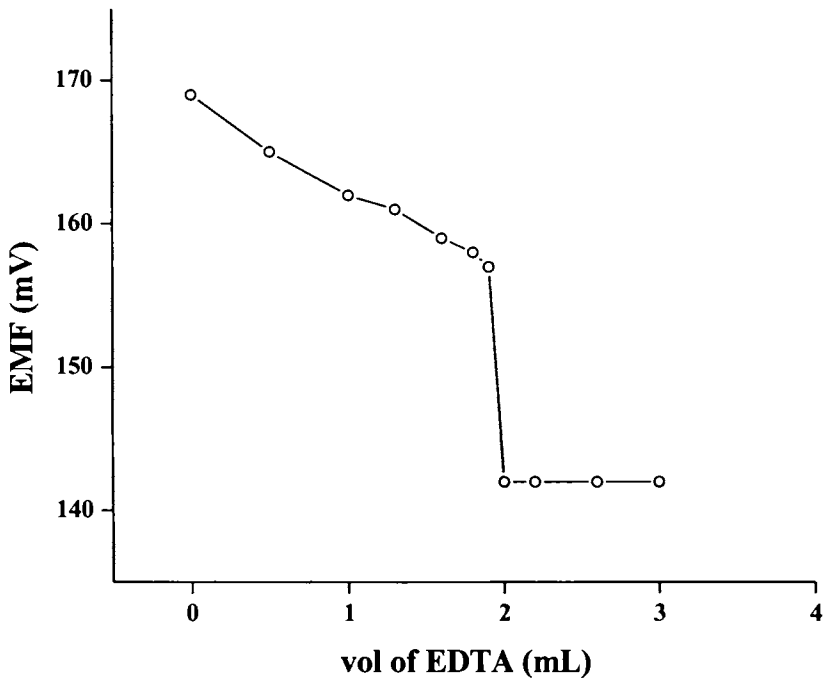

Figure 7.19 – Potentiometric titration curve of 10.0 mL of 2.0×10^{-3} M Pb^{2+} solution with 1.0×10^{-2} M EDTA using the CMCPE type sensor Dc_3 as an indicator electrode at pH 5.0.

Table 7.1 - Optimization of the PVC membrane ingredients for the PVC membrane (Da) and CPE-PVC type (Db) of sensors based on HBD[a]

Sensor	% w/w composition of each membrane				Working concentration range (M)	Slope (mV decade^{-1})	Response time (s)
	PVC	HBD	Plasticizer	NaTPB			
Da_1	96	2	0	2	$1.0 \times 10^{-1} - 5.0 \times 10^{-6}$	22.9(±0.3)	87
Da_2	30	1	DOP, 67	2	$1.0 \times 10^{-1} - 6.1 \times 10^{-7}$	26.3(±0.9)	24
Da_3	30	3	DOP, 65	2	$1.0 \times 10^{-1} - 1.8 \times 10^{-7}$	29.7(±0.6)	10
Da_4	30	5	DOP, 63	2	$1.0 \times 10^{-1} - 5.6 \times 10^{-7}$	25.2(±0.1)	30
Da_5	30	3	DBP, 65	2	$1.0 \times 10^{-1} - 2.9 \times 10^{-6}$	21.6(±0.5)	25
Da_6	30	3	DOA, 65	2	$1.0 \times 10^{-1} - 5.4 \times 10^{-4}$	15.7(±0.4)	55
Da_7	30	3	DOS, 65	2	$1.0 \times 10^{-1} - 3.7 \times 10^{-5}$	11.8(±0.5)	74
Db_1	0	0	0	0	$1.0 \times 10^{-1} - 1.0 \times 10^{-5}$	~0.0	100
Db_2	30	3	DOP, 65	2	$1.0 \times 10^{-1} - 8.8 \times 10^{-8}$	29.8(±0.9)	22

[a] Values in parentheses are RSDs based on three replicates

Table 7.2 - Optimization of the ionophore composition for the CMCPE type of sensor based on HBD[a]

Sensor	Ionophore	Graphite	Working concentration range (M)	Slope (mV decade^{-1})	Response time (s)
Dc_1	0	100	1.0×10^{-1} - 1.0×10^{-4}	1.4(±0.1)	150
Dc_2	5	95	1.0×10^{-1} - 2.8×10^{-6}	25.2(±0.4)	39
Dc_3	10	90	1.0×10^{-1} - 5.9×10^{-8}	30.2(±0.5)	27
Dc_4	20	80	1.0×10^{-1} - 7.9×10^{-6}	39.8(±0.3)	45
Dc_5	30	70	1.0×10^{-2} - 1.6×10^{-5}	31.2(±0.3)	60
Dc_6	50	50	1.0×10^{-2} - 9.2×10^{-4}	37.5(±0.5)	76

[a] Values in parentheses are RSDs based on three replicates.

Table 7.3 – Effect of partially non-aqueous medium on the slope of the sensors Da_3, Db_2 and Dc_3

Non-aqueous content (% v/v)	Slope (mV decade^{-1})		
	Da_3	Db_2	Dc_3
0	29.7	29.8	30.2
Ethanol			
10	29.7	29.8	30.1
20	29.1	28.8	28.7
25	28.5	26.4	26.2
30	28.4	25.2	22.1
Methanol			
10	29.6	29.7	30.2
20	29.0	28.7	28.8
25	28.5	26.5	26.3
30	28.1	25.3	22.2

Table 7.4 – Selectivity coefficients for the sensors Da_3, Db_2 and Dc_3 using fixed interference method at 1.0×10^{-2} M concentration of interfering ion.

Interfering ion (X)	Da_3	Db_2	Dc_3
Na^+	5.8×10^{-3}	4.0×10^{-3}	4.7×10^{-3}
K^+	3.2×10^{-3}	2.9×10^{-3}	3.7×10^{-3}
NH_4^+	2.5×10^{-2}	2.7×10^{-2}	2.3×10^{-2}
Ag^+	9.4×10^{-1}	9.1×10^{-1}	8.9×10^{-1}
Mg^{2+}	7.2×10^{-3}	8.4×10^{-3}	6.2×10^{-3}
Ca^{2+}	4.8×10^{-3}	3.1×10^{-3}	3.8×10^{-3}
Ba^{2+}	7.2×10^{-3}	8.9×10^{-3}	7.9×10^{-3}
Mn^{2+}	6.5×10^{-3}	7.0×10^{-3}	5.3×10^{-3}
Co^{2+}	4.3×10^{-3}	4.9×10^{-3}	3.8×10^{-3}
Ni^{2+}	1.8×10^{-3}	1.1×10^{-3}	1.5×10^{-3}
Zn^{2+}	8.3×10^{-3}	7.9×10^{-3}	6.2×10^{-3}
Cd^{2+}	2.7×10^{-1}	4.1×10^{-1}	5.9×10^{-1}
Hg^{2+}	9.4×10^{-2}	8.6×10^{-2}	8.2×10^{-2}
Cu^{2+}	5.4×10^{-3}	4.8×10^{-3}	5.5×10^{-3}
Fe^{3+}	2.0×10^{-2}	2.9×10^{-2}	2.1×10^{-2}

Table 7.5 - Determination of the Pb^{2+} content in Eveready battery waste sample

Sample	Da_3* ppm	Db_2* ppm	Dc_3* ppm	ICP-AES ppm
Eveready battery waste	18.22 ± 0.04	18.21 ± 0.05	18.26 ± 0.07	18.11

* RSDs based on three replicates.

Table 7.6 – Response characteristics of the sensors Da_3, Db_2 and Dc_3

Parameter	Response characteristics		
	Da_3	Db_2	Dc_3
Working concentration range (M)	1.0×10^{-1} – 5.0×10^{-7}	1.0×10^{-1} – 1.0×10^{-7}	1.0×10^{-1} – 1.0×10^{-7}
Slope (mV $decade^{-1}$)	29.7 ± 0.6	29.8 ± 0.9	30.2 ± 0.5
Detection limit (M)	1.8×10^{-7}	8.8×10^{-8}	5.9×10^{-8}
Response time	10 s	22 s	27 s
pH range	2.6-6.0	3.0-6.5	3.0-7.0
Non aqueous tolerance limit	25%	20%	10%
Shelf life	6 months	3.5 months	4 weeks

Table 7.7 -Comparison of characteristics of the sensor with some reported sensors

No.	Working concentration range (M)	Slope (mV decade^{-1})	pH range	Lifetime	Ref. No.
1	$4.3 \times 10^{-3} - 1.0 \times 10^{-6}$	Nernstian	2.0-6.0	4 months	180
2	$5.0 \times 10^{-2} - 2.0 \times 10^{-5}$	Nernstian	NM*	NM	188
3	$1.0 \times 10^{-2} - 5.0 \times 10^{-5}$	Nernstian	NM	10 months	190
4	$1.0 \times 10^{-2} - 1.0 \times 10^{-5}$	Nernstian	4.5-7.0	3 months	191
5	$1.0 \times 10^{-1} - 1.0 \times 10^{-5}$	Nernstian	4.0-8.0	12 weeks	184
6	$1.0 \times 10^{-2} - 1.0 \times 10^{-6}$	Nernstian	4.0-7.0	1 month	193
7	$1.0 \times 10^{-2} - 4.0 \times 10^{-6}$	Near Nernstian	4.5-7.0	2 weeks	194
8	$1.0 \times 10^{-1} - 6.0 \times 10^{-7}$	Nernstian	1.5-6.0	5 months	198
9	$1.0 \times 10^{-1} - 5.0 \times 10^{-6}$	Nernstian	5.0-9.0	3 months	199
10	$1.0 \times 10^{-1} - 6.0 \times 10^{-7}$	Nernstian	3.0-6.0	2 months	197
11	$6.1 \times 10^{-4} - 2.2 \times 10^{-8}$	Nernstian	6.0	NM	201
12	$5.0 \times 10^{-2} - 2.5 \times 10^{-6}$	Nernstian	1.6-6.0	5 months	164
13	$1.0 \times 10^{-1} - 5.0 \times 10^{-7}$	Nernstian	2.6-6.0	6 months	**Da_3**
14	$1.0 \times 10^{-1} - 1.0 \times 10^{-7}$	Nernstian	3.0-6.5	3.5 months	**Db_2**
15	$1.0 \times 10^{-1} - 1.0 \times 10^{-7}$	Nernstian	3.0-7.0	4 weeks	**Dc_3**

*NM – not mentioned

Chapter 8

CONCLUSIONS

This chapter presents the important milestones and future outlook of the work embodied in this thesis.

8.1 Important Milestones

The main objectives of the present work include the following

- Synthesis of the ionophores
- Characterization of the synthesized ionophores by elemental analysis and infrared spectroscopic methods
- Fabrication of different types of sensors
- Investigation of the response of the developed sensor to different cations
- Optimization of the membrane composition
- Study of the response characteristics of the developed sensor
- Analytical applications
- Comparison with other reported sensors

As part of the present investigations, a total of fourteen potentiometric sensors have been developed and fabricated. A three fold approach has been taken in developing the sensors, viz., PVC plasticized membrane sensor, carbon paste electrode and chemically modified carbon paste electrode. All the sensors are highly useful in the determination of metal ions such as manganese(II), nickel(II), copper(II), mercury(II) and lead(II). A thorough analytical study has been carried out with respect to

each sensor developed. Based on these studies, optimum conditions have been developed for the quantitative determinations of the selected metal ions using the sensors. Systematic application studies have also been carried out for all the developed sensors and the results revealed that the presently developed sensors are far superior than most of the sensors reported.

The fourteen potentiometric sensors developed for the respective metal ions are

Mn^{2+} - CPE-PVC and CMCPE type. (2 nos)

Ni^{2+} - PVC membrane sensors. (2 nos)

Cu^{2+} - PVC membrane, CPE-PVC and two CMCPE type (4 nos)

Hg^{2+} - PVC membrane, CPE-PVC and CMCPE type (3 nos)

Pb^{2+} - PVC membrane, CPE-PVC and CMCPE type (3 nos)

8.2 Future Outlook

The field of sensors is rapidly developing and efforts are being made to design sensors, which are cost effective, simple in operation, reliable, a small instrumental arrangement and most of all portability. Attempts are being made for the fabrication of sensors with disposable characteristics as it avoids electrode poisoning from repeated usage of the same sensor surface for successive analyses. It is hoped that the developed potentiometric sensors can find wide applications in the future analytical chemistry.

References

1. H. Haraguchi, *Bull. Chem. Soc. Jpn.*, **72**, 1163 (1999).
2. J. Mendham, R. C. Denney, J. D. Barnes and M. Thomas, *Vogel's Textbook of Quantitative Chemical Analysis*, 6th Edn, Pearson Education Ltd, Singapore (2002).
3. C. L. Wilson and D. W. Wilson (eds), *Comprehensive analytical chemistry*, Elseiver, Amsterdam (1960).
4. D. Malinin and J. H. Yoe, *J. Chem. Edu.*, **38**, 129 (1961).
5. K. Girish Kumar and R. Muthuselvi, *Asian J. Chem.*, **131**, 337 (2001).
6. K. Girish Kumar and R. Muthuselvi, *Microchim. Acta*, **137**, 25 (2001).
7. K. Girish Kumar and R. Muthuselvi, *J. Anal. Chem.*, **61**, 28 (2006).
8. C. M. A. Brett and A. M. Oliveira Brett. *Electroanalysis*, Oxford University Press, Oxford (1998).
9. C. M. A. Brett, *Pure Appl. Chem.*, **73**, 1969 (2001).
10. A.J. Bard and L.R. Faulkner, *Electrochemical methods, fundamentals and applications*, Wiley, New York (1980).
11. J. Wang, *Analytical Electrochemistry*, 2nd ed., Wiley-VCH, Weinheim (2000).
12. R. W. Cattrall, *Chemical Sensors*, Oxford Chemistry Primers, New York (1997).
13. M. Cremer, *Z. Biol.*, **47**, 562 (1906).
14. F. Haber and Z. Klemensiewicz, *Z. Physik. Chem.*, **67**, 385

(1909).

15. M. Dole, *The Glass Electrode*, New York (1941).
16. R. Buck and E. Lindner, *Anal. Chem.*, **73**, 88A (2001).
17. M. S. Frant and J. W. Ross, *Science*, **154**, 1553 (1966).
18. R. A. Durst (Editor), *Ion-Selective Electrodes*, Natl. Bur. Stand. Spec. Publ., Washington (1969).
19. J. Ross, *Science*, **156**, 1378 (1967).
20. G. J. Moody, R. B. Oke and J. D. R. Thomas, *Analyst*, **95**, 910 (1970).
21. J. Ruzicka and J. C. Tjell, *Anal. Chim. Acta*, **49**, 349 (1970).
22. S. Mesaric and E. A. M. F. Dahmen, *Anal. Chim. Acta*, **64**, 431 (1973).
23. W. R. Heineman, H. J. Wieck and A. M. Yacynych, *Anal. Chem.*, **52**, 345 (1980).
24. G. Price and P. L. Drake, *React. Funct. Polym.*, **66**, 109 (2006).
25. S. Baniwal, S. Chandra, A. Panwar and A. K. Singh, *Talanta*, **50**, 499 (1999).
26. M. R. Ganjali, P. Norouzi, L. Shamsolahrari and A. Ahmadi, *Sens. Actuators B*, **114**, 713 (2006).
27. V. K. Gupta, A. K. Singh and B. Gupta, *Anal. Chim. Acta*, **575**, 198 (2006).
28. Z. Yan, Y. Lu and X. Li, *Sens. Actuators B*, online (2006).
29. K. Girish Kumar, K. Saji John and C. J. Indira, *Indian J. Chem. Tech.*, **13**, 13 (2006).
30. M. Shamsipur, A. Soleymanpour, M. A. Khond, H. Sharghi and A. R. Hasaninejad, *Sens. Actuators B*, **89**, 9 (2003).

31. M. M. Ardakani, M. Salavati-Niasari and M. Jamshidpoor, *Sens. Actuators B*, **101**, 302 (2004).

32. K. Girish Kumar, Sareena John, Remalakshmy Poduval and Pearl Augustine, *The Chinese Pharm. Jour.*, **57**, 29 (2005).

33. S. S. M. Hassan, W. H. Mahmoud, M. A. F. Elmosallamy and M. H. Almarzooqi, *J. Pharm. Biomed. Anal.*, **39**, 315 (2005).

34. W. Simon, H. R. Wuhrmann, M. Vasak, L. A. R. Pioda, R. Dohner and Z. Stefanac, *Angew. Chem.*, **82**, 433 (1970).

35. R. P. Buck and E. Lindner, *Pure Appl. Chem.*, **66**, 2527 (1994).

36. E. B. Buchanan Jr. and J. L. Seago, *Anal. Chem.*, **40(3)**, 517 (1968).

37. H. Hirata and K. Higashiyama, *Talanta*, **19**, 391 (1972).

38. U. S. Lal, M. C. Chattopadhyaya, M. C. Ghosh and A. K. Dey, *Indian Agric.*, 139 (1982); *Chem. Abstr.*, **99**, 15614w (1983).

39. D. Midgley and D. E. Mulchay, *Talanta*, **32**, 7 (1985).

40. V. Agarwala and M. C. Chattopadhyaya, *Anal. Lett.*, **22**, 1451 (1989).

41. B. Y. Sun and Y. H. Qi, *Fenxi Huaxue*, **22**, 1138 (1994).

42. X. H. Dong, *Fenxi Huaxue*, **24**, 494 (1996).

43. A. K. Singh, P. Saxena and A. Panwar, *Sens. Actuators B*, **110**, 377 (2005).

44. S. Morazzani-Pelletier and M. A. Baffier, *J. Chim. Phys.*, **62**, 429 (1965).

45. E. Pungor, K. Toth and J. Havas, *Microchim. Acta*, **4/5**, 689 (1966).

46. T. N. Dobbelstein and H, Diehl, *Talanta*, **16**, 1341 (1969).

47. E. A. Materova, V. V. Muchovikov and M. G. Grigorieva, *Anal. Lett.*, **8**, 167 (1975).
48. C. Luca, P. Maria and M. Nicolae, *Rev. Chim.*, **27**, 1088 (1976).
49. E. V. Smirnova, O. M. Petrukhin and S. L. Rogatinskaya, *Zh. Anal. Khim.*, **37**, 2137 (1982).
50. U. S. Lal, M. C. Chattopadhyaya and A. K. Dey, *J. Indian Chem. Soc.*, **49**, 493 (1982).
51. M. D. Hampton, C. A. Peters and L. A. Wellington, *Anal. Chim. Acta*, **194**, 171 (1987).
52. S. P. Aswathi, V. T. Kulkarni and M. Sundaresan, *J. Electrochem. Soc. India*, **37**, 309 (1988).
53. H. P. Bhatt and N. V. Thakkar, *Indian J. Chem.*, **33A**, 436 (1994).
54. G. N. Rao, S. Srivastava, S. K. Srivastava and M. Singh, *Talanta*, **43**, 1821 (1996).
55. V. K. Gupta, A. K. Jain, L. P. Singh and U. Khurana, *Anal. Chim. Acta*, **355**, 33 (1997).
56. V. K. Gupta, R. Prasad, P. Kumar and R. Mangla, *Anal. Chim. Acta*, **420**, 19 (2000).
57. V. K. Gupta, R. Prasad and A. Kumar, *Sensors*, **2**, 384 (2002).
58. V. K. Gupta, R. N. Goyal, S. Agarwal, P. Kumar and N. Bachheti, *Talanta*, online (2006).
59. A. K. Jain, V. K. Gupta, R. D. Singh, U. Khurana and L. P. Singh, *Sens. Actuators B.*, **40**, 15 (1997).
60. A. K. Jain, V. K. Gupta, P. A. Ganeshpune and J. R. Raisoni, *Anal. Chim. Acta*, **553**, 177 (2005).
61. M. F. Mousavi, N. Alizadeh, M. Shamsipur and N. Zohari, *Sens.*

Actuators B., **66**, 98 (2000).

62. M. Shamsipur and S. Y. Kazemi, *Electroanalysis*, **12**, 1472 (2000).
63. M. R. Ganjali, M. R. Fathi, H. Rahmani and H. Pirelahi, *Electroanalysis*, **12**, 1138 (2000).
64. M. R. Ganjali, M. Hosseini, M. Salavati-Niasari, T. Poursaberi, M. Shamsipur, M. Javanbakht, and O. R. Hashemi, *Electroanalysis*, **14**, 526 (2002).
65. A. Abbaspour and A. Izadyar, *Microchem. J.*, **69**, 7 (2001).
66. A. K. Singh, C. L. Sharma, S. Baniwal and A. Panwar, *Electroanalysis*, **13**, 1209 (2001).
67. A. K. Singh and R. Singh, *J. Inclusion Phenom. Macrocyclic Chem.*, **53**, 249 (2005).
68. A. K. Singh and P. Saxena, *Sens. Actuators B*, online (2006).
69. M. Mazloum, M. S. Niassary and M. K. Amini, *Sens. Actuators B*, **82**, 259 (2002).
70. M. H. Mashhadizadeh and A. Momeni, *Talanta*, **59**, 47 (2003).
71. M. H. Mashhadizadeh, I. Sheikhshoaie and S. Saeid-Nia, *Sens. Actuators B*, **94**, 241 (2003).
72. L. P. Singh and J. M. Bhatnagar, *Sensors*, **3**, 393 (2003).
73. K. Belhamel, R. Ludwig and M. Benamor, *Microchim. Acta*, **149**, 145 (2005).
74. A. Yari, S. Azizi and A. Kakanejadifard, *Sens. Actuators B*, online (2006).
75. Orion Research Inc., *Cupric Ion Electrode (Model 94-29)*, Instruction Manual (1971).

76. B. Chatterjee and D. K. Mitra, *J. Indian Chem. Soc.*, **32**, 751 (1955).

77. H. Hirata, K. Higashiyama and K. Date, *Anal. Chim. Acta*, **51**, 209 (1970).

78. H. Hirata and K. Date, *Talanta*, **17**, 883 (1970)

79. M. Sharp and G. Johansson, *Anal. Chim. Acta*, **54**, 13 (1971).

80. M. Neshkova and H. Sheytanov, *Talanta*, **32**, 654 (1985).

81. M. Neshkova and H. Sheytanov, *Talanta*, **32**, 937 (1985).

82. S. Kamata, A. Bhale, Y. Funkanaga and H. Murata, *Anal. Chem.*, **60**, 2464 (1989).

83. S. Kamata, H. Murata, Y. Kubo and A. Bhale, *Analyst*, **114**, 1029 (1989).

84. A. K. Jain, P. Singh and L. P. Singh, *Ind. J. Chem.*, **33**, 272 (1994).

85. A. K. Jain, V. K. Gupta, L. P. Singh and J. R. Raisoni, *Talanta*, **66**, 1355 (2005).

86. C. Sun, Y. Sun, X. Zhang, H. Xu and J. Shen, *Anal. Chim. Acta*, **312**, 207 (1995).

87. Z. Chen and P. W. Alexander, *Electroanalysis*, **9**, 141 (1997).

88. M. J. Gismera, M. A. Mendiola, J. R. Procopio and M. T. Sevilla, *Anal. Chim. Acta*, **385**, 143 (1999).

89. M. J. Gismera, J. R. Procopio, M. T. Sevilla and L. Hernandez, *Electroanalysis*, **15**, 126 (2003).

90. M. Shamsipur, S. Rouhani, M. R. Ganjali, H. Eshghi and H. Sharghi, *Microchem. J.*, **63**, 202 (1999).

91. N. Alizadeh, S. Ershad, H. Naeimi, H. Sharghi and M. Shamsipur,

Fresenius J. Anal. Chem., **365**, 511 (1999).

92. M. Shamsipur, Javanbakht, M. F. Mousavi, M. R. Ganjali, V. Lippolis, A. Garau, L. Tei, *Talanta*, **55**, 1047 (2001).
93. K. C. Gupta and M. J. D'Arc, *Sens. Actuators B*, **62**, 171 (2000).
94. K. C. Gupta and M. J. D'Arc, *Anal. Chim. Acta*, **437**, 199 (2001).
95. M. B. Saleh, *Anal. Lett.*, **33(8)**, 1501 (2000).
96. P. J. Kumari and M. C. Chattopadhyaya, *J. Inst. Chem. (India)*, **72(2)**, 65 (2000).
97. K. K. Tiwari and M. C. Chattopadhyaya, *Indian J. Chem.*, **40A**, 619 (2001).
98. S. J. Park, O. J. Shon, J. A. Rim, J. K. Lee, J. S. Kim, H. Nam and H. Kim, *Talanta*, **55**, 297 (2001).
99. M. B. Gholivand and N. Nozari, *Talanta*, **54**, 597 (2001).
100. L. Tymecki, M. Jakubowska, S. Achmatowicz, R. Koncki and S. Glab, *Anal. Lett.*, **34**, 71 (2001).
101. C. C. Su, C. H. Ueng and L. K. Liu, *J. Chinese Chem. Soc.*, **48**, 733 (2001).
102. M. R. Ganjali, T. Poursaberi, L. H. Babaei, S. Rouhani, M. Yousefi, M. K. Razi, A. Moghimi, H. Aghabozorg and M. Shamsipur, *Anal. Chim. Acta*, **440**, 81 (2001).
103. T. Poursaberi, L. H. Babaei, M. Yousefi, S. Rouhani, M. Shamsipur, M. K. Razi, A. Moghimi, H. Aghabozorg and M. R. Ganjali, *Electroanalysis*, **13**, 1513 (2001)
104. M. R. Ganjali, M. Emani and M. S. Niasari, *Bull. Korean Chem. Soc.*, **23**, 1394 (2002).
105. A. R. Firooz, M. Mazloum, J. Safari and M. K. Amini, *Anal.*

Bioanal. Chem., **372**, 718 (2002).

106. A. Abbaspour and S. M. M. Moosavi, *Talanta*, **56**, 91 (2002).
107. A. Abbaspour and M. A. Kamyabi, *Anal. Chim. Acta*, **455**, 225 (2002).
108. M. R. Al-Saraj, S. M. Saadeh, M. S. Abdel-Latif and S. Monzir, *Anal. Lett.*, **36**, 2417 (2003).
109. M. R. Al-Saraj, S. M. Saadeh, M. S. Abdel-Latif and S. Monzir, *Chemical Sciences*, **58**, 658 (2003).
110. S. Sadeghi, M. Eslahi, M. A. Naseri, H. Naeimi, H. Sharghi and A. Shameli, *Electroanalysis*, **15**, 1327 (2003).
111. S. Yoshimoto, H. Mukai, T. Kitano and Y. Sohrin, *Anal. Chim. Acta*, **494**, 207 (2003).
112. V. K. Gupta, R. Prasad and A. Kumar, *Talanta*, **60**, 149 (2003).
113. V. K. Gupta, R. N. Goyal, N. Bachheti, L. P. Singh and S. Agarwal, *Talanta*, **68**, 193 (2005).
114. V. K. Gupta, A. K. Jain, G. Maheshwari, H. Lang and Z. Ishtaiwi, *Sens. Actuators B*, online (2006).
115. M. M. Ardakani, M. Salavati-Niasari, M. K. Kashani and S. M. Ghoreishi, *Anal. Bioanal. Chem.*, **378**, 1659 (2004).
116. L. P. Singh and J. M. Bhatnagar, *Talanta*, **64**, 313 (2004).
117. A Michalska, M. Ocypa and K. Maksymiuk, *Electroanalysis*, **17**, 327 (2005).
118. M. Ocypa, A Michalska and K. Maksymiuk, *Electrochim. Acta*, **51**, 2298 (2006).
119. A. R. Fakhari, T. A. Raji and H. Naeimi, *Sens. Actuators B*, **104**, 317 (2005).

120. S. S. M. Hassan, E. M. Elnemma and A. H. K. Mohamed, *Talanta*, **66**, 1034 (2005).

121. Z. Szigeti, I. Bitter, K. Tóth, C. Latkoczy, D. J. Fliegel, D. Günther and E. Pretsch, *Anal. Chim. Acta*, **532**, 129 (2005).

122. A. K. Singh, S. Mehtab and A. K. Jain, *Anal. Chim. Acta*, **575**, 25 (2006).

123. I. A. M. de Oliveira, M. Pla-Roca, L. Escriche, J. Casabó, N. Zine, J. Bausells, J. Samitier and A. Errachid, *Mater. Sci. Eng., C*, **26**, 394 (2006).

124. J. Ruzicka and J. Chr. Tjell, *Anal. Chim. Acta*, **51**, 1 (1970).

125. G. E. Baiulescu and V. V. Cosofret, *Talanta*, **23**, 677 (1976).

126. G. E. Baiulescu and N. Ciocan, *Talanta*, **24**, 37 (1977).

127. V. V. Cosofret, P. G. Zugravescu and G. E. Baiulescu, *Talanta*, **24**, 461 (1977).

128. W. Szczepaniank and J. Oleksy, *Anal. Chim. Acta*, **189**, 237 (1986).

129. M. T. Lai and J. S. Shih, *Analyst*, **111**, 891 (1986).

130. Y. Masuda and E. Sekido, *Bunseki Kagaku*, **39**, 683 (1990).

131. M. Pietraszkiewicz, R. Gasiorowski and Z. Brzózka, *J. Inclusion Phenom. Mol. Recognit. Chem.*, **9**, 259 (1990).

132. Z. Brzózka and M. Pietraszkiewicz, *Electroanalysis*, **3**, 855 (1991).

133. S. K. Srivastava, V. Sahgal and H. Vardhan, *Sens. Actuators B*, **13**, 391 (1993).

134. D. Siswanta, K. Nagatsuka, H. Yamada, K. Kumakura, H. Hisamoto, Y. Shichi, K. Toshima and K. Suzuki, *Anal. Chem.*, **68**,

4166 (1996).

135. D. Siswanta, M. Kin, H. Hisamoto and K. Suzuki, *Chem. Lett.*, **25**, 1011 (1996).
136. S. Amemiya, P. Bühlmann and Y. Umezawa, *Anal. Chem.*, **70**, 445 (1998).
137. V. K. Gupta, S. Jain and U. Khurana, *Electroanalysis*, **9**, 478 (1997).
138. V. K. Gupta, S. Chandra and H. Lang, *Talanta*, **66**, 575 (2005).
139. A. R. Fakari, M. R. Ganjali and M. Shamsipur, *Anal. Chem.*, **69**, 3693 (1997).
140. M. Javanbakht, M. R. Ganjali, H. Eshghi, H. Sharghi and M. Shamsipur, *Electroanalysis*, **11**, 81 (1999).
141. X. Yang, D. B. Hibbert and P. W. Alexander, *Anal. Chim. Acta*, **372**, 387 (1998).
142. A. K. Jain, S. M. Sondhi and V. K. Sharma, *Electroanalysis*, **12**, 301 (2000).
143. R. D. Marco, B. Pejcie and S. Cook, *Lab. Robotics Automat.*, **12**, 194 (2000).
144. L. Perez-Marin, E. Otazo-Sánchez, G. Macedo-Miranda, P. Avila-Pérez, J. Alonso-Chamaro and H. López-Valdivia, *Analyst*, **125**, 1787 (2000).
145. M. Mazloum, M. K. Amini and I. Mohammadpoor-Baltork, *Sens. Actuators B*, **63**, 80 (2000).
146. S. S. M. Hassan, M. B. Saleh, A. A. A. Gaber, R. A. H. Mekheimer and N. A. A. Kream, *Talanta*, **53**, 285 (2000).
147. M. N. Abbas and G. A. E. Mostafa, *Anal. Chim. Acta*, **478**, 329

(2003).

148. R. K. Mahajan, I. Kaur and T. S. Lobana, *Talanta*, **59**, 101 (2003).
149. R. K. Mahajan, R. Kaur, I. Kaur, V. Sharma and M. Kumar, *Anal. Sci.*, **20**, 811 (2004).
150. M. Bagheri, M. H. Mashhadizadeh, S. Razee and A. Momeni, *Electroanalysis*, **15**, 1824 (2003).
151. M. H. Mashhadizadeh and I. Sheikhshoaie, *Talanta*, **60**, 73 (2003).
152. J. Lu, X. Tong and X. He, *J. Electroanal. Chem.*, **540**, 111 (2003).
153. A. K. Singh, G. Bhattacharjee and R. Singh, *Sens. Actuators B*, **99**, 36 (2004).
154. M. J. Gismera, D. Hueso, J. R. Procopio and M. T. Sevilla, *Anal. Chim. Acta*, **524**, 347 (2004).
155. G. Ye, Y. Chai, R. Yuan and J. Dai, *Anal. Sci.*, **22**, 579 (2006).
156. A. A. Khan and Inamuddin, *Sens. Actuators B*, online (2006).
157. H. Hirata and K. Higashiyama, *Anal. Chim. Acta*, **54**, 415 (1971).
158. E. Lindner, K. Toth and E. Pungor, *Anal. Chem.*, **56**, 1127 (1984).
159. Y. G. Vlasov, E. A. Bychkov and A. V. Legin, *Zh. Anal. Khim.*, **40**, 1839 (1985).
160. V. Tyagi and A. K. Jain, *Indian J. Chem.*, **29A**, 608 (1990).
161. S. K. Srivastava, V. K. Gupta and S. Jain, *Analyst*, **120**, 495 (1995).
162. V. K. Gupta, R. Mangla and S. Agarwal, *Electroanalysis*, **14**, 1127 (2002).
163. A. K. Jain, S. M. Sondhi and S. Rajvanshi, *Indian J. Chem.*, **42A**,

819 (2003).

164. A. K. Jain, V. K. Gupta, L. P. Singh and J. R. Raisoni, *Electrochim. Acta*, **51**, 2547 (2006).
165. V. K. Gupta, A. K. Jain and P. Kumar, *Sens. Actuators B*, online (2006).
166. N. M. Sheina, N. V. Shvedene and L. B. Kulakova, *Zh. Anal. Khim.*, **45**, 113 (1990).
167. E. Malinowska, *Analyst*, **115**, 1085 (1990).
168. E. Malinowska, J. Jurczak and T. Stankiewicz, *Electroanalysis*, **5**, 489 (1993).
169. E. Malinowska, Z. Brzózka, K. Kasiura, R. J. M. Egberink and D. N. Reinhout, *Anal. Chim. Acta*, **298**, 253 (1994).
170. W. Wroblewski and Z. Brzózka, *Anal. Chim. Acta*, **326**, 163 (1996).
171. W. Wroblewski and Z. Brzózka, *New J. Chem.*, **20**, 419 (1996).
172. S. Kamata and K. Onoyama, *Anal. Chem.*, **63**, 1295 (1991).
173. S. R. Sheen and J. S. Shih, *Analyst*, **117**, 1691 (1992).
174. K. Anuar and S. Hamdan, *Talanta*, **39**, 1653 (1992).
175. A. S. Attiyat, R. D. Christian, C. V. Cason and R. A. Bartsch, *Electroanalysis*, **4**, 51 (1992).
176. E. Bakker, M. Willer and E. Pretsch, *Anal. Chim. Acta*, **282**, 265 (1993).
177. N. Tavakkoli and M. Shamsipur, *Anal. Lett.*, **29**, 2269 (1996).
178. N. Tavakkoli, Z. Khojasteh, H. Sharghi and M. Shamsipur, *Anal. Chim. Acta*, **360**, 203 (1998).
179. A. Rouhollahi, M. R. Ganjali and M. Shamsipur, *Talanta*, **46**,

1341 (1998).

180. M. R. Ganjali, A. Rouhollahi, A. R. Mardan, M. Hamzeloo, A. Mogimi and M. Shamsipur, *Microchem. J.*, **60**, 122 (1998).
181. H. R. Pouretedal, A. Forghaniha, H. Sharghi and M. Shamsipur, *Anal. Lett.*, **31**, 2591 (1998).
182. O. R. Hashemi, F. Raoufi, M. R. Ganjali, A. Moghimi, M. Kargar-Razi, H. Aghabozorg and M. Shamsipur, *Anal. Sci.*, **16**, 1221 (2000).
183. M. Shamsipur, M. R. Ganjali and A. Rouhollahi, *Anal. Sci.*, **17**, 935 (2001).
184. S. Sadeghi, G. R. Dashti and M. Shamsipur, *Sens. Actuators B*, **81**, 223 (2002).
185. S. Riahi, M. F. Mousavi, M. Shamsipur and H. Sharghi, *Electroanalysis*, **15**, 1561 (2003).
186. X. Yang, N. Kumar, H. Chi, D. B. Hibbert and P. W. Alexander, *Electroanalysis*, **9**, 549 (1997).
187. F. Cadogan, P. Kane, M. A. Mckervery and D. Diamond, *Anal. Chem.*, **71**, 5544 (1999).
188. A. Abbaspour and F. Tavakal, *Anal. Chim. Acta*, **378**, 145 (1999).
189. D. Xu and T. Katsu, *Talanta*, **51**, 365 (2000).
190. M. F. Mousavi, S. Sahari, N. Alizadeh and M. Shamsipur, *Anal. Chim. Acta*, **414**, 189 (2000).
191. M. F. Mousavi, M. B. Barzegar and S. Sahari, *Sens. Actuators B*, **73**, 199 (2001).
192. M. M. Zareh, A. K. Ghoneim and M. H. Abd El-Aziz, *Talanta*, **54**, 1049 (2001).

193. J. Lu, R. Chen and X. He, *J. Electroanal. Chem.*, **528**, 33 (2002).

194. S. S. M. Hassan, M. H. A. Ghalia, A. E. Amr and A. H. K. Mohamed, *Talanta*, **60**, 81 (2003).

195. M. M. Ardakani, A. A. Ensafi, H. Naeimi, A. Dastanpour and A. Shamlli, *Sens. Actuators B*, **96**, 441 (2003).

196. M. M. Ardakani, M. K. Kashani, M. Salavati-Niasari and A. A. Ensafi, *Sens. Actuators B*, **107**, 438 (2005).

197. H. R. Zare, M. M. Ardakani, N. Nasirzadeh and J. Safari, *Bull. Korean Chem. Soc.*, **26**, 51 (2005).

198. V. S. Bhat, V. S. Ijeri and A. K. Srivastava, *Sens. Actuators B*, **99**, 98 (2004).

199. H. Agarwal, A. P. Gupta and G. L. Verma, *J. Indian Chem. Soc.*, **81**, 666 (2004).

200. T. Jeong, H. K. Lee, D-C. Jeong and S. Jeon, *Talanta*, **65**, 543 (2005).

201. M. J. Gismera, M. T. Sevilla and J. R. Procopio, *Anal. Sci.*, **22**, 405 (2006).

202. P.W. Alexander and R.J. Sleet, *Aust. J. Chem.*, **23**, 1183 (1970).

203. E. N. Jacobsen in I. Ojima (Ed.), *Catalytic Asymm Syntheses*, VCH Publishers, New York (1993).

204. G. L. Eichhorn and J. C. Bailar, *J. Am. Chem. Soc.*, **75**, 2905 (1953).

205. C. A. McAuliffe, A. Werfalli, W. E. Hill and D. M. A. Minahan, *Inorg. Chim. Acta*, **29**, 241 (1978).

206. M. Grigoras, C. O. Catanescu and G. Colotin, *Macromol. Chem. Phys.*, **202**, 2262 (2001).

207. I. H. Bukhari, A. Haleem, A. Jabbar and H. N. Bati, *Biosci. Res.*, **2(3)**, 142 (2005).

208. M. Harimohan and F. L. Urbach, *Inorg. Chem.*, **8**, 556 (1969).

209. M. Yildiz, B. Duelger, S. Y. Koyuncu and B. M. Yapici, *J. Ind. Chem. Soc.*, **81(1)**, 7 (2004).

210. P. Koper, Z. Sndelar, M. Biler and R. Klicka, *Pol. J. Chem*, **72(9)**, 2060 (1998).

211. R. A. Robinson and R. H. Stokes, *Electrolyte solutions, the measurement and interpretation of conductance, chemical potential, and diffusion in solutions of simple electrolytes*, 2nd Edn, Butterworths, London (1968).

212. U.S Environmental Protection Agency, Integrated Risk Information System (IRIS) on Manganese, Environmental Criteria and Assessment Office, Office of Health and Environmental Assessment, Office of Research and Development, Cincinnati, OH (1993).

213. W. E. Morf, D. Ammann and W. Simon, *Chimia*, **28**, 65 (1974).

214. U. Schaller, E. Bakker, U. E. Spichiger and E. Pretsch, *Anal. Chem.*, **66**, 391 (1994).

215. P. Bühlmann, S. Yajima, K. Tohda and Y. Umezawa, *Electrochim. Acta*, **40**, 3021 (1995).

216. P. Bühlmann, S. Yajima, K. Tohda, K. Umezawa, S. Nishizawa and Y. Umezawa, *Electroanalysis*, **7**, 811 (1995).

217. S. Yajima, K. Tohda, P. Bühlmann and Y. Umezawa, *Anal. Chem.*, **69**, 1919 (1997).

218. S. Ameniya, P. Bühlmann, E. Pretsch, B. Rusterholz and Y.

Umezawa, *Anal. Chem.*, **72**, 1618 (2000).

219. D. Ammann, *Ion-selective microelectrodes: Principles, design and application*, Springer-Verlag, Berlin (1986).
220. D. Ammann, W. E. Morf, P. Anker, P. C. Meier, E. Pretsch and W. Simon, *Ion-Sel. Electrode Rev.*, **5**, 3 (1983).
221. P. C. Meier, W. E. Morf, M. Laubli and W. Simon, *Anal. Chim. Acta*, **156**, 1 (1984).
222. R. Eugster, P. M. Gehrig, W. E. Morf, U. E. Spichiger and W. Simon, *Anal. Chem.*, **63**, 2285 (1991).
223. W. E. Morf, G. Kahr and W. Simon, *Anal. Lett.*, **7**, 9 (1974).
224. M. Huser, P. M. Gehrig, W. E. Morf, W. Simon, C. Lindner, J. Jeney, K. Toth and E. Pungor, *Anal. Chem.*, **63**, 1380 (1991).
225. E. Bakker, E. Malinowska, R. D. Schiller and M. E. Meyerhoff, *Talanta*, **41**, 881 (1994).
226. E. Bakker, P. Bühlmann and E. Pretsch, *Chem. Rev.*, **97**, 3083 (1997).
227. E. Bakker, E. Pretsch and P. Bühlmann, *Anal. Chem.*, **72**, 1127 (2000).
228. T. P. Coogan, D. M. Latta, E. T. Snow and M. Costa, *CRC Crit. Rev. Toxicol.*, **19**, 341 (1989).
229. E. Berman, *Toxic metals and their analysis*, Heyden & Sons, London, (1980).
230. D. A. Skoog, D. M. West and F. J. Holler, *Fundamentals of analytical chemistry*, Saunders College Publishing, USA, (1996).
231. Z. Marczenko, *Separation and spectrophotometric determination of elements*, John Wiley & Sons, New York, (1986).

232. W. Zhang, L. Jenny and U. E. Spichiger, *Anal. Sci.*, **16**, 11 (2000).

233. P.C. Heier, D. Ammann, W.E. Morf and W. Simon in J. Koryta (ed), *Medical and Biological Application of Electrochemical Devices*, Wiley, New York, (1980).

234. K. Cammann, *Working with ion-selective electrodes*, Springer-Verlag, Berlin, (1979).

235. M. D. A. A. Perez, L. P. Martin, J. C. Quintana and M. Yazdani-Perdram, *Sens. Actuators B,* **89**, 262 (2003).

236. D. Ammann, E. Pretsch, W. Simon, E. Lindler, A. Bezegh and E. Pungor, *Anal. Chim. Acta*, **171**, 119 (1985).

237. Cecil, *Essential of Medicine*, 4th edn, Medtronic Ed., (1997).

238. M. Valko, H. Morris and M. T. D. Cronin, *Current Medicinal Chemistry*, **12(10)**, 1161 (2005).

239. H. Scheinberg and A.G. Morell, *Inorganic Biochemistry*, Elsevier, Amsterdam, (1973).

240. R. D. Macro, *Anal. Chem.*, **66**, 3202 (1994).

241. L. W. Potts, *Quantitative Analysis- Theory and Practice*, Harper and Row, New York (1987).

242. J. Fries and H. Getrost, *Organic reagents for trace analysis*, E. Merck, Darmstadt, (1977).

243. O. Haasw, M. Klarre, J. A. C. Broaekaert and K. Krengel-Rothensee, *Analyst*, **123**, 1219 (1998).

244. P. C. Rudner, A.G. de Torres, J. M. C. Pavon and E. R. Castellon, *J. Anal. Atom. Spectrom.*, **13**, 243 (1998).

245. A. Ali, H. Shen and X. Yin, *Anal. Chim. Acta*, **369**, 215 (1998).

246. P. Shetty and N. Shetty, *Ind. J. Chem. Tech.*, **11**, 163 (2004).

247. H. M. Secolaga, J. Pereziglesisa, J. M. Fernandezolis, J. M. Castroromero, V. G. Rodrigues, *Anal. Lett.*, **31**, 2747 (1998).

248. A. Y. Elsayed, *Anal. Lett.*, **31**, 1905 (1998).

249. M. W. Hinds, *Spectrochm. Acta B Atom. Spectrosc.*, **53**, 1063 (1998).

250. P. Bemejobarrera, E. M. Venduracostenla, A. Moredapinerio and A. Bemejobarrera, *Anal. Chim. Acta*, **398**, 263 (1999).

251. K. H. Lee, S. J. Jiang and H. W. Liu, *J. Anal. Atom. Spectrom.*, **13**, 1227 (1998).

252. M. Sandor, F. Geistmann and M. Schuster, *Anal. Chim. Acta*, **388**, 19 (1999).

253. M. Plasecke, R. Czol and H. J. Ache, *Anal. Chim. Acta*, **304**, 107 (1995).

254. L. Bennum, V. H. Gillette, E. D. Greaves, *Spectrochm. Acta B Atom. Spectrosc.*, **54**, 1291(1999).

255. E. A. Viltchinskaia, L. L. Zeigman, D. M. Gracia, P. F. Santos, *Electroanalysis*, **9**, 633 (1997).

256. J. E. Ferguson, *The Heavy Elements: Chemistry, Environmental Impact and Health Effects*, Pergamon Press, Oxford, (1990).

257. J. Schwartz, *Environ. Res.*, **66**, 105 (1994).

258. B. Welz, *Atomic Absorption Spectroscopy*, VCH, Amsterdam, (1985).

259. I. Sekerka and I. Lechner, *Anal. Chim. Acta*, **254**, 49 (1991).

Research papers published

1. K. Girish Kumar, K.Saji John and Remalakshmy Poduval, Polystyrene anchored vanillin schiff base – Complexation and ion removal studies, *J. Appl. Polym. Sci.*, **98**, 1536 (2005).
2. K. Girish Kumar, Sareena John, Remalakshmy Poduval and Pearl Augustine, Electrochemical determination of terazosin in pure form and in dosage forms, *The Chinese Pharm. Jour.*, **57**, 29 (2005).
3. K. Girish Kumar, Pearl Augustine, Remalakshmy Poduval and Sareena John, Voltammetric studies of sparfloxacin and application to its determination in pharmaceuticals, *Pharmazie*, **61(4),** 291 (2006).
4. K. Girish Kumar, Remalakshmy Poduval, Sareena John and Pearl Augustine, A PVC plasticized membrane sensor for nickel ions, *Microchim. Acta*, online (2006).
5. K. Girish Kumar, Remalakshmy Poduval, Pearl Augustine, Sareena John and Beena S., A PVC plasticized sensor for Ni (II) ion based on a simple ionophore, *Anal. Sci.*, (in Press).
6. K. Girish Kumar, Sareena John, Pearl Augustine, Remalakshmy Poduval and Beena S., A novel mebendazole selective membrane sensor and its application to pharmaceutical analysis, *Anal. Sci.*, under revision (2006).
7. K. Girish Kumar, Remalakshmy Poduval, Pearl Augustine and Sareena John, A chemically modified carbon paste sensor for copper ion using a Schiff base as ionophore, *Indian J. Chem. Sec.A*, (submitted).

Papers presented / accepted

1. A novel Manganese selective plasticized membrane sensor using a Schiff base as ionophore (National seminar on Emerging Trends and New Vistas in Chemistry, Calicut University, Kerala, 2005).
2. Fabrication of a Novel Potentiometric Sensor for the Determination of Terazosin (National seminar on Emerging Trends and New Vistas in Chemistry, Calicut University, Kerala, 2005).
3. Differential Pulse Voltammetric Determination of Sparfloxacin in Pure Form and in Dosage Forms (National seminar on Emerging Trends and New Vistas in Chemistry, Calicut University, Kerala, 2005).
4. Nickel(II) selective plasticized membrane potentiometric sensor using a Schiff base (The 6^{th} East Asia Conference on Chemical Sensors, Gulin, China, 2005).
5. Fabrication of a nickel ion sensor (National Seminar on Frontiers in Chemistry, Cochin University of Science and Technology, Kochi, India, 2006).
6. Fabrication of a novel tetracycline membrane sensor and its application to pharmaceutical analysis (National Seminar on Frontiers in Chemistry, Cochin University of Science and Technology, Kochi, India, 2006).
7. Fabrication of a PVC membrane sensor for the determination of nimesulide in pharmaceutical formulation (National Seminar on Frontiers in Chemistry, Cochin University of Science and Technology, Kochi, India, 2006).